SURVEYING THE METABOLIC VERSATILITY OF BIOFILM-FORMING *EPSILONPROTEOBACTERIA*: A STUDY INTO DEVELOPING ECOSYSTEMS AT EXTREME ENVIRONMENTS

By

CHARLES EDWARD O'BRIEN

A Dissertation submitted to the Graduate School – New Brunswick

Rutgers, The State University of New Jersey

and

The Graduate School of Biomedical Sciences

University of Medicine and Dentistry of New Jersey

In partial fulfillment of the requirements

For the degree of

Doctor of Philosophy

Graduate Program in Microbiology and Molecular Genetics

Written under the direction of

Professor Costantino Vetriani

And approved by

_____

_____

_____

_____

New Brunswick, New Jersey

May 2013

ABSTRACT OF THE DISSERTATION

Surveying the metabolic versatility of biofilm-forming *Epsilonproteobacteria*:

a study into developing ecosystems at extreme environments

By CHARLES EDWARD O'BRIEN

Dissertation Director:

Dr. Costantino Vetriani

At deep-sea hydrothermal vents, mixing of reduced, super-heated, hydrothermal fluids with cold, oxygenated, seawater creates steep temperature and chemical gradients that support chemosynthetic primary production and rich communities of invertebrates. In 2006, an eruption occurred on East Pacific Rise at 9° 50'N, 104° 17'W. Direct observations of the post-eruptive diffuse flow vents clearly indicated that the earliest colonizers were microbial biofilms. A series of cruises in 2006-07 allowed us to monitor the recovery of the ecosystem.

The main objectives of this dissertation are to assess the taxonomic and functional diversity of chemosynthetic bacteria following the eruption, and to correlate it to macrofaunal colonization. To this end, I investigated several microbial biofilms that developed at the bottom of the ocean during exposure to different temperature, redox and biological regimes. Furthermore, I selected pure cultures of

vent bacteria representative of these biofilms and designed experiments to investigate their expression of diagnostic genes involved in carbon fixation and respiration. Finally, I used the information obtained from the pure cultures and from metatranscriptomic studies of the vent biofilms to design experiments for the detection of gene transcripts in chemosynthetic microbial biofilm communities collected from deep-sea hydrothermal vents, and to interpret the results.

My data showed that the biofilm communities that were exposed to active venting were substantially different from the ones that formed at control sites, and that vent invertebrates could only be detected at the former sites. Furthermore, I found that various members of the *Epsilonproteobacteria* dominated the chemosynthetic biofilm communities, and that these bacteria fixed carbon dioxide *in-situ* via the reverse tricarboxylic acid (rTCA) cycle and that they expressed different terminal reductases in response to variable temperature and redox conditions.

I demonstrated for the first time that different respiratory pathways (*e.g.,* nitrate reduction, sulfur oxidation/reduction, microaerobic respiration) are expressed simultaneously in chemosynthetic biofilms. In turn, these results imply that the extremely dynamic conditions found at diffuse flow vents, where reduced hydrothermal fluids mix with oxic seawater, provide the biofilm bacteria with a diverse "metabolic menu" in the form of different redox couples that they can use to conserve energy.

ACKNOWLEDGEMENTS

I would like to thank the members of my dissertation committee, Dr. Costantino Vetriani, Dr. Max Häggblom, Dr. Lee Kerkhof, and Dr. Kay Bidle, for all of their help and support in completing this dissertation work. All of the insightful questions really got me to think about my project more deeply. I am extremely grateful to Costa for taking me in when I had no where else to turn. The work I have done in his lab will be the basis for all I do in the future. My other committee members have been so understanding through all of this, give me bits of advice about writing, job hunting or otherwise.

A number of Vetriani lab members had a hand in this work. Jessica, Kai Li, and Matt all were tremendous helper in starting up all of the experiments. I also built upon work by Melitza and James, so I thank them for framing this work. To Ileana, Ashley, Sushmita, Nicole, Ramadalis, Don and Pat, Matt, Linda and Patty (in no particular order), All of you have made my time here very enjoying and interesting. For the others: Richard, Kyle, Lynnicia, Leticia, Jessica, Caroline, Kristin, Lissette, Moises and Hema, I wish I had more opportunities to get to know all of you better. Thank you also to anybody I may have skipped, it was unintentional.

Dave, Yon, Yi, Aashish, Jayanta and everyone else from the Ebright lab, you will always have a place in my heart. It was so much fun working with all of you. Kathy Maguire, Caroline Ambrose and Diane Murano were such awesome administrators. Any question I had, regardless of how stupid, would be always be answered with a smile. Thank you to Dr. Drew Vershon and Dean Barbara Bender for being so kind during my transition.

Costa, Richard, Max, Diane, Tamar, Gavin and Ines all deserve my gratitude for letting me teach and mentor students. Teaching has been the best part of my journey. I couldn't have asked for a better group of kids (and I say that lovingly) to teach. Being in class and mentoring students in lab has been a major impact on my academic and personal growth.

Finally, to my family and friends. What a bumpy ride, right? You have always been so comforting even when I wasn't making sense. Just spending time with any of you would always bring me joy.

Dedication

I want to dedicate this to Fiona. I always had your picture as my computer desktop. Any time I closed a program on my computer, your face would be there shining back at me. I wish we could be as close in distance as you are to my heart.

Table of Contents

LIST OF FIGURES

LIST OF TABLES

Chapter 1 – Introduction

Background

Extremophiles have inhabited hostile environments, which are not suitable for most life on our planet for billions of years and may predate any other organisms (130). Some of these ancient extremophiles include ones living in geothermal environments with high temperatures and usually high concentrations of toxic chemical species (146). Hydrothermal vents are one of these types of environments with temperatures reaching up to 400 ^{o}C, pressures in excess of several hundred atmospheres, and high concentrations of hydrogen sulfide (often in excess of 1 mM) and many heavy metals (e.g. Cu, Zn, Fe, Cd, Pb) (163). Deep-sea hydrothermal vents are probably the most extreme environments on Earth at which life flourishes.

The hydrothermal vent systems are marked by points of volcanic activity and are generally covered in layers of basalt. Exposed rocks allow for water circulation and nutrient recycling (28). The cold seawater surrounding the system seeps into the Earth's crust, effectively removing oxygen and oxygenated compounds (63). The higher temperature of the magma beneath the surface allows highly reduced compounds, such as sulfides, and heavy metals to dissolve into the water. As the fluids become rich with reduced materials, the magma super-heats the water, making it less dense. The water then rises up, trying to find points of escape (Figure 1). At focused points of escape, the water cools down very quickly allowing for the formation of metal-sulfide compounds (5). These metal-sulfides either deposit on the surface, creating chimney-like structures, or create a plume of "black smoke"

(124; 143). If the water does not find a focused point of escape, it cools down more slowly as it filters through the crust and comes in contact with cold, oxygenated seawater. These types of vents are known as diffuse-flow vents, which are typically colonized by vent invertebrates (Figure 1). As the hydrothermal vent systems are volcanic in nature, they can go through renewal cycles based on volcanic eruptions and resulting earthquakes (134).

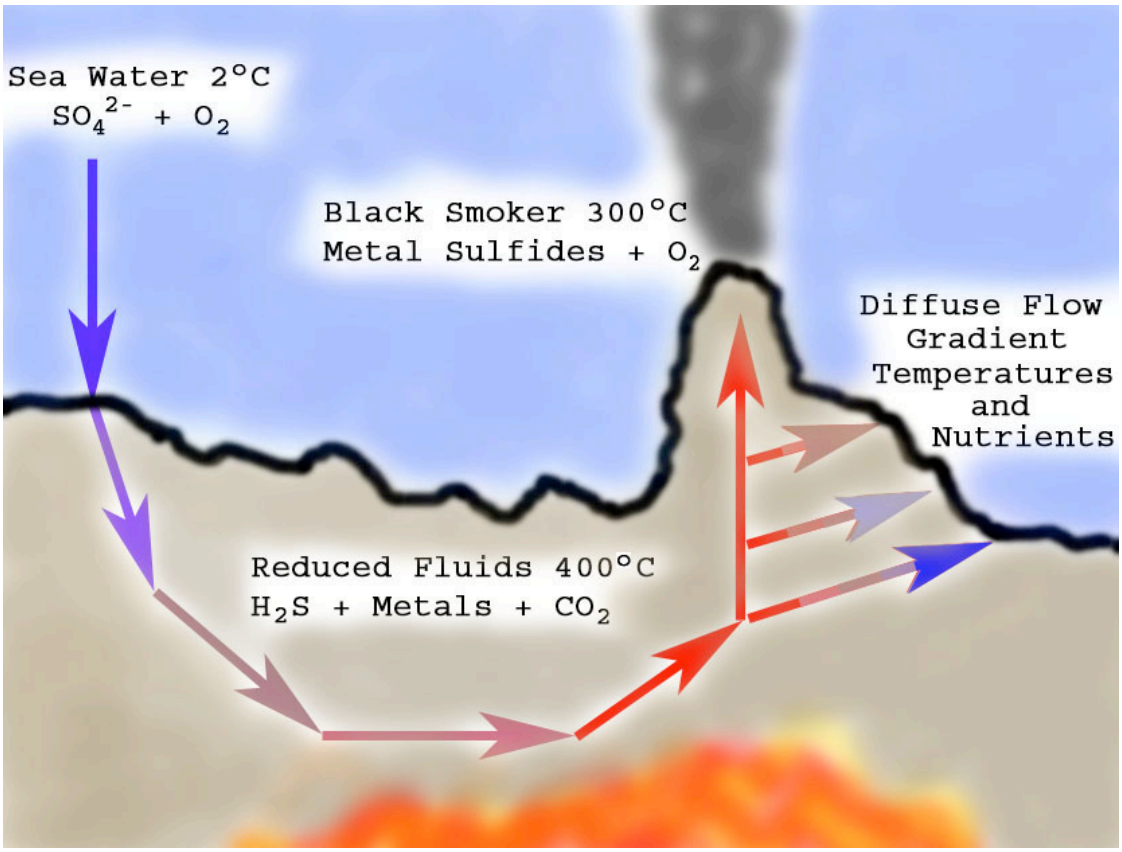

Figure 1: Diagram of a hypothetical deep-sea hydrothermal vent. Seawater seeps into the earth's crust, removing oxidized compounds. Metals and reduced compounds dissolve into the water. The magma below the surface degasses CO_2 and heats the water, making it less dense. The water can rise up and out of chimney-like structures. The temperature decreases rapidly, forming metal sulfides to give a black smoke appearance. Water can also diffuse through the crust and escape through cracks in the surface. These points of diffuse flow can have varying concentrations of nutrients and temperatures.

Eruptions on East Pacific Rise (EPR) at 9°N, 104°W

The East Pacific Rise (EPR) is a mid-oceanic ridge system that runs from Antarctica to the Gulf of California, becoming the San Andreas Fault in California (Figure 2) (16). The EPR is a fast spreading ridge system, meaning that the tectonic plates move apart at speeds ranging from 70 mm/yr in some areas to ~160 mm/yr (16; 77; 157). This movement leads to volcanic eruptions and earthquakes (16; 142; 157). Two eruptions have been documented at EPR 9°N, off the coast of Mexico; once in 1991 and then again in 2005-2006 (Figure 3) (23; 47; 142; 157). Because of this rapidly changing environment, the system at 9°N of the EPR contains some of the most studied hydrothermal vents for geological, geochemical, macrofaunal, and microbiological development (46; 136; 162; 170).

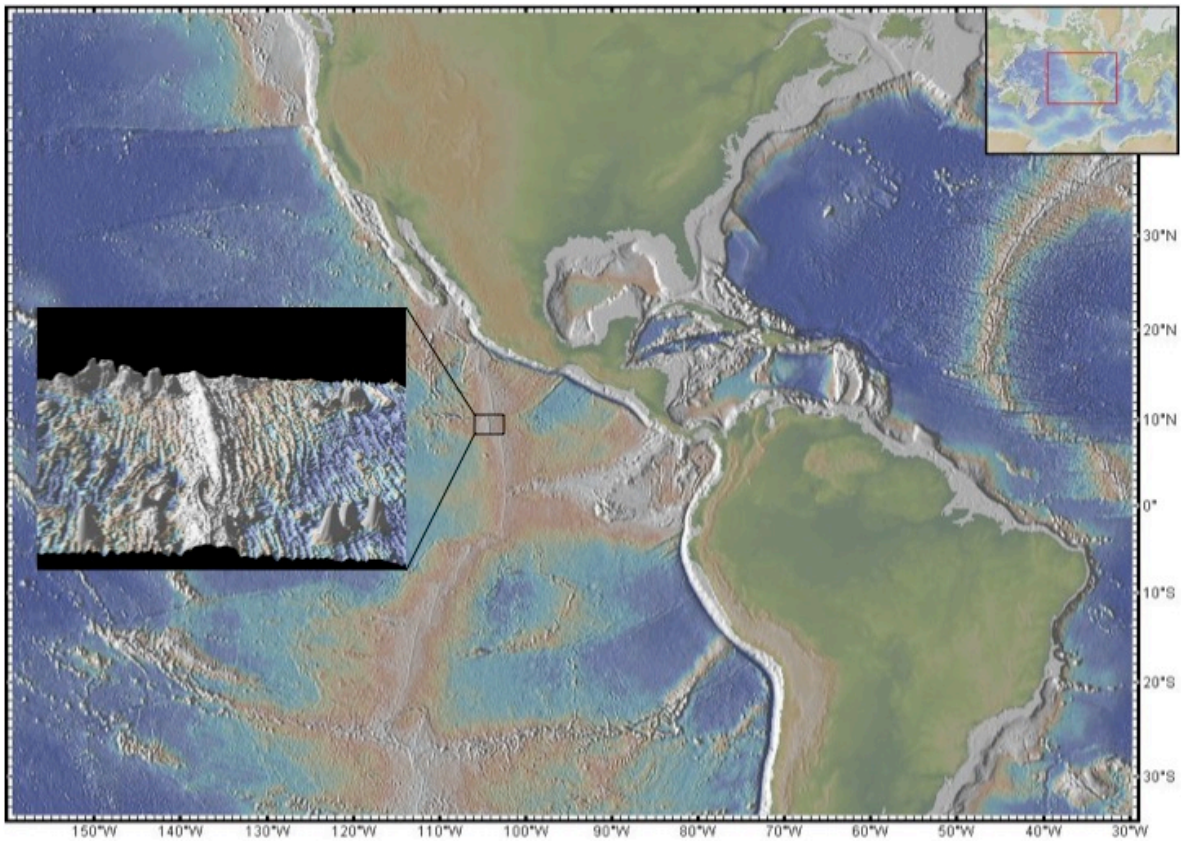

Figure 2: A topographical map showing the East Pacific Rise. The section zoomed in depicts our vent system of interest at 9°N.

Since the 1991 eruption along 9°N of the EPR, outlined in Figure 3, studies have been conducted investigating the changes in the ecosystem at this site (26; 170). Temperature, fluid chemistry and macrofaunal progression were all reported over the time period from 1991 to 2000 (136; 162). At most sites, the succession of the biological ecosystem slowly shifted from white microbial biofilms to large colonies of tubeworms to mussels (as depicted in Figure 3 and (105)). These patterns of microbial colonization and macrofaunal development were variable and present only where hydrothermal fluid emissions occurred (40; 106; 136).

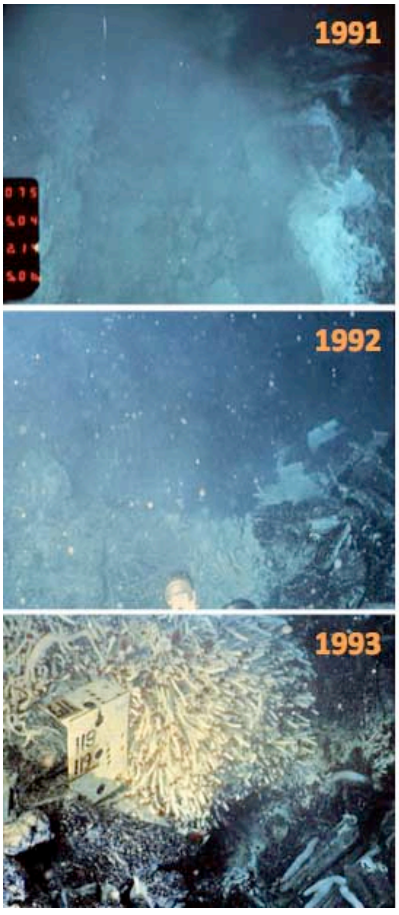

1989	Discovery of 9°50'N venting areas
1990	
1991	Eruption
1992	Secondary eruption
1993	Magmatic diking
1994	
1995	Cracking event
1996	
1997	Black smokers emerge
1998	
1999	
2000	
2001	
2002	
2003	Tica black smokers emerge
2004	
2005	Eruption
2006	New areas of diffuse flow

Figure 3: Hydrothermal vent development at 9°N on the East Pacific Rise. (left) The progression of the ecosystem beginning with white microbial biofilms and developing into colonies of macrofauna (pictures courtesy of Dr. Tim Shank and Dr. Richard Lutz). (right) Timeline of events surrounding the 1991 and 2006 eruptions (modified from www.interridge.org by Dr. Tim Shank).

The extended time-course observation of this region was halted in April 2006. Some of the ocean bottom seismometers (OBS), for detecting earth-quakes, failed to respond or could not be recovered (88). Subsequent surveys by the R/V *Knorr* also suggested that a second volcanic eruption had occurred along the EPR between 9°48'N and 9°51'N. A rapid response cruise of the R/V *New Horizon* tested the area for conductivity, temperature and depth (CTD), collected water from the plume using hydrocasts, and performed digital image surveys. This confirmed that the recent eruption was more extensive than previously thought, covering the area between ~9°46'N and 9°57'N (23). The analysis of the data recovered from still functional OBS showed that the seafloor began to crack in late 2005, followed by major earthquakes in the end of January 2006 (88). More rapid response dives were initiated along the ridge crest. It was observed that areas with vigorous diffuse flow system were covered in white microbial biofilms, while lacking in any visible macrofaunal species. During the R/V *Alvin* expeditions (June 2006), and in the course of subsequent visits in January 2007 to the 9°N post-eruptive area and to the vents located at 12°48'N (referred to 13°N), we collected microbial biofilms using experimental microbial colonizers (Figure 4), and we coordinated *in situ* fluid chemical measurements.

Epsilonproteobacteria **as pioneer colonizers of deep-sea vents**

Microbial biofilms represent a critical step in the primary colonization of deep-sea hydrothermal vents, as they allow microorganisms to maximize access to nutrient and energy sources in an environment typically characterized by high turbulence (1; 78). Studies of the microbial communities of diffuse flow vents have

established the relevance of chemolithoautotrophic *Epsilonproteobacteria* as primary producers, early colonizers, as well as metazoan epi- and endosymbionts at deep-sea hydrothermal vents (12; 13; 15). Phylogenetically, the *Epsilonproteobacteria* fall into five clades: *Campylobacterales*, *Nautiliales*, two unnamed families including *Arcobacter* spp. and *Sulfurospirillum* spp., , and a cluster of marine-related isolated predominantly from sulfidic environments (e.g. hydrothermal vents or hot-springs) (12). The *Campylobacterales* include many host-associated organisms from the genus *Wolinella* and the human pathogenic genera *Helicobacter* and *Campylobacter* (95). The *Nautiliales* group includes the hydrogen-oxidizing thermophilic genera *Nautilia*, *Caminibacter* and *Lebetimonas* that generally reside in a close proximity to the hydrothermal fluid emissions at temperatures between 35 and 60°C (12). The other *Epsilonproteobacteria* found at hydrothermal vents are found in biofilms attached to vent surfaces, in the discharged vent fluids or as symbionts of the vent macrofauna (12; 76; 103).

Although the composition of newly formed hydrothermal vent biofilms and symbiotic relationships have been examined, we have not advanced with respect to defining microbial activity (51; 53). We have a limited understanding of the metabolic pathways and functions, or *in situ* measurements of *Epsilonproteobacteria* metabolism (139). Experimental microcolonizers, utilizing many different colonization surfaces, have demonstrated that these bacteria adhere to the solid support, in the vicinity of active flow, and dominate the resulting biofilms (Figure 4). By having a post-eruptive time-zero study, we were able to start determining the

correlation between microbial biofilm community structure, fluid chemical composition, and the macrofaunal species that colonize the site.

Figure 4: Metal mesh colonizer deployed at an actively diffusing vent at 9°N on the EPR. This particular colonizer shown here was utilized for the metatranscriptome work in this dissertation. This picture was taken before the biofilm was preserved for future studies.

Interestingly, only regions with active flow contain macrofaunal development (2; 27). These regions of active flow are generally marked by higher temperature and the geochemical regimes are constrained by the inorganic reduced species dissolved in the fluids (92). These fluids contain abundant amounts of reduced sulfur species (91). There are also volatile compounds dissolved into the fluids as the magma beneath the Earth's crust degasses (75; 91). These compounds

include significant quantities of methane, molecular hydrogen, and carbon dioxide (150). At the interface between the ambient seawater and points of escape, the two fluids mix together to form steep redox gradients (92; 93). All of these factors create thermal and redox gradients that can be exploited by chemosynthetic prokaryotes, including *Epsilonproteobacteria* (15). At newly formed diffuse flow vents, the *Epsilonproteobacteria* are the pioneer colonizers of this harsh environment and, as episymbionts of vent invertebrates, they might facilitate macrofaunal colonization (15).

CO_2 fixation and respiratory metabolism in *Epsilonproteobacteria*

Pure cultures of *Epsilonproteobacteria* isolated from deep-sea hydrothermal vents are chemolithoautotrophs, meaning that they fix carbon dioxide using energy derived from inorganic chemical species (25; 111). As no significant amount of light penetrates below the euphotic zone, reaching the deep ocean, chemosynthesis rather than photosynthesis is the basis for primary production at deep-sea hydrothermal vents (25; 62; 70; 100). Furthermore, only around 0.1% of the organic carbon derived from photosynthetic surface water dweller reaches the seafloor, which is not sufficient to support the rich communities of invertebrates that inhabit deep-sea vents (52; 63). The recently available genome sequences of vent *Epsilonproteobacteria* provide the necessary information for reconstructing their metabolic processes (see Figure 5; (14; 35; 112; 138; 140)). However, the presence of certain genes and pathways in the genome of an organism suggest the potential to carry out such functions, but further evidence, in the form or gene expression or enzyme activity, is necessary.

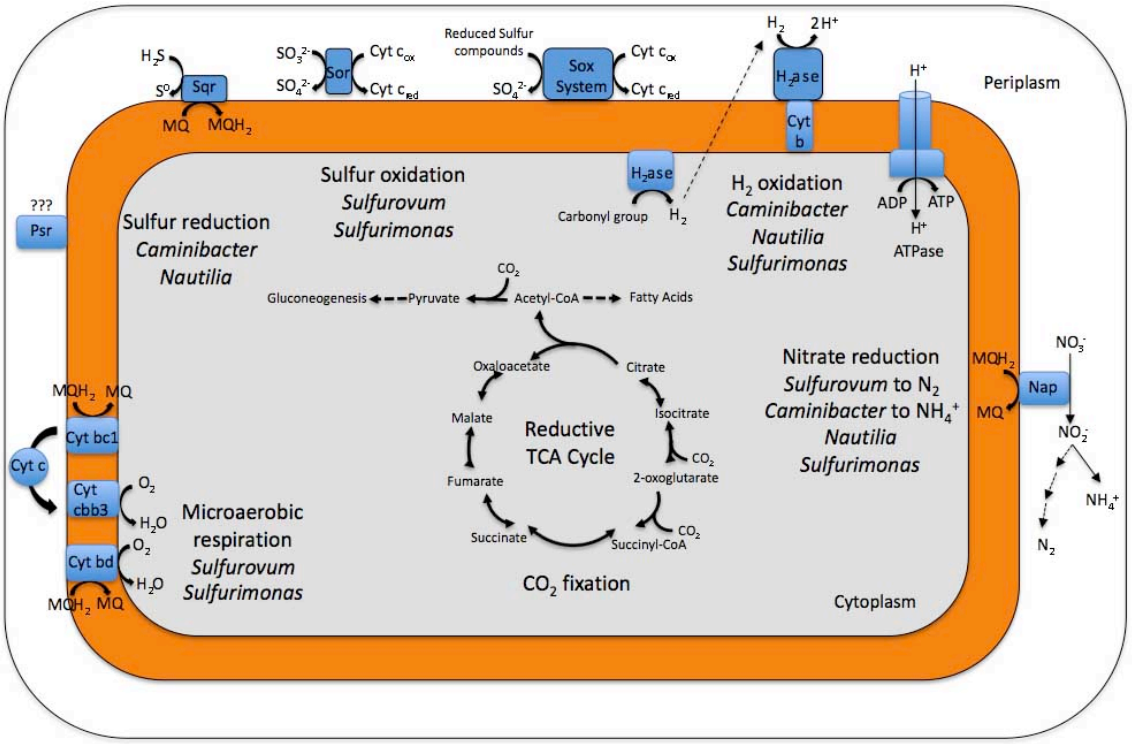

Figure 5: Central metabolic pathways in *Epsilonproteobacteria*. The genomes included come from two mesophilic organisms, *Sulfurovum* sp. NBC37-1 and *Sulfurimonas autotrophica*, and two thermophilic organisms, *Nautilia profundicola* Am-H and *Caminibacter mediatlanticus* TB-2 (35; 111; 140).

At deep-sea vents, carbon dioxide is produced by the magma degassing from beneath the Earth's crust (150). The *Epsilonproteobacteria* utilize the reductive tricarboxylic acid cycle (rTCA) for assimilating this carbon dioxide into biological material (55; 56; 123). The rTCA cycle contains ten reaction steps, utilizing many of the same enzyme from the Krebs cycle (131). The only three steps that are unique to the rTCA cycle are citrate to oxaloacetate and acetyl CoA, fumarate to succinate, and 2-ketoglutarate to isocitrate (131). Carbon dioxide is reduced via the rTCA cycle with electrons originally derived from the oxidation of primary electron donors (e.g. hydrogen and reduced sulfur species) (131). Out of all of the metabolic pathways in

vent *Epsilonproteobacteria*, the rTCA cycle is the best characterized, as enzyme activities in several organisms have even been reported for each of the reactions necessary for a complete cycle (165). However, no *in situ* studies have been performed on the vent biofilms.

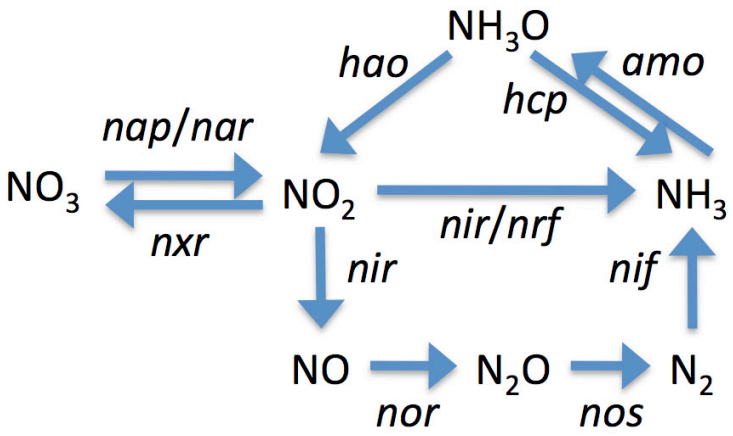

Figure 6: Nitrogen cycle modified from the KEGG Pathway Database.

Characterized hydrothermal vent *Epsilonproteobacteria* pure culture isolates have shown that many of these organisms can couple nitrate reduction to the oxidation of hydrogen and/or reduced sulfur species. For example, *Sulfurimonas paralvinellae* and *Sulfurovum lithotrophicum* can couple the oxidation of thiosulfate and elemental sulfur to the reduction of nitrate (60; 152). *Caminibacter mediatlanticus* and *Nautilia nitratireducens* can utilize hydrogen as an electron donor with nitrate as the terminal electron acceptor (119; 166). From the genome sequences of these organisms and their relatives (35; 112), we can reconstruct the pathways these organisms utilize for nitrate respiration (Figure 6). *S. paralvinellae* and *S. lithotrophicum* have the genes for denitrification (112). The denitrification pathway starts with periplasmic nitrate reductase (*nap*) to reduce nitrate to nitrite and a *nir* nitrite reductase to produce nitric oxide. Nitric oxide is further reduced to

nitrous oxide (*nor*), and finally reduced with a nitrous oxide reductase (*nos*) to leave N_2 as an end product (Figure 6) (68; 112). Other *Epsilonproteobacteria*, such as *C. mediatlanticus* and *N. nitratireducens*, have the genes required for the nitrate ammonification pathway (35). Ammonification can be accomplished in two steps, starting with Nap to reduce nitrate to nitrite, followed by a nitrite reductase similar to *nrf* ferredoxin-nitrite reductase (the exact gene is yet to be identified in vent *Epsilonproteobacteria*) to produce ammonia as an end product (Figure 6) (35).

Bacterial hydrogenases have been studied for over a century (145; 160). Some organisms couple the hydrogenase activity directly to the dehydrogenases of the electron transport chain. Others produce hydrogenases to couple molecular hydrogen oxidation with the reduction of oxygen, nitrate, reduced sulfur species, some oxidized metals, and CO_2, among other substrates (108; 145). The chemolithoautotrophic *Epsilonproteobacteria* carry the genes for 3 classes of hydrogenases: membrane bound hydrogen-uptake hydrogenases; hydrogen-sensing hydrogenases; and membrane bound hydrogen-evolving hydrogenases (111). Hydrogenases have been studied extensively in the pathogenic *Epsilonproteobacteria* (50; 61; 90). Only recent studies into vent *Epsilonproteobacteria* have begun to investigate the exact function hydrogenases play in their metabolism (116; 149) (Figure 5).

Epsilonproteobacteria split into two categories with regards to sulfur metabolism. Generally, sulfur oxidation has been identified in aerobic or microaerobic environments (32; 71). As the temperature of a diffuse flow vent decreases, it allows for more oxygenated sea water to mix into the fluids (64). In

contrast, the higher temperature fluids have less oxygen available for sulfur oxidation (92; 93). This may explain why the thermophilic *Epsilonproteobacteria* are mostly anaerobes (14; 35; 139), and most of the microaerobic, *Epsilonproteobacteria* are mesophiles that thrive at the oxic/anoxic boundary by coupling the oxidation of reduced sulfur species to the oxidation of oxygen (111; 138140). Based on the genome sequences of the *Epsilonproteobacteria, Caminibacter mediatlanticus* TB-2, *Sulfurimonas denitrificans* and *Nautilia profundicola* (14; 35; 138), the genes for sulfur oxidoreductase (*sqr*) and polysulfide

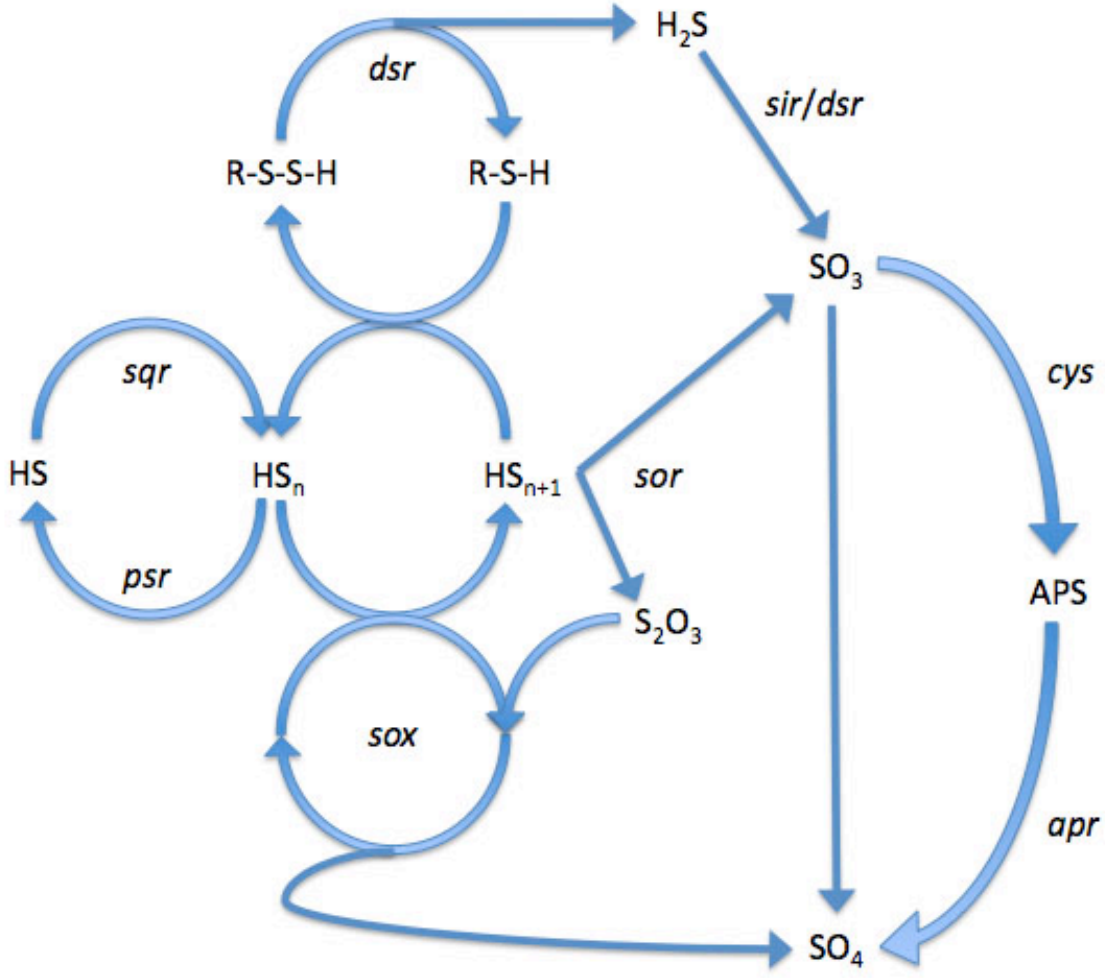

Figure 7: Possible reconstruction of the sulfur cycle in deep-sea vent organisms. Pathways were assembled using information on the KEGG Pathway Database and literature referring to sulfur reduction and oxidation (9; 41; 126; 171).

reductase (*psr*) are present (Figure 7). Other than what is found in the genomes, and minimal work performed on the host-associated *Campylobacterales* order (61), nothing is known about how these enzymes actually function in *Epsilonproteobacteria* (149).

The thiosulfate oxidase (*sox*) is one of the most well characterized components of the sulfur cycle (32; 71). The *sox* system is a complex series of reactions for complete oxidation of thiosulfate ending with sulfate (31; 32; 71). The genes necessary for *sox* have recently been identified in vent *Epsilonproteobacteria* genomes (Figure 5) (111; 138; 140). In addition to the *sox* system, alternate genes for sulfur oxidation have been identified in *Epsilonproteobacteria* (Figure 5), including sulfide quinone reductase (*sqr*) and sulfite oxidase (*sor*) (111; 138; 140) (Figure 7). The general view of the *sqr* mechanism is the oxidation of hydrogen sulfide to inorganic sulfur (42); however, more recent studies suggest an alternative function for *sqr* related to the formation of polysulfide chains (9). One example of these polysulfide chains comes from the mesophilic *Epsilonproteobacterium*, *Arcobacter* sp., which is known to produce polysulfide filaments, most likely through *sqr* activity (154). The *sor* system is related among sulfur oxidizing bacteria, however the exact mechanisms are unknown. The general consensus is that it either involves a reversible reaction of converting sulfides to sulfite and thiosulfate or requires a disproportionation event (31). Both types of reactions require oxygen.

Oxygen respiration occurs through cytochrome oxidases. Microaerophilic *Epsilonproteobacteria* utilize a menaquinone coupled oxidase reaction for reducing oxygen (122). As with the other metabolic pathways in *Epsilonproteobacteria*, most

of the work on oxygen respiration has been done on the pathogenic species (73; 118; 158). One type of cytochrome oxidase, the cbb3-type cytochrome oxidase (*cco*), is found almost exclusively in *Proteobacteria* (74; 122). *Helicobacter pylori* only contains the genes for cbb3-type oxidase (158), while *Campylobacter jejuni* contains both the cbb3-type oxidase and a bd-type oxidase (118). The vent microaerobic *Epsilonproteobacteria* have a cbb3/bd-type oxidase similar to the enzyme found in *C. jejuni* (111; 138) (Figure 5).

Study scope and objectives

On the EPR, volcanic eruptions can destroy the ecosystem and bury all microbial biofilms and macrofaunal communities under fresh lava or sediment (46; 47). These environments rebuild through the formation of focused-flow chimneys and diffuse flow vents (85; 128). The chemical regimes of the newly formed vents can be unstable and relatively different from the established vents that preceded the eruption (161). Variable fluid dynamics include changes in chemistry, temperature or pH that have direct impact on the microbes and macrofauna that colonize the new vents (49; 63; 136). The interactions between the bacteria and macrofaunal organisms are known to change along these gradients (99; 107). However, the exact mechanism that links bacterial survival in the environment to macrofaunal succession in post-eruptive hydrothermal vent systems has not been studied. Chemosynthetic *Epsilonproteobacteria* are the foundation species in vent biofilms and their activities may facilitate colonization of other microbial or macrofaunal organisms. The wealth of knowledge obtained from vent bacterial pure culture isolates opens avenues to explore how these organisms function in their natural

communities. We are interested in finding out how the hydrothermal vent *Epsilonproteobacteria* fill their role in newly formed vent systems.

Studies that integrate microbial physiology and genetics provide insight on gene expression in response to changing conditions, and are valuable tools to understand how microorganisms interact with each other, as symbionts and with their environment. With over 4000 published microbial genomes, and many more genomes and metagenomes still in the pipeline, we are in the midst of a genome revolution (http://www.ncbi.nlm.nih.gov/genomes). A few of the vent *Epsilonproteobacteria* now have had their genomes sequenced (14; 19; 35; 111) (their metabolic pathways are reconstructed in Figure 5). These genomes, along with pure culture information, gives us a starting point for formulating hypotheses on how these organisms adapt to their environments.

In general, *Epsilonproteobacteria* are known to inhabit harsh environments. For instance, the *Epsilonproteobacteria* pathogen, *Helicobacter pylori* thrives in the human stomach, where the pH is very low. While the majority of information on the *Epsilonproteobacteria* is related to the human pathogens *Campylobacter jejuni* and *Helicobacter pylori*, the most diversity in this group of bacteria comes from the organisms living at deep-sea hydrothermal vents (109). As determined by the genome sequences of *C. jejuni* and *H. pylori*, the pathogens have many metabolic genes that are homologous with their vent relatives (118; 158). This includes the genes for the reductive TCA cycle, nitrate reductase, hydrogenase, and oxidase. By studying the chemosynthetic vent *Epsilonproteobacteria*, we may also provide insight into the adaptability of the *Epsilonproteobacteria* pathogens. We hypothesize

that the *Epsilonproteobacteria* species make such great pioneers at deep-sea hydrothermal vents because of their versatile metabolism. This general hypothesis can be broken down into the following sub-hypotheses:

- The presence or absence of macrofaunal colonists at newly formed deep-sea hydrothermal vents is determined by the interaction between the bacterial biofilm community and the different temperature and redox regimes in the environment.
- The *Epsilonproteobacteria* respond to environmental constraints by expressing the genes necessary for fixing carbon dioxide via the reductive tricarboxylic acid cycle (rTCA) and for utilizing the diverse redox regimes.

I had two main objectives to test the above hypotheses:

- Correlating the *Epsilonproteobacteria* dominated biofilm communities with the vent environment and the macrofauna during colonization of post eruptive vents.
- Comparing expression of genes involved in the central metabolism of *Epsilonproteobacteria* from *in situ* vents biofilms to *in vivo* pure culture vent isolates.

Chapter 2 – Interactions among microbial biofilms, fluid chemistry and faunal colonization at hydrothermal vents on the East Pacific Rise

In collaboration with Timothy Shank, Breea Govenar (invertebrate identification) and George Luther (fluid chemistry)

Introduction

Biologists have proposed that the chemical composition of deep-sea hydrothermal vent fluids serves as a settlement cue for fauna to colonize hydrothermal vents along mid-oceanic ridges (81; 107); however, the hypothesis remains largely untested. In addition, microbial community composition in vent fluids and the development of microbial biofilms at vent openings are expected to vary in response to vent fluid chemistry, and may facilitate or inhibit the settlement of invertebrate species (39; 63). The types of sulfur species present in the hydrothermal fluids are generally driven by the temperature and physical characteristics of the vent and can vary when new vents are formed (113; 135). Because of the high concentration of total sulfur, the pioneer microbes developing the biofilm communities are predominantly sulfur oxidizing or reducing *Epsilonproteobacteria* (22; 76; 104). What is for certain is that microbial biofilms are the first communities found at a newly formed vent (22; 43; 86). This colonization event is then followed by a gradual replacement of microbial biofilms by a succession of macrofauna (136).

Ecological processes following disturbances can be key determinants of the subsequent colonization and development of marine communities. In December 2003, we initiated colonization studies at Tica vent on the northern East Pacific Rise

(EPR; a site known as the Ridge 2000 Program's EPR Integrated Study Site), to examine the effect developing microbial communities may have on the colonization of vent endemic fauna. In ~ November 2005, volcanic seafloor eruptions destroyed hydrothermal vent habitats and buried benthic communities in fresh lavas (23; 157). These eruptions also created more than 20 nascent vent habitats, establishing a time-zero for subsequent biological colonization and community development. Previous studies have documented post-eruptive changes in chemical concentrations in diffuse-vent fluids (162). The variability in fluid chemistry, temperature or pH in vent habitats is considered to influence primary production and the distribution of microbes and metazoans, and biological interactions have been shown to vary along a gradient in fluid flux. However, studies that simultaneously examine microbial community structure of early microbial colonists, macrofaunal colonization and fluid chemistry in varying environmental conditions have not been conducted previously. We hypothesize that the chemical composition and flow of hydrothermal fluids and microbial community assembly control the colonization dynamics of later microbial and faunal colonists. Ultimately, geological-chemical-microbial-metazoan interactions may drive the ecological patterns in these disjunct and ephemeral habitats and provide insights into the evolution of life in other chemosynthetic ecosystems.

We conducted time-series *in situ* experiments examining patterns of microbial community structure coincident with assessments of fluid chemistry and vertebrate colonization at different temporal scales along the East Pacific Rise. The primary objective of our integrated research is to understand biological-

geochemical interactions during initial colonization of basalt at deep-sea hydrothermal vents through time-series studies that combine molecular genetic characterization of microbial communities and metazoan colonists with *in situ* measurements of H_2, H_2S, pH and temperature. Through these integrated studies, we have identified marked differences in short-term microbial community development and vent-endemic metazoans. The goal of the present study was to examine for the first time co-located linkages between hydrothermal fluid chemistry, microbial colonization and metazoan colonization. Specifically, amongst newly formed post-eruptive vents, we aimed to: 1) characterize the composition of microbial colonizers; 2) assess physiological and functional attributes of microbial colonizers; and 3) correlate patterns within each of the linkage groups that are involved in hydrothermal vent ecosystem development.

Materials and Methods

Integrated colonization experiments. To compile and expose the linkages of hydrothermal fluid composition with microbial and metazoan colonization, we designed and deployed experimental colonizers that permit the coordination and integration of these data (Figure 2). Deploying artificial substrates provides the opportunity to "control" the natural environmental conditions by choosing specific habitats. The experimental colonizers, referred to as TAMS (Temporal Autonomous Multi-disciplinary Substrates) were designed to allow hydrothermal fluids to pass through the colonization surface (Figure 1). Each colonizer was constructed from a 4 x 4" polyetheylene frame with two layers of 1mm (opening) polyester mesh to

allow flow permeability and a 100 μm layer to provide substrate for microbial colonization. Each TAMS hosted an attached Vemco™ temperature probe for continuous monitoring of the temperature throughout the deployment (see Figure 1). Four TAMS were deployed for sampling each of the habitat types that were actively venting but not yet colonized with megafauna. Four TAMS were also deployed on neighboring basalt at controls. The active vents were distinguished by observing autonomous temperature loggers. Detailed close-up imaging of each associated habitat was conducted to examine recent tubeworm colonists.

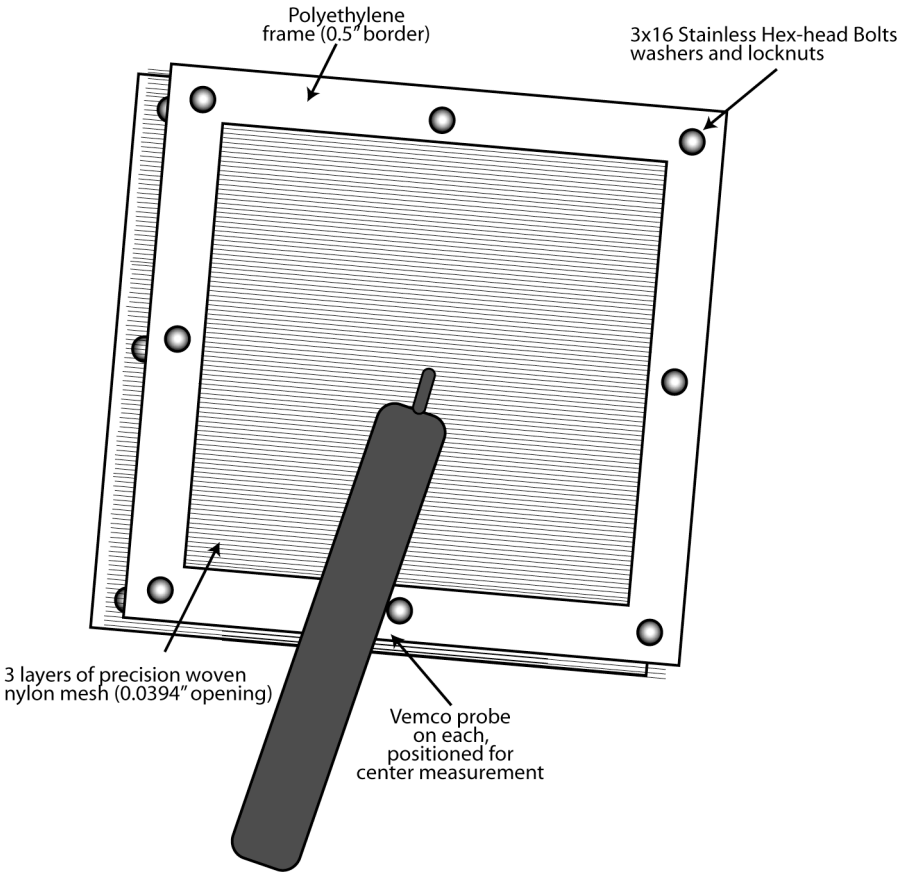

Figure 1. TAMS (Temporal Autonomous Multi-disciplinary Substrates) design.

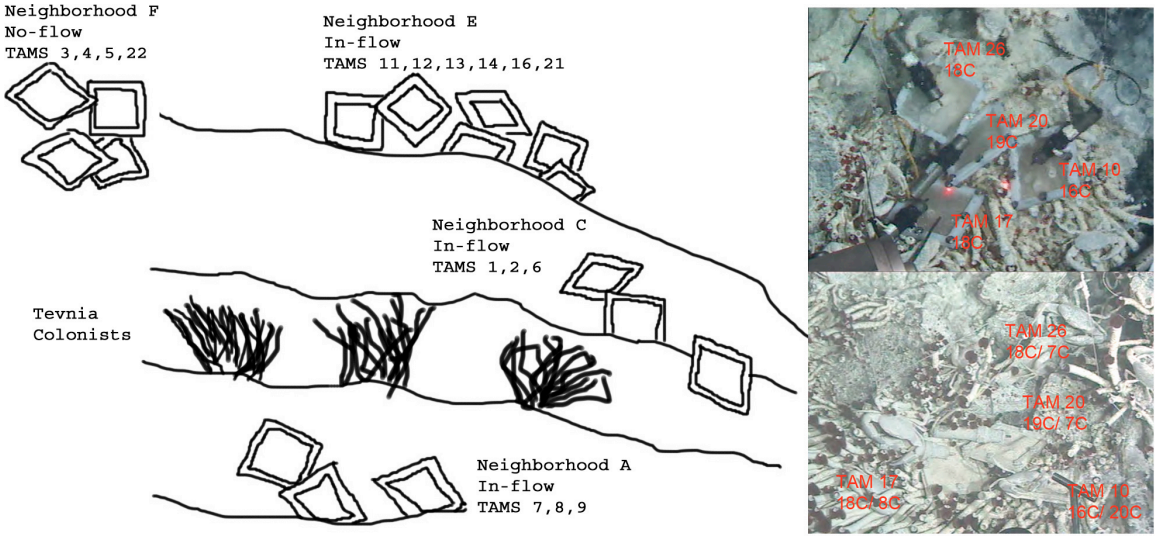

Figure 2. (left) Rough sketch of TAMS colonizers deployed at Tamtown. The neighborhoods are categorized by the diffusing vent ridges and proximity to fully growth *Tevnia* colonies. (top right) Photo taken of the diffuse-flow TAMS at Marker 19 just after deployment. (bottom right) Photo taken before recovering the colonized TAMS at Marker 19, 6 weeks after deployment.

In designing our deployment strategy, we recognized that spatial and temporal heterogeneity of fluid chemistry and temperature associated with vent habitats at a given site does not allow the deployment of multiple colonizers that could be considered "replicates" (Table 1; (87; 133). Thus, for our data integration, we consider each colonization surface as an individual sampling unit. Our TAMS design and deployment strategy is designed to obtain *in situ* (continuous) temperature and chemical measurements at each TAM to assess, correlate, and identify the patterns recruitment and colonization of microbial and metazoan species in chemically different habitats.

TAMS deployment. TAMS were transported to the seafloor in filtered seawater to prevent contamination by surface-water microbial and metazoan populations and were recovered either in individual temperature-insulated

containers ("bioboxes") or into a container that was flooded with a preservative for *in-situ* fixation.

Table 1. Quadrants (I, II, III, IV) of TAMS colonized (+) or uncolonized (0) by vestimentiferans at Tamtown (June 2006- Jan 2007, x: 4663, y: 77660, depth: 2504 m), Marker 19 (Nov 2006- Jan 2007, x: 5528, y: 72694, depth: 2510 m). Letters in parentheses are different locations of diffuse-flow within the Tamtown area.

Site	Treatment	TAM ID	I	II	III	IV
Tamtown	Diffuse-flow (A)	7	0*	+	+*	+
	Diffuse-flow (A)	8	+	+*	0	0*
	Diffuse-flow (A)	9	+	0*	+	+*
	Diffuse-flow (E)	11	+	0*	0	+*
	Diffuse-flow (E)	12	+*	+	+*	+
	Diffuse-flow (E)	13	0	+*	0	0*
	Diffuse-flow (E)	14	0	0	0	+
	Diffuse-flow (E)	16	+	+	+*	+*
	Diffuse-flow (E)	21	+*	+*	+*	+*
	Diffuse-flow (C)[1]	1	N/A	N/A	N/A	N/A
	Diffuse-flow (C)	2	+*	+	+*	+
	Diffuse-flow (C)	6	0*	0	0*	0
	Control	3	0	0	+*	+
	Control	4	0	0	0	0*
	Control	5	0*	0	0	0
	Control	22	0	0	0*	0
Marker 19	Diffuse-flow	17	+	0	0	+
	Diffuse-flow	20	+*	+	+*	+
	Diffuse-flow	26	+	+	+	+
	Diffuse-flow	10	0	0	0*	0
	Control	29	0	0*	0	0
	Control	37	0	0	0*	0
	Control	19	0	0	0	0*
	Control	18	0*	0	0	0

[1]Recovered in November 2006.
*Microbially analyzed mesh quadrants.

The locations with the highest number of deployed TAMS colonizers were collectively labeled as "Tamtown" for the purpose of identification. The Tamtown sites were established during Alvin dives 4203 and 4207 (Figure 2). Neighborhood A was the first site established on dive 4203. The location was in a crack just below a *Tevnia*-covered rock face. Neighborhood B (not used in this study) was slightly

east of A, situated in the same crack. Neighborhood C was situated slightly north of A, on a ridge above the *Tevnia*-covered rock. Neighborhood E was established on dive 4207. The location was northwest of C, on the other side of the ridge. Each of the neighborhoods A, B, C, E were all established on actively diffusing vents. Neighborhood D was established as a control site, outside of the diffusing vents slightly south of A, on dive 4203. TAMS colonizers 3, 4 and 5 were all located at neighborhood D until they were moved to neighborhood F on dive 4207. TAMS colonizer 22 was added to the no-flow group, all situated slightly east of Marker 11.

TAMS were deployed with Marker 20, south of P vent on AT 15-13 (dive 4283) (Table 1). On this cruise, no TAMS were collected, but temperature (2.5- 12 °C on dive 4300) and electrochemical scans were conducted for each substrate. In this area, lava flows in transit were very rubbly and broken up, like a thin "shell/veneer" of sheet flow that was then collapsing.

Compiled *in situ* fluid chemistry. Fluid chemistry measurements were carried out by our collaborator, Dr. George Luther at the University of Delaware. A submersible-mounted and an autonomous in-situ electrochemical sensor (82) were used to measure H_2S/HS^-, FeS, Fe_2^+, Mn_2^+, O_2, pH and T°C on the surface of each TAMS at deployment and recovery. At Tamtown, an autonomous *in situ* electrochemical analyzer (ISEA Insect) (102), hosting four gold-amalgam working electrodes (each coupled with a Vemco™ temperature probe) capable of measuring O_2, H_2S, iron and sulfur species, was deployed. The submersible manipulator facilitated the precise placement of the electrodes to minimize its effect on the flow field. Electrochemical scans directly above were obtained from four electrodes and

the TAMS Vemco™ temperature loggers every 15 seconds. Working details of the voltammetric analyzer, as well as standardization and conditioning of the electrodes well performed as previously described (7; 83; 84). Voltage is scanned while monitoring current; each electroactive substance gives a current that is proportional to concentration at a specific voltage. Detection limits (DL) in μM are 0.2 for H_2S, 3 for O_2, 5 for Mn(II), and 10 for Fe(II), and replicate scans agree within 2 to 5%. DL are based on a 100-μm diameter electrode but can be extended by changing electrode size and increasing scan rate (6). Sulfide limits of detection are at least an order of magnitude better than the commonly used method (20) on which most sulfide measurements are based (102). During Dive 4297, the ISEA insect was recovered after the six-month deployment.

TAMS recovery. TAMS were deployed during AT15-6 (RESET06) with Insect at both Markers 8 and 11, when *Tevnia* colonization and active diffuse-flow were observed. Hydrothermal fluid flux waned by November, when TAMS 1 was recovered during AT15-13. The Insect and remaining TAMS were recovered during January 2007. Neighborhood E, where Marker 24 was deployed, neighborhood F, and neighborhood A, where Marker 25 was deployed, were all collected during these dives. TAMS were also deployed at Marker 19 on dive 4282. TAMS were recovered and Marker 31 samples were deployed on dive 4304. TAMS were also deployed at Marker 33 on dive 4305 (x: 5057, y: 74926) in an area of diffuse-flow, containing white staining, and colonized by *Tevnia.* These TAMS, recovered on dive 4312 and preserved *in situ* in RNAlater, will be utilized for future studies

investigating the co-expression of genes by microbes and macrofauna, and not utilized in the current study.

Upon recovery, the TAMS were placed into the 2°C "cold room" on the ship for further processing. The TAMS were visually divided into quadrants, following a systematic numbering scheme (starting on the left side of the Vemco™ temperature probe as one and progressing clockwise), inspected and documented with digital imaging. The frame was disassembled in either cold filtered seawater (or preservative, depending on the method of recovery/ collection), and both sides of the mesh were carefully examined for microbial and metazoan colonists. Sessile metazoan colonists were documented by high-quality digital imaging at 10x magnification, physically removed from the mesh, measured (for body length), and frozen individually. After rinsing the mesh gently in the filtered seawater to retain the meio- and macrofaunal colonists, the mesh was cut into the four quadrants. For every quadrant, one sheet was used for microbial inoculations and the other two sheets were used for phylogenetic analyses. The filtered seawater was passed through a 250 μm sieve to retain and separate the associated meiofaunal and macrofaunal communities.

Macrofaunal colonist enumeration. Identification and enumeration of TAM metazoan colonists was conducted via microscopy by our collaborators, Dr. Tim Shank and Dr. Breea Govenar at Woods Hole Oceanographic Institution. Larvae (and juvenile) macrofauna, particularly vestimentiferans, too small for unambiguous morphological identification were identified using Restriction Fragment Length Polymorphism (RFLP) analyses; see (21; 30; 105; 137) and DNA sequencing of

mtCOI. Comparisons of community structure and composition analyzed with standard parametric and non-parametric statistics, including several subroutines offered by PRIMER v.5 (38). Analysis of similarities (ANOSIM) was used to determine whether significant differences in the community composition existed between TAM substrates within a habitat-type and among the habitat-types. SIMPER tests were used to determine the species or the group of species that contribute(s) the highest percentage of the variability among the significantly different communities. Each independent datum, including environmental conditions, the composition of the microbial biofilms and the macrofaunal colonists, will be compared using the BIOENV statistical analysis (18; 38).

DNA extraction. Colonizer sections selected for microbial analysis were stored at -80 ^{o}C until processed. Genomic DNA extracts were compared from a 3 cm x 1 cm piece, 1 cm x 1 cm piece and a combination of four 1 cm x 1 cm squares in the TAMS 9 Quadrant 4. The communities did not vary between the three methods, so 1 cm x 1 cm squares were used for the remaining colonizers. Total genomic DNA was extracted from the squares cut from the center of the quadrants using an UltraClean Soil DNA extraction kit (Mo Bio, Carlsbad, CA) according to the protocol supplied with the kit. The DNA purity was checked using a 1% agarose gel. The number of replicates for each TAMS biofilm community, used in microbial analysis, was either one or two depending on how the TAMS colonizer quadrants were distributed after collection (Table 1).

16S rRNA gene amplification by PCR. The 16S rRNA genes were PCR amplified using forward primer 8F (5'-AGAGTTTGATCCTGGCTCAG-3') and the

reverse primer 1517R (5'-ACGGCTACCTTGTTACGACTT-3'). Reactions were subjected to the following program in a thermal cycler (Perkin-Elmer, Waltham, MA): 94 ^{o}C for 2 min; 35 cycles of denaturation at 94 ^{o}C for 30 s, annealing at 50 ^{o}C for 30 s, and extension at 72 ^{o}C for 30 s; with a final extension at 72 ^{o}C for 7 min on the last cycle.

Fragments of the 16S rRNA gene for Denaturing Gradient Gel Electrophoresis **(**DGGE) analyses were PCR amplified using forward primer 338F (5'-ACTCCTACGGGAGGCAGCAG-3') with a GC clamp on the 5' end (5'-CGCCCGCCGCGCGCGGCGGGCGGGGCGGGGGCACGGGGGG-3') and reverse primer 519R (5'-GWATTACCGCGGCKGCTG-3'). Reactions were subjected to the following program: 94 ^{o}C for 5 min; 10 cycles of denaturation at 94 ^{o}C for 30 s, annealing at 61 ^{o}C for 1 min and extension at 72 ^{o}C for 1 min.; followed by 20 cycles of denaturation at 94 ^{o}C for 30 s, annealing at 56 ^{o}C for 1 min, and extension at 72 ^{o}C for 1 min; with a final extension at 72 ^{o}C for 10 min on the last cycle.

Denaturing gradient gel electrophoresis (DGGE). DGGE analysis was performed as previously described (159). Samples (18.0 μl) were applied onto a 6% (wt/vol) polyacrylamide gels in 1x TAE (40 mM Tris, 20 mM acetate, 1 mM EDTA) with denaturant gradient from 40 to 60% (where 100% denaturant contains 7 M urea and 40% formamide). Electrophoresis was performed at a constant voltage of 57 V for 16 h at 60 ^{o}C with a 10 min initial run at 200 V. After electrophoresis, gels were incubated for 15 min in ethidium bromide (0.5 mg/L), rinsed for 10 min in distilled water and photographed with a UV Foto Analyst imaging system (Fotodyne, Inc.).

Construction of clonal libraries. In order to increase the efficiency of cloning, a round of a-tailing was performed. The 16S rRNA gene PCR products were diluted 3 fold into PCR Master Mix (Qiagen) containing *Taq* Polymerase. Clone libraries were then constructed using the TOPO TA cloning kit (Invitrogen) following the manufacturers' recommendations. Amplified 16S rRNA gene fragments were cloned in a pCR4-TOPO plasmid vector (Invitrogen) and the ligation products were used to transform competent *E. coli* TOP10 cells. Clones were grown in Luria Bertani media containing 100 μg/ml ampicillin overnight at 37 ^{o}C and kept for long-term storage at -80 ^{o}C in 96-well plates. Recombinant plasmids were extracted using the QIAprep spin miniprep kit (Qiagen) as described in the manufacturers' instructions. Six 16S rRNA gene libraries (Table 3) were constructed and a total of 500 randomly selected colonies were analyzed. The clones are designated TAMSXXQuadY_#, where XX indicates the TAMS colonizer number, Y identifies the quadrant the sample was taken from and # represents the clone number.

Restriction fragment length polymorphism (RFLP) screening. Clonal inserts of 16S rRNA gene fragments were digested for 2 h at 37 ^{o}C on a thermocycler using the tandem tetrameric restriction endonucleases *Hae*III and *Msp*I (Promega). A 3% (w/v) Metaphor agarose gel containing ethidium bromide was prepared using manufacturer's specifications (Lonza). The restriction products were run for 1.5 h at 75 V an 4 ^{o}C on the Metaphor gel and visualized under UV light.

Sequencing and phylogenetic analysis. Representative bacterial 16S rRNA gene clones with unique RFLP patterns were sequenced utilizing an automated DNA

sequencer (3100 Avant Genetic Analyzer; Applied Biosystems). The sequence reaction was carried out using the 8F, 1517R and 515F (5'-GTGCCAGCMGCCGCGGTAA- 3') universal primers with the following program: 96 ^{o}C for 30 s; 35 cycles of denaturation at 96 ^{o}C for 10 s, annealing at 50 ^{o}C for 5 s and extension at 60 ^{o}C for 4 min.

The sequences obtained were assembled using the AutoAssembler Program (Applied Biosystems). Each sequence was compared with an existing database of rRNA gene sequences from the cultivated microorganisms and environmental clones using the BLAST search program of the National Center for Biotechnology Information. The Check_Chimera version 2.7 program of the Ribosomal Database Project II (http://wdcm.nig.ac.jp/RDP/html/analyses.html) was used to detect possible chimeric sequences, (89). Any chimeric sequences were removed from further analysis. Clones from each unique RFLP pattern had their 16S rRNA gene sequenced were the results were aligned using ClustalX (155). Seaview was used to manually adjust the alignment before plotting the tree topology in Phylo_win (33). The phylogenetic distances were calculated using the Jukes-Cantor model and neighbor joining method. The robustness of the tree was tested by bootstrap analysis based on 500 resamplings.

Statistical analysis on the microbial communities was performed using NTSYS-PC software package version 2.0 (127). The clones were sorted into their most closely related class of bacteria and recorded into a matrix. Clustering analysis used the Sequential, Agglomerative, Hierarchical and Nested (SAHN, (141) method based on Unweighted Pair Group Method with Arithmetic Mean (UPGMA) to

formulate a dendrogram. Rarefaction analysis was performed using the Analytical Rarefaction Calculator program that is found at: http://www.uga.edu/strata/software/Software.html.

Results

Colonizer selection. Our collaborator, Dr. George Luther, measured the environmental parameters (e.g., temperature, inorganic sulfur species) at the time of deployment for all Tamtown samples and at the time of recovery for Marker 19 samples. Visual inspection of each deployment location was used for determining diffuse-flow or no-flow status. For each sample the temperature was measured directly, as well as compiled over the time of deployment using Vemco™ temperature probe attached to the colonizer. During deployment or collection, measurements for H_2S, volatilized sulfur (AVS) and O_2 were taken (Dr. Luther's data is listed in Table 2).

Dr. Tim Shank and his team at the Woods Hole Oceanographic Institution sectioned the colonizers and preserved them for future study. Before preserving, they counted and removed the invertebrates (vestimentiferans) from the bacterial biofilms. Fragments of the same colonizers were designated for microbial studies and given to us (Table 1). These colonizers were picked based on the presence or absence of tubeworm colonists, diffuse-flow or no-flow location, and the chemical and temperature regimes during the deployment. In order to obtain a general overview of the community composition from these selected biofilms, DGGE analysis was performed (Figure 3). In general, the banding patterns for each of the biofilms or conditions (samples shown in Table 1), revealed that the corresponding

Table 2. Temperature and chemical analysis taken at deployment or recovery of TAMS colonizers.chemical

TAMS #	29	18	20	26	10	19	17	7	8	9	3	4	5
Wand (dive)	4304	4304	4304	4304	4304	4304	4304	4297	4299	4297	4300	4300	4300
Wand-temp, degC (avg)	2.79	2.50	7.17	7.57	8.25	2.50	8.32	4.30	5.90	5.10	3.75	2.50	2.65
Wand-temp, degC (stdev)	0.27	0.00	0.57	1.00	3.12	0.000	0.683	0.422	0.709	0.316	0.354	0.00	0.242
Wand-temp, degC (max)	3.00	2.50	8.00	9.50	15.0	2.50	9.50	5.00	7.00	5.50	4.00	2.50	3.00
Wand-temp, degC (min)	2.50	2.50	6.50	6.50	4.50	2.50	7.00	3.50	4.00	4.50	3.00	2.50	2.50
Wand-H_2S, uM (avg)	2.53	10.6	54.2	41.4	57.9	2.84	60.7	3.84	21.1	8.24	5.74	0.618	0.868
Wand-H_2S, uM (stdev)	0.26	0.274	19.3	32.1	40.2	1.40	1.72	2.10	9.36	1.29	4.97	.284	0.194
Wand-H_2S, uM (max)	2.88	1.37	67.3	63.4	104	5.70	63.2	8.37	36.1	9.81	14.7	1.11	1.38
Wand-H_2S, uM (min)	2.14	0.713	BDL	BDL	1.49	1.83	57.4	1.60	BDL	6.83	1.56	0.312	0.712
Wand-O_2, uM (avg)	78.5	82.4	21.5	22.2	7.87	88.5	10.6	53.7	63.4	20.6	43.4	57.1	49.8
Wand-O_2, uM (stdev)	12.9	5.35	17.7	16.3	17.3	11.0	11.8	6.34	9.21	5.57	5.65	6.30	4.76
Wand-O_2, uM (max)	92.9	88.3	47.4	49.3	55.6	103.0	26.7	63.3	93.0	28.4	52.6	65.7	57.2
Wand-O_2, uM (min)	51.5	75.0	BDL	BDL	BDL	70.8	BDL	44.7	52.1	9.82	36.3	43.6	38.4
Vemco	1116	2898	8656	2876	2879	2897	8652		2883	1107	1129	1115	2354
Vemco (housing)	115	254	268	230	216	241	201		243	203	233	239	209
Vemco-temp, degC (avg)	1.8	1.7	9.2	10.4	8.4	2.0	9.5		4.9	4.9	4.8	2.3	1.6
Vemco-temp, degC (stdev)	0.1	0.2	2.6	2.8	2.7	0.2	2.6		3.1	2.9	2.4	0.5	0.3
Vemco-temp, degC (max)	4.5	4.5	25.2	26.9	20.2	4.5	21.1		22.0	23.5	18.6	5.2	3.1
Vemco-temp, degC (min)	1.6	1.4	2.6	2.9	2.1	1.8	3.0		1.9	1.8	1.7	1.8	1.2

Table 3. Subset of bacterial 16S rRNA gene clones analyzed including one sample and one control from each location.

Location	Treatment	#Clones picked	#Used in RFLP	#Sequenced	α	δ	ε	γ	CFB	Unassigned
Tamtown TAMS 4	Control	32	22	5	0	0	0	5	0	0
Tamtown TAMS 9	Diffuse-flow	45	34	17	1	1	14	1	0	0
Marker 19 TAMS 29	Control	37	36	14	0	0	4	10	0	0
Marker 19 TAMS 20	Diffuse-flow	71	41	31	0	2	26	0	2	1
Total		185	133	67	1	3	44	16	2	1

microbial communities were similar, but not identical. Those communities with unique DGGE patterns (or one community from a group of similar fingerprints) were then used for further analyses. While the DGGE analysis is useful to obtain a general overview of the different microbial biofilms, it does not provide a detailed assessment of the composition of such communities. In order to accomplish this goal, shotgun clone libraries were created from total genomic DNA extracted from the biofilms. Two no-flow samples (Tamtown TAMS 4 and Marker 19 TAMS 29) were chosen as representative no-flow controls for each location. From Marker 19, TAMS 20 quadrant 3 was chosen for study because it was the only Marker 19 diffuse-flow colonizer that was stored for microbial analysis. At Tamtown, TAMS 12 and 16 were chosen for further study because they had many unique DGGE bands and had the highest and lowest [H2S] out of the diffuse-flow Tamtown colonizers, respectively. TAMS 9, from Tamtown, was chosen because this colonizer had quadrants with and without vestimentiferans colonists. TAMS 13 was not included in the analysis because there was no environmental analysis to correlate results to.

TAMS invertebrate colonists. All macrofaunal work was reported to us by our collaborators Dr. Tim Shank and Dr. Breea Govenar, performed at Woods Hole Oceanographic Institution. Each TAM was colonized by 80 to 3786 individuals of macrofaunal invertebrates, representing between 5 to 20 species (Dr. Shank's and Dr. Govenar's work is shown in Table 4). The community composition of the macrofaunal colonists was significantly different between sites (Table 4; ANOSIM, $R = 0.622$, $p = 0.001$), habitat-types (ANOSIM, $R = 0.584$, $p = 0.001$), but not between habitat-types within a site. The differences in the community composition between

sites and between habitat-types were due to the relative dominance of the gastropod limpets *Lepetodrilus tevniatus* and *L. elevatus* at Tamtown and in diffuse-flow habitats (SIMPER).

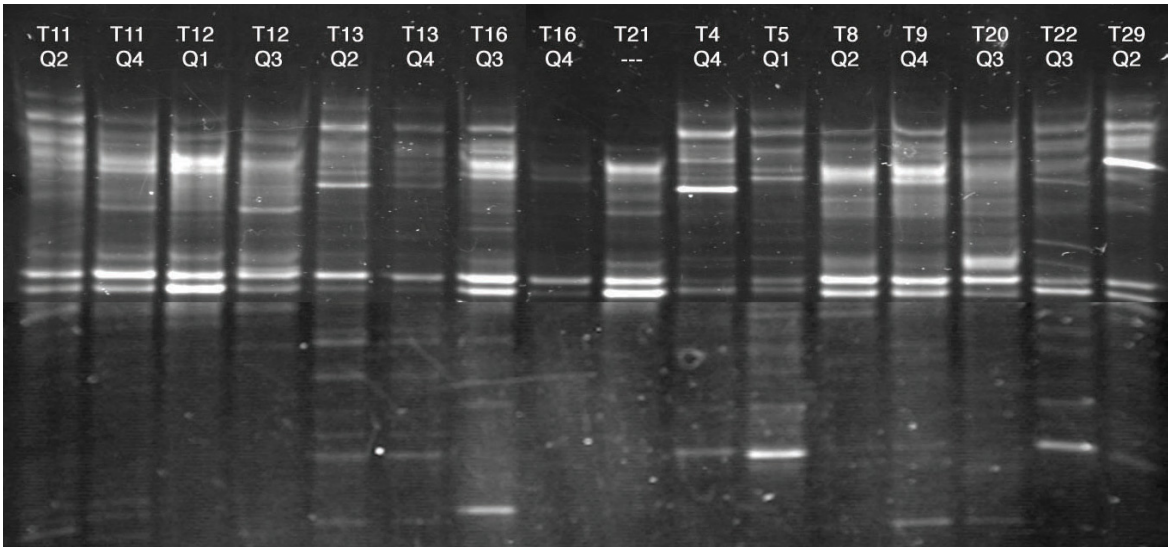

Figure 3: DGGE profiles of microbial biofilm communities colonizing the TAMS. The colonizer and quadrant are designated as T# Q#.

Foundation species, including siboglinid tubeworms and bathymodiolin mussels, colonized TAMS in both diffuse-flow and bare basalt habitats. For the TAM deployed in the bare basalt habitat that was colonized by both tubeworms and mussels, the maximum recorded temperature was 18.6°C; and for the TAM colonized by mussels only, the maximum recorded temperature was 5.2°C.

Among TAMS for which the siboglinid tubeworm colonists were identified to species, *Tevnia jerichonana* was identified on every TAM and had the greatest relative abundance (Table 4). As many as two individuals of the siboglinid tubeworm species *Riftia pachyptila* were identified on three TAMS, and one

individual *Oasisia alvinae* was identified on two TAMS. One larva of the mussel *Bathymodiolus thermophilus* was identified on each of six TAMS, at Tamtown only.

Table 4. Quantities of macrofaunal eggs and larvae embedded in the bacterial biofilms for each TAMS colonizer.

	9	**12**	**16**	**4**	**20**	**29**
Riftia pachyptila	1	2	2	0	0	0
Tevnia jerichonana	15	19	50	0	9	0
Oasisia alvinae	0	1	0	0	0	0
unidentified vestimentiferans (total)	5	4	32	0	0	0
Archinome rosacea	0	0	0	4	0	0
Amphisamytha galapagensis	3	2	2	1	0	0
Galapagomystides aristata	0	0	1	0	0	0
Hesiospina vestimentifera	4	0	0	1	0	0
Paralvinella pandorae	0	5	3	0	4	0
Prionospio sandersi	0	19	29	0	0	0
Ophyrhotrocha akessoni	128	221	251	258	18	1
TAM worm	16	0	8	17	0	0
Branchinotogluma hessleri	0	0	0	0	0	0
Lepidonotopodium williamsae	3	5	3	4	0	3
Polynoid sp. nov.	0	0	0	1	0	0
juvenile (non-vestimentiferan) polychaetes	4	7	30	6	0	0
mystery worm (not a polychaete)	0	0	1	0	0	0
Bathymodiolus thermophilus	1	0	0	1	0	0
Cyathermia naticoides	0	0	0	0	0	0
Clypeosectus delectus	8	0	0	14	0	1
Eulepetopsis vitrea	4	0	0	5	0	1
Gorgoleptis spiralis	2	0	1	30	0	1
non-Lepetodrilid juvenile gastropods	0	0	0	43	0	2
Lepetodrilus elevatus	147	1212	837	82	2	0
Lepetodrilus tevniatus	248	1437	1587	46	0	0
Lepetodrilus c.f. pustulosus	0	0	0	0	0	0
Lepetodrilus juveniles	163	206	312	239	0	117
Amphipod sp. 1	0	0	0	0	0	0
Ventiella sulfuris	4	53	58	0	283	2
Dahlella caldariensis	0	0	0	0	3	0
Copepods	63	0	15	695	438	72
Ostracods	21	0	6	234	0	34
Platyhelminthes	3	19	8	3	2	0
Nemertean	0	6	0	0	0	0
Sipunculid	0	0	0	0	0	0
Aplacophoran	0	3	14	1	0	0
Ophiuroid	0	0	0	0	0	0

TAMS bacterial colonists. The microbial community was characterized for 6 TAMS (Table 3 and Figure 5). Strong correlations among specific microbial groups and macrofaunal species were found. Organisms most closely related to *Gammaproteobacteria* of the genus *Leucothrix* were the numerically dominant bacterial group or species on TAMS in no flow area that were not colonized by siboglinid tubeworms and were almost completely absent on TAMS that were colonized by tubeworms (Figures 4 and 5). Microbes closely related to the *Epsilonproteobacterium Sulfurovum lithotrophicum,* were present on all TAMS colonized by tubeworms and were almost completely absent in TAMS that were not colonized by tubeworms. In contrast, other *Sulfurovum* species were relatively abundant among all TAMS, both colonized and not colonized by tubeworms. Other groups of bacteria that were present on at least one TAM from either diffuse-flow or no-flow include the phylum *Bacteroidetes* and the classes *Alphaproteobacteria* and *Deltaproteobacteria*. None of these samples aligned close enough to a known pure culture isolate (>95%) to assign a genus or species (data not shown). Thirteen out of the 323 clones were determined to be chimeras and removed from the phylogenetic analysis. The remaining 310 clones fell into 131 RFLP fingerprints – with some duplicates between biofilm samples.

Temperature and chemistry of hydrothermal fluids. Data loggers recorded temperatures directly above the mesh of each TAMS. Four of the 24 data loggers failed, but the working data loggers recorded temperatures during the course of the full deployment. The maximum temperatures ranged from 3.1 to 26.9°C, and the minimum temperatures ranged from ambient seawater

temperatures (1.8°C) to 3.0°C (see Table 2 for Dr. Luther's findings). The average, median, maximum, and minimum recorded temperatures did not differ significantly by site or by habitats at Tamtown, but all four metrics of temperature variation were significantly greater in the diffuse-flow habitats than the bare basalt habitats at Marker 19.

The *in situ* electrochemical and temperature sensor ("wand") did not record temperatures as high or as low as those recorded by the data loggers, possibly due to the extreme spatial variability and the height difference between the data logger that was attached to the frame of the TAM and positioned directly above the mesh and the wand that was held by the manipulator arm of the submersible directly above (< 1 cm) the mesh. The maximum measured H_2S concentrations were as high as 103.7 μM, and like temperature, there were no significant differences between sites or between habitat types at Tamtown, but H_2S concentrations were significantly greater in the diffuse-flow habitats than the bare basalt habitats at Marker 19 (Table 2; t_{avg} = -11.997, p = 0.0012). The maximum measured O_2 concentrations among TAMS ranged from 46.5 to 103.0 μM, and the minimum O_2 concentrations ranged from non-detectable to 79.6 μM. Thus for some TAMS, the minimum O_2 concentrations were greater than the maximum O_2 concentrations for other TAMS. The O_2 concentrations were also significantly greater at Marker 19 than Tamtown (t_{avg} = 13.238, p < 0.0001; t_{max} = 10.371, p < 0.0001; t_{min} = 4.388, p = 0.0163) and significantly greater in the basalt habitat type than the diffuse-flow, but only at Marker 19 (t_{avg} = 15.687, p < 0.0001; t_{min} = 2.78, p = 0.032). All temperature

and chemical calculations were reported to us by Dr. Luther and his team at the University of Delaware.

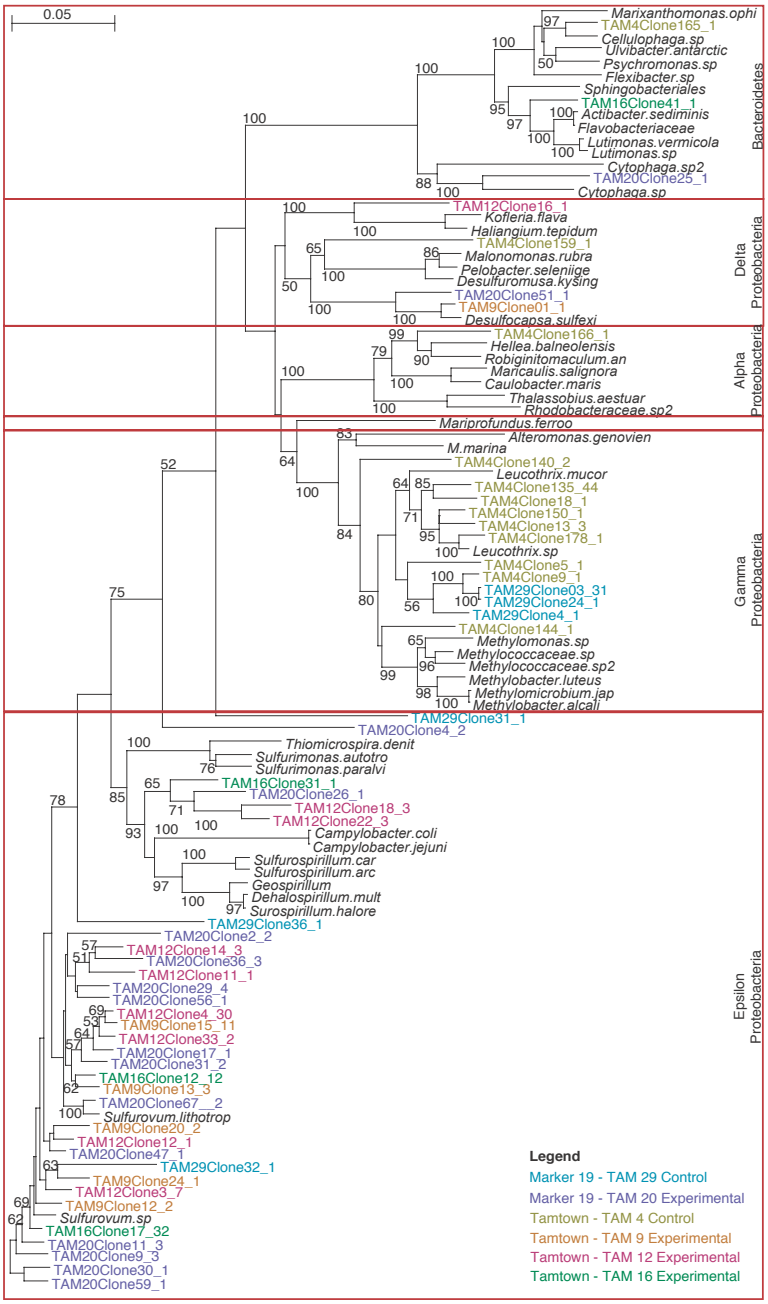

Figure 4. Phylogenetic analysis of bacterial 16S rRNA gene sequences from bacterial biofilm communities at 9ºN in the EPR. The tree was constructed using the neighbor-joining method from a similarity matrix based on the Jukes-Cantor distance model. Most of the clones had greater than 1300 basepairs of unambiguous sequence. Representative sequences of 16S rRNA genes obtained in this study are highlighted in color based on their colonizer of origin. The number of replicates found for each sequence are listed after each clone number.

Discussion

This study represents one of the first attempts to find a link between the environment, bacterial communities, and the macrofauna associated with the vent ecosystem at an early stage of colonization. The hydrothermal vent ecosystem develops by first having chemosynthetic bacteria attach to the basalt substrates in proximity of the vent emissions, which provide the microorganisms with energy and carbon sources (1). The macrofauna later colonize and may use the same pioneer bacteria as endo- or epi-symbionts (8; 72; 79). The vent emissions are marked by higher temperature and higher concentrations of sulfur species than the ambient seawater (75; 162). Because of chemical shifts from water mixing, there is a steep gradient of sulfur concentration, diffused oxygen and temperatures (107). Our sample locations at Tamtown and Marker 19 follow similar patterns to other vent systems. We made the prediction that changes in sulfur species concentrations and temperature would alter the bacterial community composition, allowing the macrofauna to colonize. The local chemical and physical characteristics would then be assumed to drive the microbial population (83; 93). As the ecosystem develops, the initial bacterial biofilms co-develop with the macrofauna colonizing the area (28). This interaction and development was our main focus in our work here. As the ecosystem does shift during development, it was imperative for us to have a zero time point. The OBS warnings and data of the 2005-2006 eruptions gave us this opportunity (157). Rapid response dives at EPR 9^{o}N (23) give us the opportunity to study the developing microbial biofilms before the macrofauna invaded the area. In this study we report a comparison of the bacterial communities from diffuse-flow

(directly exposed to hydrothermal fluids) and no-flow (not directly exposed to vent fluids) sites. This data was then correlated to the concentration of sulfur and the presence of tubeworm colonists.

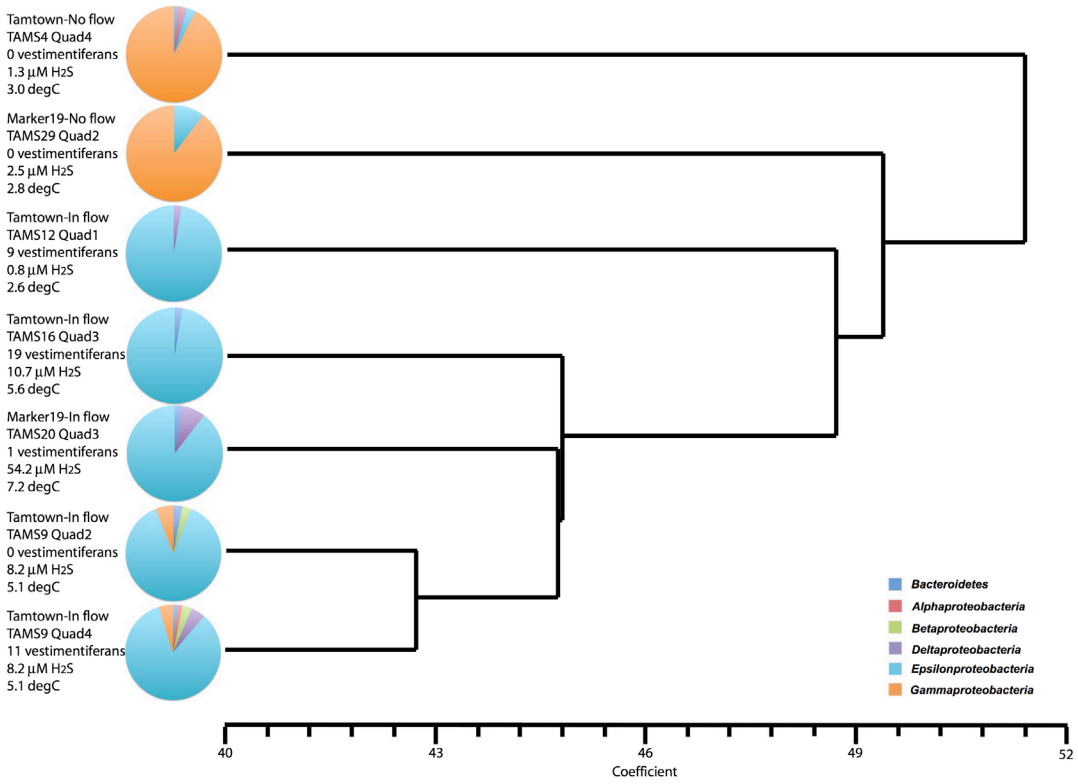

Figure 5. Dendrogram showing the relatedness of each biofilm community. Each community is associated with the location, experiment, TAMS designation, number of tubeworm colonists found on the mesh, the concentration of hydrogen sulfide and temperature of the surrounding seawater. The pie charts depict the relative percentages for each class of bacteria found in the community.

The 16S rRNA gene sequences that were shotgun cloned provide a general picture of the bacterial communities. Previous studies on this ecosystem do show the same trend of *Epsilonproteobacteria* dominating the diffuse-flow vents and *Gammaproteobacteria* replacing the former in region not affected by geothermal activity (1; 78; 148). There was a clear similarity between samples from diffuse-flow and no-flow sites, with the diffuse-flow biofilms containing around 90% or greater

Epsilonproteobacteria and the no-flow communities containing around 90% *Gammaproteobacteria* (Figure 5). Even if only the dominant members of each biofilm community were detected, this general picture is still useful to infer associations with environmental parameters and invertebrates. Further studies using deep sequencing technologies may be used for getting a more complete picture of microbial diversity from diffuse-flow or no-flow sites.

The 16S rRNA gene libraries show a clustering pattern where the diffuse-flow and no-flow biofilms are more similar to each other, respectively (Figure 5). *Epsilonproteobacteria* dominated all the diffuse-flow biofilms from the TAMS 9, 12, 16, and 29 colonizers (Figure 5). When the environmental factors for diffuse-flow and no-flow samples (i.e. TAMS 9, 12, and 16 vs. 4 at Tamtown and TAMS 20 vs. 29 at Marker 19) are compared to the community composition, there is a clear relationship. In each case, the *Epsilonproteobacteria* were dominant in the samples within a higher temperature and H_2S concentration environment. This supports the conclusion that chemosynthetic *Epsilonproteobacteria*, mostly relating to the genera *Sulfurovum* (Figure 4), are probably driven by a combination of elevated temperature (compared to ambient bottom seawater) and concentration of hydrogen sulfide. The almost complete absence of these organisms from the no-flow vents is most likely related to the strong dominance of heterotrophs in the communities. Recent comparisons of other vents environments show similar community distribution to our samples at EPR 9^{o}N (1; 78; 148).

It was interesting that the *Epsilonproteobacteria* were dominating diffuse-flow biofilms at both sites. The lower concentrations of sulfide at Tamtown (as

compared to Marker 19) was indicative that the Tamtown vents were beginning to die (86). This was confirmed upon visual inspection at the collection times, where the amount of hydrothermal fluids being expelled was visually decreased. Generally, the percentage of *Epsilonproteobacteria* in a microbial biofilm decreases when the flux of vent fluids decrease and the vent dies (148). However, the biofilms at the Tamtown diffuse-flow community had just as much or even a higher percentage of *Epsilonproteobacteria* than the Marker 19 diffuse-flow biofilm (Figure 5).

Vestimentiferan tubeworms colonized TAMS that were deployed among recent vestimentiferan colonists on basalt and on "bare" basalt that appeared to be uncolonized by any sessile megafauna. Vestimentiferans only colonized TAMS with *Epsilonproteobacteria* biofilms and maximum measured temperatures > 18°C and did not colonize TAMS with maximum measured temperatures < 5°C (Table 4). Non-vestimentiferan tubeworm larvae were found outside of flow. This suggests that vestimentiferan tubeworms are either relying on nutrition from chemoautotrophic bacteria or that there were periods of exposure to hydrothermal fluids. Mussels only colonized TAMS at Tamtown (on colonized and uncolonized basalt), where the hydrothermal fluid flux apparently decreased over the 6-month duration of the experiment. This supports the theory that macrofaunal succession is driven by changes in microbial biofilm communities as the vent fluids fluctuate or diminish (87; 114; 148).

The control samples from Tamtown TAMS 4 and Marker 19 TAMS 29 showed evidence of heterotrophic *Gammaproteobacteria* dominating the biofilms (Figures 4 and 5). The most abundant hits were related to the organism *Leucothrix mucor* (10).

Leucothrix is a close relative of the marine organisms *Beggiatoa* and *Thiothrix* (45; 168). While all three are known for forming filamentous mats close to sulfide deposits (168), *Beggiatoa* and *Thiothrix* have extremely versatile metabolism as they can function as autotrophs, heterotrophs, and mixotrophs depending on the conditions, while *Leucothrix* is predominantly heterotrophic (37; 45; 115; 168). *Leucothrix* and *Thiothrix* also known for their interactions with marine macrofauna (10; 34). While many *Gammaproteobacteria* and *Leucothrix* species are known for their beneficial relationships, *Leucothrix mucor* is known to have parasitic tendencies by disrupting egg and larval development in many higher trophic marine species (65). This may be the same case for vestimentiferans colonists embedding themselves into bacterial biofilms that we see here. The eggs and larvae may colonize a no-flow biofilm, but fail to develop because of the high incidence of *Leucothrix mucor*.

Epsilonproteobacteria are known to be epibionts of the hydrothermal vent tubeworms, *Alvinella pompejana*, and can form biofilms on the external surface of the tubes in other species (44; 94; 120; 147). The vestimentiferans found in this study were embedded in the bacterial biofilms. However, this only occurred in the *Epsilonproteobacteria* dominated diffuse-flow biofilms. Our findings support previous conclusions on tubeworm development (57). Horizontal endosymbiont transmission refers to the tubeworms having an undeveloped trophosome when they are born (117). They acquire their symbionts in the larvae stages of development (117). Seeing as the vestimentiferans were embedded in the diffuse-flow biofilms that contained low quantities of *Gammaproteobacteria*-type

endosymbionts, the tubeworms must be utilizing a filter process of selecting a specific bacterium to develop symbiotic relationships with. These symbionts may come from a very small component of the community or from the hydrothermal fluids diffusing into the environment (44).

In each of the two TAMS 9 quadrants analyzed, there was a single close match (~97% sequence identity) to a *Leucothrix* species. Even though this type of *Gammaproteobacterium* might be detrimental to either egg or larval development (66), vestimentiferans worms were able to colonize the biofilm. The other diffuse-flow TAMS colonizers, 12, 16 and 20, may also have a *Gammaproteobacteria* component that was not detected. This suggests that the percentage or abundance of filamentous heterotrophs has a greater effect on larval development than just their presence. The higher concentrations of sulfur species and lower concentrations of oxygen in diffusing environments allows for a dominance of chemosynthetic *Epsilonproteobacteria*. Because the species like *Leucothrix mucor* are outgrown, the tubeworm eggs and larvae may have the time needed for their initial stages of development.

Acknowledgements

This work was supported by National Science Foundation grants OCE-0327261, OCE-0451983, and OCE-0451983 to TMS), OCE-9529819 (to RAL), OCE-0327353 (to RAL and CV), MCB-0456676 (to CV), and OCE-03264634 (to GWL), and the Office of Ocean Exploration of the National Oceanic and Atmospheric Administration, grant NA04OAR4600084 (to TS), as well as by the Deep Ocean

Exploration Institute of the Woods Hole Oceanographic Institution (to TS and BG). We also wish to express our gratitude to the Captain and crew of the R/V Atlantis and the pilots and crew of the DSV Alvin, as well to Craig Cary, Karen Von Damm, and the shipboard scientific parties of the AT11-0, AT11-09, AT11-10, AT11-27, AT15-6, AT15-13, and AT15-15 cruises.

Chapter 3 –Detection of gene transcripts for autotrophic carbon fixation and respiratory metabolism in pure cultures and natural biofilms from deep-sea hydrothermal vent

Introduction

Studies have shown that *Epsilonproteobacteria* dominate bacterial biofilms in both diffused and focused flow hydrothermal vent systems (1; 12; 78). It is the general consensus that these organisms are the initial pioneers at newly formed vents (1; 15). Surveys of microbial diversity, based on analyses of the 16S rRNA gene, indicated that the *Epsilonproteobacteria* genera *Sulfurovum* and *Sulfurimonas* are the most abundant in lower temperature biofilms (1; 78). In the high temperature biofilms, the dominant *Epsilonproteobacteria* are from the genera *Nautilia* and *Caminibacter* (165). Studies of pure cultures of *Epsilonproteobacteria* and their genomes showed that these bacteria use the reductive tricarboxylic cycle (rTCA) to fix CO_2 and conserve energy by coupling the oxidation of reduced sulfur species and/or H_2 with the reduction of nitrate, oxygen or elemental sulfur (12; 108).

The rTCA cycle contains ten reaction steps, utilizing many of the same enzymes from the Krebs cycle (Figure 1 (56; 131)). The only three steps that are unique to the rTCA cycle are citrate to oxaloacetate and acetyl CoA, fumarate to succinate, and 2-ketogluterate to isocitrate (131). The unidirectional step that converts citrate to oxaloacetate and acetyl CoA is catalyzed by the ATP dependant citrate lyase enzyme, which is encoded by the *aclA*/*B* gene (56; 131). Hence, the *aclA*/*B* gene can be used as a diagnostic marker for autotrophic CO_2 fixation via the

rTCA cycle (11). Several studies have characterized ATP citrate lyase enzymatic activity in pure cultures and *aclA* or *B* phylogenetic distribution in vent *Epsilonproteobacteria* (Table 1) (48; 55; 56; 149; 165). However, we are not aware of *in situ* expression studies of the *aclA/B* in vent biofilm communities.

Table 2 Specific activities [nmol min^{-1} (mg cell protein)$^{-1}$] of enzymes of the reductive TCA cycle in *C. mediatlanticus*

Enzyme activity tested	*Caminibacter mediatlanticus*
Assay temperature (°C)	55
ATP citrate lyase	275
2-Oxoglutarate:BV oxidoreductase	330
Pyruvate:BV oxidoreductase	160
Fumarate reductase (BV)	710
Isocitrate dehydrogenase (NAD)	45
Isocitrate dehydrogenase (NADP)	7,800
Malate dehydrogenase (NADH)	4,080
2-Oxoglutarate dehydrogenase (NAD)	n.d.
2-Oxoglutarate dehydrogenase (NADP)	n.d.
Pyruvate dehydrogenase (NAD)	n.d.
Pyruvate dehydrogenase (NADP)	n.d.

Mean values were obtained from at least five measurements. Standard errors were less than ±20%. n.d., no activity detected, detection limit <1 nmol min^{-1} (mg cell protein)$^{-1}$

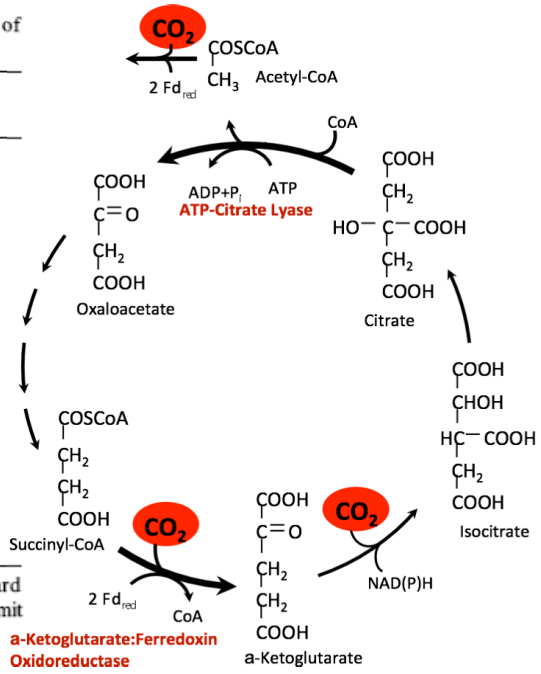

Figure 1: Previous studies involving autotrophic carbon fixation in pure culture isolates. (left) Enzyme activity assays reported from *C. mediatlanticus* cell lysates (table was taken from (165)). (right) Diagram of the reaction steps of the rTCA cycle (56).

In order to gain the energy for CO_2 fixation, the *Epsilonproteobacteria* can perform anaerobic respiration using nitrate as a terminal electron acceptor. Denitrification is the reduction of nitrate to dinitrogen gas via a multi step pathway (Figure 3) (167; 172). Many mesophilic vent organisms have this general denitrification ability (Figure 2) (111; 139). However, thermophilic vent *Epsilonproteobacteria* reduce nitrate to ammonia (Figure 2) (35; 139), a process called dissimilatory reduction of nitrate to ammonia (DNRA) (172). The first step in

both mesophilic and thermophilic pathways is the reduction of nitrate to nitrite, which is catalyzed by two nitrate reductases: the periplasmic nitrate reductase (*nap*) and the membrane-bound nitrate reductase (*nar*) (Figure 3). The genome sequences of several *Epsilonproteobacteria* has shown that these organisms only encode for the periplasmic nitrate reductase, *napA* (14; 35; 111; 138; 140).

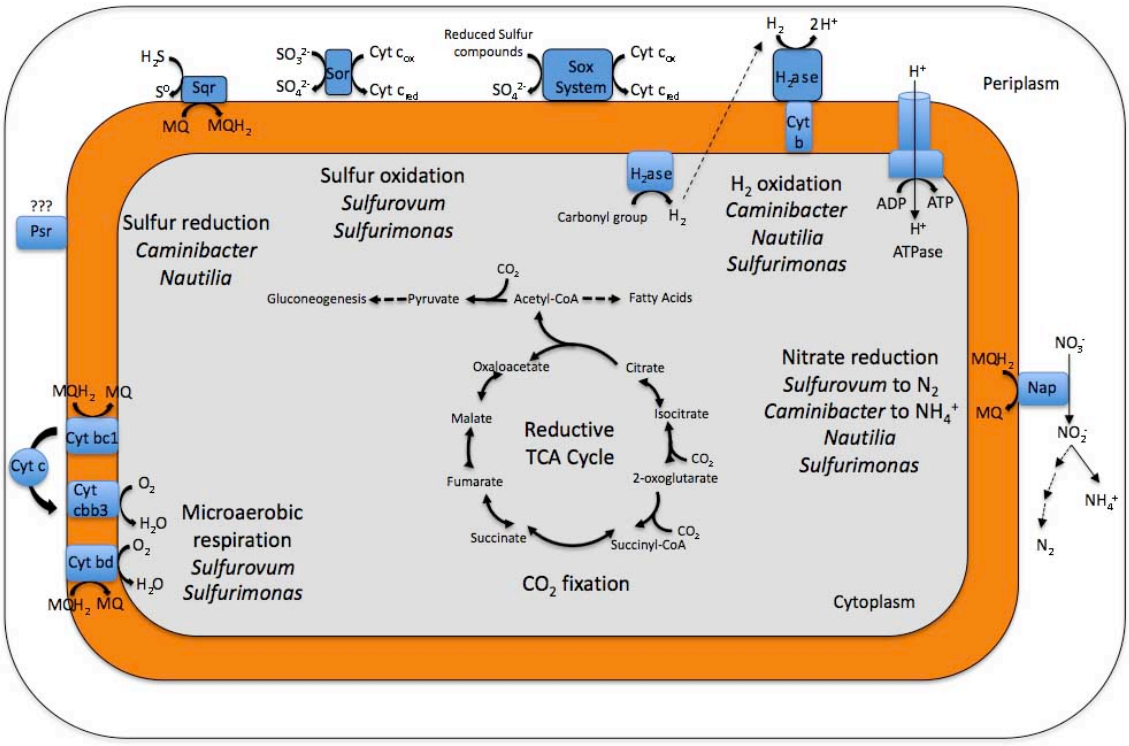

Figure 2: Central metabolic pathways in *Epsilonproteobacteria*. The genomes included come from two mesophilic organisms, *Sulfurovum* sp. NBC37-1 and *Sulfurimonas autotrophica*, and two thermophilic organisms, *Nautilia profundicola* Am-H and *Caminibacter mediatlanticus* TB-2 (35; 111; 140).

Other than respiring nitrate, some vent *Epsilonproteobacteria* microaerobically use O_2 as a terminal electron acceptor. Most proteobacterial oxygen respiration is mediated through a cbb3-type cytochrome oxidase (*cco*) coupled reaction (122). The microaerobic vent *Epsilonproteobacteria* utilize the cbb3-type cytochrome oxidase (118; 139; 158). While most of thermophilic

Epsilonproteobacteria are strict anaerobes, *Hydrogenimonas thermophila*, *Nitratiruptor tergarcus*, and *Caminibacter profundus* can also respire oxygen (101; 110; 151). The only information that we have on vent *Epsilonproteobacteria* cytochrome oxidase derives from the few available genome sequences (Figure 2) (111; 138), which include the *cco* gene families. However, none of the thermophilic microaerobic *Epsilonproteobacteria* have been sequenced. The work presented here is the first look at both the phylogenetic diversity and the expression of the cbb3-type cytochrome oxidase gene *cco* in hydrothermal vent organisms.

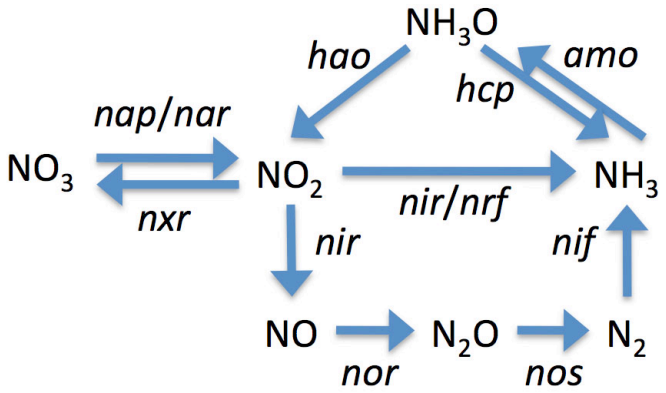

Figure 3: Nitrogen cycle modified from the KEGG Pathway Database.

Reduced sulfur species play a critical role in the respiratory metabolism of vent microorganisms. The reconstruction of possible respiratory pathways based on the genome sequence of vent *Epsilonproteobacteria* revealed at least three possible sulfur oxidation enzymes: thiosulfate oxidase (*sox*), sulfite oxidase (*sor*), and sulfide quinone reductase (*sqr*) as well as a possible polysulfide reductase (*psr*) that may be involved in sulfur reduction (Figures 2 and 4) (3; 31; 144; 153). Previous work showed that the main function assigned to the sulfide quinone reductase is oxidizing hydrogen sulfide to elemental sulfur (42). The *sqrA* gene (encoding for the sulfide quinone reductase) is found in the genomes of both mesophilic (e.g., *Sulfurovum*

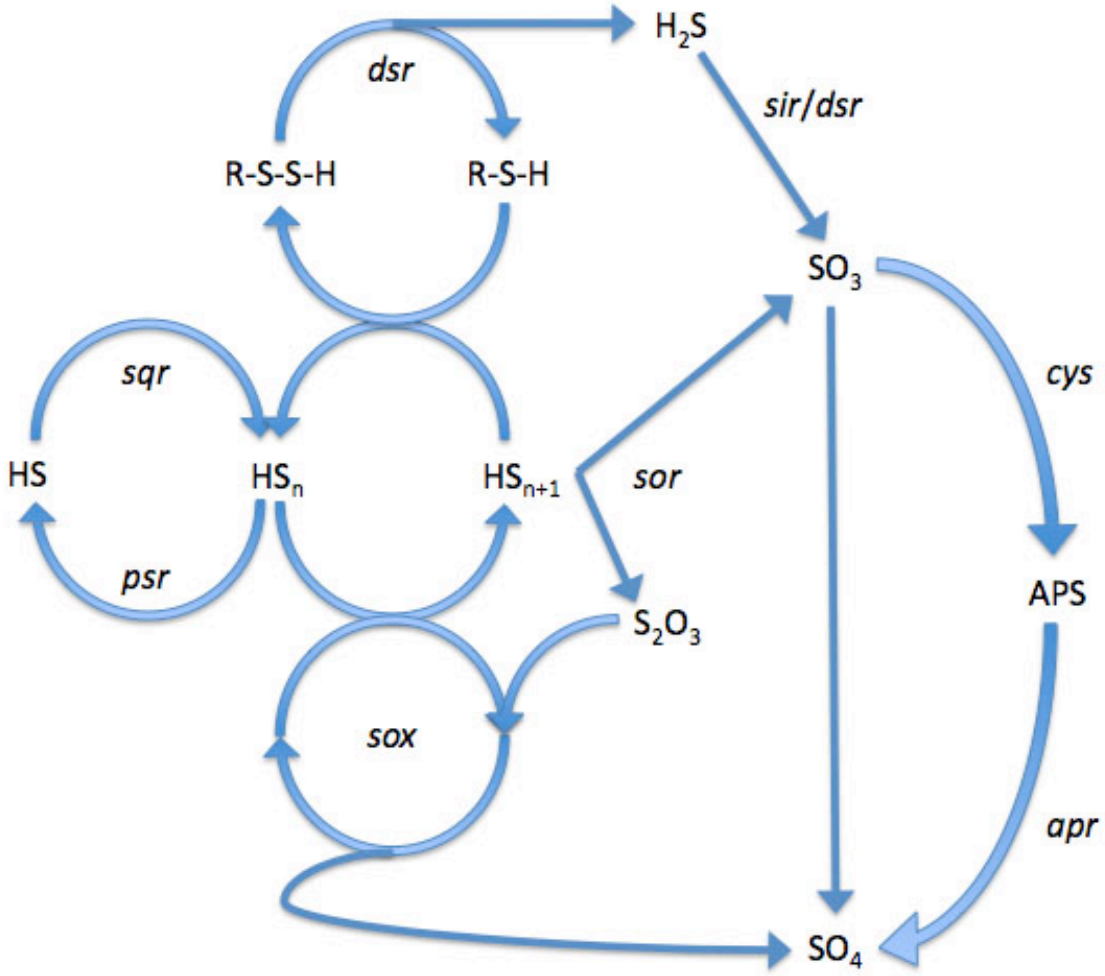

Figure 4: Possible reconstruction of the sulfur cycle in deep-sea vent organisms. Pathways were assembled using information on the KEGG Pathway Database and literature referring to sulfur reduction and oxidation (9; 41; 126; 171).

lithotrophicum) and thermophilic (e.g., *Caminibacter mediatlanticus*) *Epsilonproteobacteria* (Figure 2) (35). However, the *sqrA* gene from *S. lithotrophicum* and *C. mediatlanticus* have only about 52% sequence identity, suggesting that the two enzymes might have different functions in the two organisms. It is reasonable to hypothesize that the sulfide quinone reductase catalyzes sulfide oxidation in the microaerobic *S. lithotrophicum,* while in the anaerobic *C. mediatlanticus* the enzyme might be involved in the reduction of elemental sulfur to sulfide. Since most of the studies on sulfide oxidation in vent

organisms are focused on the thiosulfate oxidase (*sox*) or the sulfite oxidase (*sor*) (121; 149), I decided to provide new insight into the sulfur cycle by investigating the expression of *sqrA* gene in pure cultures of *Epsilonproteobacteria* and natural biofilm communities. Another important aspect of the sulfur cycle involves in the reduction of sulfate through adenylylsulfate (APS) reductase (*apr*) (Figure 4). The APS reductase, combined with APS kinase (*cys*) forms a reversible two-step reaction from sulfate to sulfite (97). APS reductase is found in the vent *Gammaproteobacterium Thiomicrospira thermophila*, however it is not present in *Epsilonproteobacteria* (Table 1) (149). Since many vent organisms contain the *apr* genes (3; 97), I decided to assess which organisms express this gene by performing a survey of the *apr* transcript in the biofilm communities.

Epsilonproteobacteria encode for hydrogen sensing, uptake and evolving hydrogenases. The NiFe-type hydrogenase, encoded by the *hyn* gene, is a hydrogen uptake hydrogenase that couples hydrogen oxidation to the reduction of nitrate, oxygen, and oxidized sulfur species for respiration (108; 145). Takai *et. al.* (2005), found hydrogenase activity in cell lysates of mesophilic (*Sulfurimonas paralvinellae*) and thermophilic (*Lebetimonas acidophila*) hydrogen oxidizing *Epsilonproteobacteria* (Table 1) (149), and the *hyn* gene is found in the genomes of these organisms and other hydrogen oxidizing *Epsilonproteobacteria* (Figure 2) (35; 138). Hence, detection of the *hyn* gene transcripts allows for the identification of active hydrogen oxidizing *Epsilonproteobacteria* in vent natural biofilm communities.

Recent studies including vent *Epsilonproteobacteria* focused on physiology and genome analyses of pure cultures (35; 111; 138), along with the detection of the diagnostic gene for CO_2 fixation via the rTCA cycle, *aclAB* (149; 164; 165) in natural communities. However, I am not aware of studies that investigated the *in situ* function of *Epsilonproteobacteria*-dominated vent biofilm communities. To fill this knowledge gap, my goal was to capitalize upon what is known from pure cultures to investigate gene expression in the biofilm communities collected from two diffuse flow vents characterized by temperatures regimes within 10-28 °C and 20-50 °C range, respectively. I hypothesize that, during the formation of these biofilms, *Epsilonproteobacteria* fix carbon dioxide via the reductive tricarboxylic acid cycle (rTCA) and express genes involved in several respiratory pathways in response to different temperature and redox regimes (i.e., hydrogen and sulfide oxidation coupled to nitrate and/or oxygen reduction, respectively).

Materials and methods

Biofilm sample collection. Experimental microbial colonizers (Figure 5) were deployed and collected from the East Pacific Rise (EPR) during dives in 2006, 2007 and 2008. For the purpose of this study, I have focused on the biofilm communities that developed on two microbial colonizers exposed to different temperature and biological regimes (Table 2). The microbial colonizer designated CV9 was deployed on a post-eruptive, diffuse-flow vent on the EPR at 9°N. The CV41 colonizer was deployed on the side of a polymetallic sulfide structure on the EPR at 13°N diffusing hydrothermal fluids. Table 2 summarizes the characteristics of the

Table 1. Detection of genes and resulting enzymatic activity for autotrophic carbon fixation and hydrogenase in pure culture vent bacteria (modified from (149)).

	Hydrogenimonas thermophila	*Sulfurimonas autotrophica*	*Sulfurimonas paralvinellae*	*Lebetimonas acidophila*	*Sulfurovum lithotrophicum*	*Nitratiruptor salsuginis*	*Thioreductor micantisoli*
Amplification of the following genes from genomic DNA							
aclB	+	+	+	+	+	+	+
hynSL	+	-	+	+	-	+	+ (only *hynL*)
Activity of the indicated enzymes (nmol of product min^{-1} mg^{-1})							
Citrate lyase	386 ± 40	222 ± 45	14.5 ± 1.8	375 ± 30	20.8 ± 3.2	73.0 ± 8.2	147 ± 18
H_2 Oxidation	32400 ± 740	ND	2180 ± 220	22500 ± 1200	ND	1700 ± 250	97400 ± 8000

Table 2: Sample sites used in this study

Colonizer	Site	Age	Temp	Depth	Location
CV9	9°N	7 day	10-28 °C	2506 m	Diffuse flow vent
CV41	13°N	3 day	20-50 °C	2621 m	Side of black smoker chimney

Table 3. Characteristics of selected pure culture isolate *Epsilonproteobacteria*

Organism	Isolated from	Optimum Temp °C	Electron donors	Electron acceptors	Reference
Caminibacter mediatlanticus	MAR, Rainbow, Chimney	55	H_2	NO_3^-, S^0	(166)
Sulfurimonas paralvinellae	MOT, Iheya, *Paralvinella*	30	H_2, $S_2O_3^=$, S^0	NO_3^-, O_2	(152)

two sites: The 9°N vent (CV9 biofilm) had temperatures between 10-28 °C and no invertebrate colonization, while the 13°N vent (CV41 biofilm) had temperatures between 20-50 °C and it was colonized by *Alvinella pompejana* tubeworms. Upon collection, the stainless steel meshes were removed from the solid support. Both the top and bottom portions of the colonizers were treated in RNAlater, a solution that allows the preservation of biomass and RNA.

***Epsilonproteobacteria* strains and conditions**. As shown in Table 3, the strains used in this study were a thermophilic *Epsilonproteobacterium, Caminibacter mediatlanticus* TB-2 (166), and a mesophilic *Epsilonproteobacterium*, *Sulfurimonas paralvinellae* (152). *C. mediatlanticus* was grown at 55 ^{o}C in HB-1 medium pH 5.5 with H_2/CO_2 gas in the headspace. *S. paralvinellae* was grown at 30 ^{o}C in MJ-N medium supplemented with KNO_3, NaS_2O_3, NaH_2CO_3 and tungstic acid under H_2/CO_2. Each organism was grown to exponential phase. For the purpose of these experiments, *C. mediatlanticus* was grown with H_2/CO_2 and KNO_3 or H_2/CO_2 and S^0. *S. paralvinellae* was grown with $S_2O_3^=$, H_2/CO_2 gas and KNO_3; $S_2O_3^=$ and $H_2/CO_2/O_2$; S^0, N_2/CO_2 and KNO_3; or $S_2O_3^=$, N_2/CO_2 and KNO_3. All redox couples tested are listed in Table 4.

RNA extraction. For biofilm community analysis, total RNA was extracted from the frozen samples stored in RNAlater solution. The steel meshes were thawed briefly just to the point where pieces of the biofilm could be removed. The RNA was then extracted using the RNAeasy kit (Qiagen) according to the manufacturer's protocol. For pure cultures, RNA from the late exponential phase was extracted by first pelleting the cells and then performing an extraction using the RNAeasy kit. For

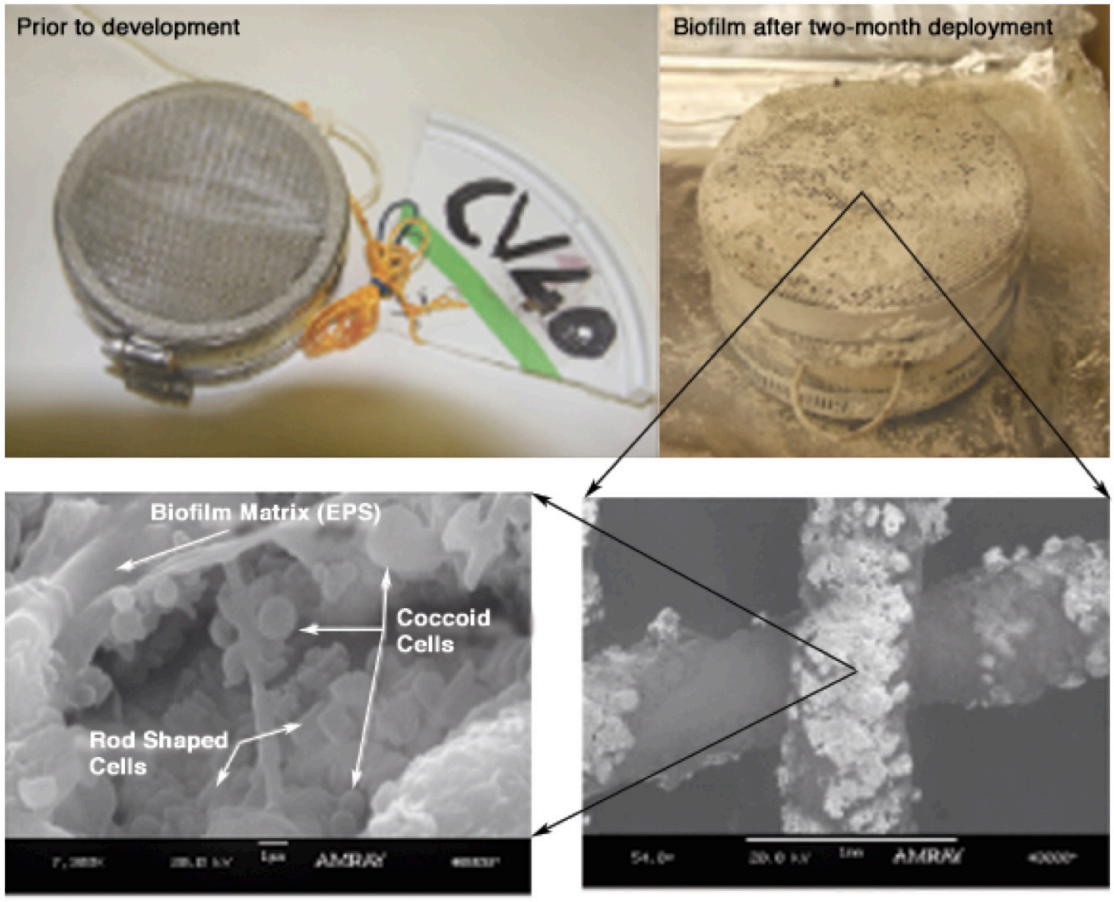

Figure 5: Biofilms forming on mesh colonizers. (Top) The stainless steel mesh colonizer before and after deployment. Hydrothermal fluids from diffuse flow vents travel through the mesh and allow microbial biofilms to attach. (top and bottom right). A SEM close up of the biofilm attached to the mesh (bottom left) showing individual cells, possibly embedded in EPS.

Table 4. Growth Conditions (Expected results from literature/Experimental result)

	H_2/NO_3^-	H_2/S^0	$S_2O_3^=/NO_3^-$	S^0/NO_3^-	H_2/O_2	$S_2O_3^=/O_2$
Caminibacter mediatlanticus	**+/+**	**+/+**	**-**	**-**	**-**	**-**
Sulfurimonas paralvinellae	**+/+±**	**-**	**+/-**	**+/+**	**+/+±**	**+/ND***

* The $S_2O_3^=/O_2$ growth condition for *S. paralvinellae* was not tested.
± Culture contained $S_2O_3^=$ in addition to the redox couple listed.

these samples, the amount of reagents was scaled depending on the size of the pellet. At minimum, twice the amount of lysozyme, RLT and ethanol was used for resuspension and lysis steps. For cultures containing S^0, up to 6 times the amount of lysozyme, RLT and ethanol were utilized, as well as a step for removing particulate sulfur. In each case, the entire lysed sample was loaded on to a single spin column after multiple spins. The rest of the extraction was performed using the manufacturer's protocol. Residual genomic DNA was removed from all samples with the TURBODNAse kit (Ambion). The only modification to the protocol was incubating twice for 30 min at 37 ^oC adding 0.5 μl of DNAse before each incubation. The samples were further checked for residual DNA contamination by PCR with bacterial 16S rRNA gene primers. PCR conditions for 16S rRNA gene amplification reactions were as follow: 35 cycles of denaturation at 94 ^oC for 30 s, annealing at 50 ^oC for 30 s, and extension at 72 ^oC for 30 s with a final extension time of 5 min.

Metatranscriptome pyrosequencing. The steps for the preparation of the total cDNA from the two biofilm communities for 454 pyrosequencing for metatranscriptome analysis were performed by Melitza Crespo-Medina and Jessica Ricci, two former members of the laboratory. However, since this part of the work on vent biofilms is relevant to my own work, I will briefly describe the procedure. Basically, RNA samples were enriched for mRNA using two procedures. The first procedure utilizes an exonuclease specific for rRNA in the mRNA-ONLY mRNA isolation kit (Epicentre). The second procedure polyadenylates and amplifies the mRNA with MessageAmp II Bacteria Kit (Ambion). Using both procedures effectively removes >95% of the rRNA transcripts (according to a personal communication

with EdgeBio, Gaithersburg, MD). In order to perform pyrosequencing on the samples, the RNA was reverse transcribed to cDNA. The cDNA was quantitated and shipped out to the University of Oklahoma for pyrosequencing.

Reverse transcription PCR. The reverse transcription and PCR reactions were performed utilizing the One-Step Reverse Transcription kit (Invitrogen). The positive control for the RT-PCR reactions was amplification of each gene using either *S. lithotrophicum* or *C. mediatlanticus* genomic DNA and the same PCR conditions. After each reaction was mixed, 10 µl was removed and placed in a separate tube to be run without the reverse transcription step (30 min hold at 55 ^{o}C) as a no-RT control. The reactions were set up according to the manufacturer's protocol with the exception of the primers and annealing temperatures adjusted for each functional gene. The primer sequences and PCR conditions are summarized in Table 5.

Construction of clone libraries. Immediately upon completion of the RT-PCRs on biofilm community samples, the products were sub-cloned into pCR4-TOPO using a TOPO-TA cloning kit (Invitrogen) according to the manufacturer's protocol. The ligations were incubated at room temperature before being transformed into One-Shot Top10 *Escherichia coli* cells (Invitrogen). The only modification to the procedure was the use of LB media in place of SOC.

RFLP analysis. Libraries were screened via RFLP to determine the amount of diversity in each sample and to consolidate the number of clones that would need to be sequenced. The isolated clones were first cultured and then subjected to PCR using the associated primers and cycle parameters listed above (Table 5). Sequences

Table 5. Primers used in this study

Primer name	Primer Sequence	Expected length	Annealing Temp	Reference
AclA-F2	TGC ATA GCA ATH GGN GGN GA	~1000	47 °Cx40	(56)
AclA-R5	CCG ATA GAN CCR TCN ACR TT			
NapA-V16F	GCN CCN TGY MGN TTY GYG G	~1200	45 °Cx40	(29)
NapA-V17R	RTG YTG RTT RAA NCC CAT NGT CCA			
CcoN-676F	CAR TGG TGG TDB GGW CAY AAY GC	628	51 °Cx10; 48 °Cx30	This study
CcoN-1303R	CAC ATC ATM CCY TGD GTR AWH CC			
SqrA-Cam-122F	GGR TYC CMT CMA AYA TTT GGG TKG G	1134	52 °Cx10; 49 °Cx30	This study
SqrA-Cam-1255R	CMA TTT CMG CCA TRS WWG CTT YDT G			
SqrA-Sulf-214F	WGC WAC ACA HGC HGC WCC C	1156	53 °Cx10; 50 °Cx30	This study
SqrA-Sulf-1369R	GAA YTG GAT HCC HTC MAA YAT HTG GG			
APS1F	TGG CAG ATC ATG ATY MAY GG	~390	60 °Cx40	(3)
APS4R	GCG CCA ACY GGR CCR TA			
HynS330F	GAR CCW AAY TTY TGG GAY AC	~1500	45 °Cx30	(149)
HynL419R	GGS GGY TTG ATC CAS GWR TAY TT			

taken from genomes of *Epsilonproteobacteria* were copied into A Plasmid Editor (ApE) to find restriction enzymes that would produce unique patterns for each. The PCR products were added directly to an enzyme mix with the chosen enzymes and the associated buffers (Promega or New England Biolabs). Digests were incubated at 37 ^{o}C for 120 min and run on 3% Metaphor Agarose (Lonza) gels for 90 min at 75 volts. The two exceptions for RFLP testing were samples for *aclA* and for *aprA*. The percentage of positive clones for *aclA* was very low and the *aprA* PCR product was too small to digest. In both cases, every positive clone was selected for sequencing.

Nucleotide Sequence Analysis. After each RT-PCR reaction, from either pure culture or biofilm community samples, the products were run on 1% agarose gels. Bands were excised and purified using a Gel-Purification kit (Qiagen) for sequencing. These sequences were used to confirm that the resulting amplicons were indeed for the correct gene transcript. Clone from libraries were selected for sequencing based primarily on unique fingerprints in the RFLP analysis. For each functional gene, one or two random samples were also selected from clusters of similar RFLP patterns (>5 of the same). The plasmids were extracted from liquid cultures using a Spin Miniprep kit (Qiagen) and the manufacturer's protocol. All of the DNA sequencing, both gel purified amplicons and plasmids, was outsourced to GENEWIZ (South Plainfield, NJ). Sequences were assembled with AutoAssembler Program (Applied Biosystems) analyzed using 4Peaks (www.mekentosj.com). The assembled fragments were assessed using the NCBI Basic Local Alignment Search Tool (BLAST).

Bioinformatics analyses. The reads from the metatranscriptome analysis were loaded into Metagenomics Analyzer (MEGAN; (58)) and Metagenomics Rapid Annotation using Subsystem Technology (MG-RAST; (98)) prior to this study. The data in MG-RAST was reanalyzed under different parameters to obtain an overview of represented organism classes and functional genes. Phylogenetic analysis for the individual functional genes was performed using the Seaview program (33), with the Clustal_W alignment matrix (156). The trees included reference sequences from the closest cultured relatives, as determined by NCBI's Basic Local Alignment Search Tool (BLAST), and were assembled using the Geneious (Biomaters) program based on the Neighbor-Joining method with the Jukes-Cantor algorithm (17; 132). The Kyoto Encyclopedia of Genes and Genomes (KEGG) database was utilized to determine whether the genes from organisms in each clade were performing the same function. Rarefaction analysis was performed in Microsoft Excel based on the number of matching RFLP fingerprints.

Results

Metatranscriptome annotation. Annotation of the transcripts obtained from the two biofilm communities, CV9 and CV41, was carried out using the MEGAN (MEtaGenome ANalyzer) software, which compares all the sequences to the GenBank database and then provides a taxonomic ranking (Figure 6). The size of the pie charts at each level (from domain to genus) indicates the relative portion of the total number of transcripts that are included in that clade (Figure 6). *Epsilonproteobacteria* dominated the two biofilms, with the majority of sequences

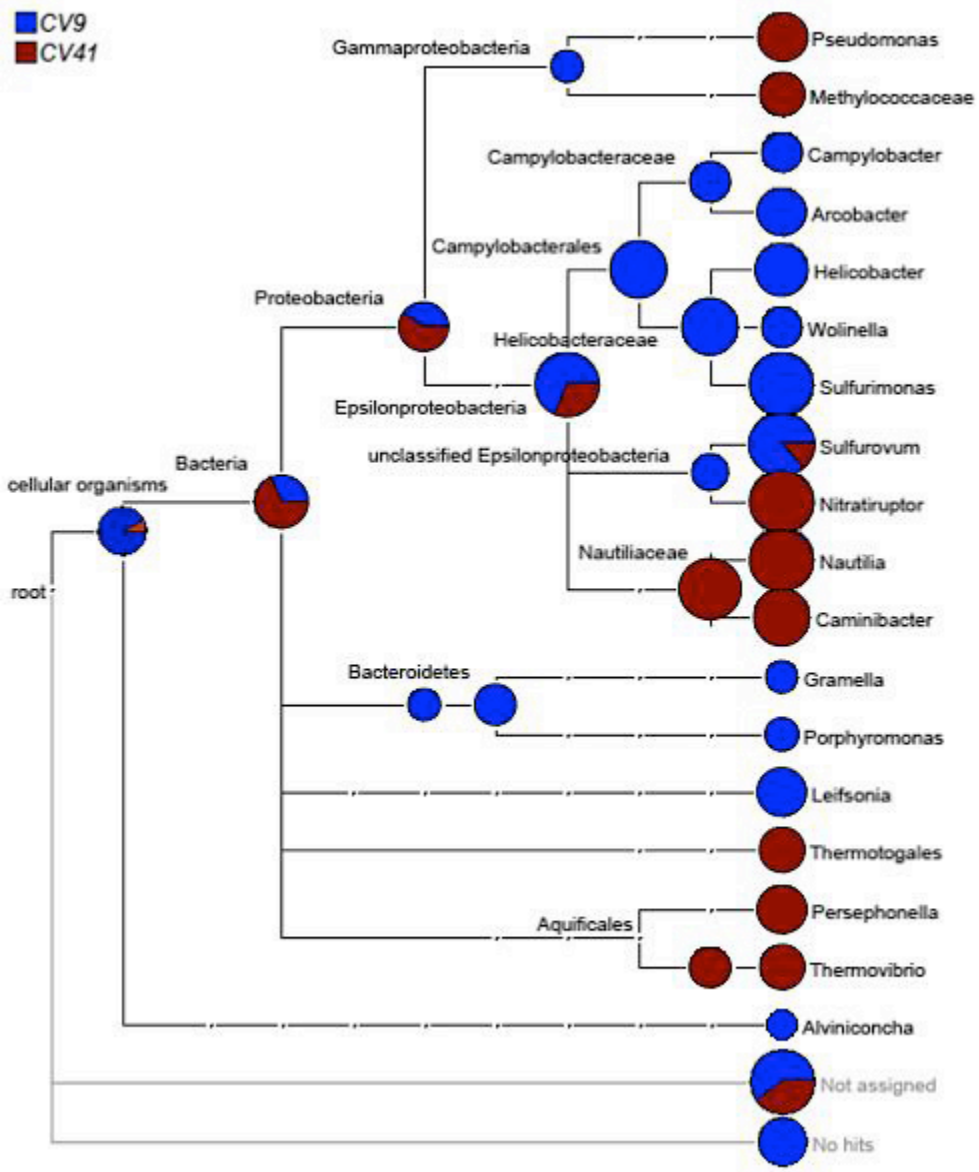

Figure 6: MEGAN analysis on the CV9 and CV41 metatranscriptome. Blue coloring in the pie charts represent data collected from the mesophilic community on the CV9 colonizer from 9°N. The red pie charts represent data collected from the thermophilic community on the CV41 colonizer from 13°N. The size of the circles indicate the total transcripts that are found in the two communities. Pie charts at each level, from domain down to genus, are resized at each step. This analysis was performed by Ricci, *et. al.* (*unpublished*) and modified to correlate with the colors used in this study.

related to *Sulfurovum* and *Sulfurimonas* spp. dominating the lower temperature CV9 biofilm, while the higher temperature CV41 biofilm contained transcripts mostly

associated to thermophilic *Epsilonproteobacteria,* including *Caminibacter, Nautilia* spp. (order *Nautiliales*), and *Nitratiruptor* spp. and two thermophilic *Aquificales* (*Thermovibrio* and *Persephonella* spp.). Interestingly, a small fraction of transcripts related to the mesophilic genus *Sulfurovum* were also detected in the CV41 biofilm community.

From the gene expression analysis using MG-RAST (a web-based metagenomic analysis tool), taxonomic assignments from both of the biofilms show that the vast majority of transcripts (>54% for CV9 and >77% for CV41) were assigned to the phylum *Proteobacteria* (Table 6). Among the *Proteobacteria*, close to 90% of the transcripts in each biofilm were from the *Epsilonproteobacteria* class. All other *Proteobacteria* were detected in lower numbers except for *Zetaproteobacteria*. Among the remaining transcripts found in the CV9 biofilm, around 1-2% each was assigned to *Bacteria* phyla *Actinobacteria, Bacteroidetes and Defferibacteres* with 5% of the transcripts assigned to the phylum *Firmicutes.* Also, around 1% were assigned to the domain *Eukaryota*. Roughly 2% of the remaining transcripts in the CV41 biofilm were assigned to the bacterial phyla *Aquificae*, *Bacteroidetes* and *Firmicutes*. Also around 2% each were given a taxonomic assignment as the domains *Archaea* and *Eukaryota*. One transcript was assigned as viral associated.

The sequences obtained in metatranscriptome analysis were not full-length transcripts for any of the genes. However, MG-RAST (a web-based metagenomic analysis tool) did assemble many of the fragments in contigs, before analysis. As expected, most of the transcripts from both biofilms were 16S rRNA sequences. MG-RAST, using its Subsystem classification, placed the rest of the transcript from the

Table 6. Taxonomic classification of biofilm community metatranscriptome data taken from EPR 9°N at a diffusing vent (CV9) and 13°N on the side of a black smoker chimney (CV41).

Taxonomic Group	CV9	CV41
Bacteria	3243	40030
Proteobacteria	1777	32122
Alphaproteobacteria	98	183
Betaproteobacteria	0	29
Epsilonproteobacteria	1538	29159
Gammaproteobacteria	24	950
Deltaproteobacteria	11	407
Unclassified *Proteobacteria*	106	2
Actinobacteria	41	0
Aquificae	0	759
Bacteroidetes	56	661
Defferibacteres	31	0
Firmicutes	176	764
Spirochaetes	10	0
Verrucomicrobia	1	0
Other *Bacteria*	1151	5724
Archaea	0	830
Euryarchaeota	0	263
Crenarchaeota	0	466
Eukaryota	18	639
Annelida	1	23
Apicomplexa	1	0
Arthropoda	0	290
Ascomycota	1	0
Chordata	0	73
Mollusca	0	1
Nematoda	3	11
Streptophyta	10	0
Other *Eukaryota*	2	241
Virus	0	1

CV9 biofilm in the following categories: ~2% genetics, <1% biosynthesis, metabolism and cellular functions (Table 7). The CV41 biofilm resulted in a much more diverse population of transcript sequences and contigs because of the two-fold

16S rRNA removal performed. The transcripts from this biofilm were associated with functions in replication (<1%), transcription (3%) and translation (<1%), biosynthesis (28%), energy metabolism (4%) and other cellular processes (1%) (Table 7). The largest fraction of the sample was classified as hypothetical or did not fit into a category during annotation. These were listed in Table 7 as "other" transcripts. All of the data compiled from MG-RAST is summarized in Tables 6 and 7.

Detection of gene transcripts in pure cultures of *Epsilonproteobacteria* and biofilm communities. *S. paralvinellae* was grown at 30 ^{o}C, while *C. mediatlanticus* was grown at 55 ^{o}C. After obtaining a pre-inoculum (1 day for *C. mediatlanticus* and ~7-10 days for *S. paralvinellae*), the cultures were transferred and grown into mid-log phase. The organisms were then transferred and grown into late exponential phase under each of the desired conditions and then harvested (Table 4). *S. paralvinellae* cultures containing $S_2O_3^{=}/NO_3^-$ without hydrogen did not grow. The S^0/NO_3^- cultures without hydrogen for *S. paralvinellae* did grow, but took twice as long to show signs of turbidity as the $H_2/S_2O_3^{=}/NO_3^-$ and $H_2/S_2O_3^{=}/O_2$ counterparts. Table 4 lists the five cultures that had enough biomass for RNA extraction as the “experimental results”.

Before analyzing the transcripts for each biofilm, genomic DNA of *C. mediatlanticus* and *S. lithotrophicum* were used for standardizing the primer sets shown in Table 5 and the obtained amplicons were sequenced to verify that the correct genes were being amplified. The genomic DNA of *C. mediatlanticus* and *Sulfurovum lithotrophicum* were also used as positive PCR controls for each functional gene transcript to be detected by RT-PCR. The RNA extractions for both

Table 7. Functional genes associated with vent biofilm community metatranscriptome analysis.

CV9	9°N	Diffuse flow vent
1	Biosynthesis	(Fatty acid)
3	Metabolism	(Carbohydrate)
2	Cell function	
	1	Membrane transport
	1	Virulence
8	Genetics	
	6	Protein translation and degradation
	2	Transcription
301	Other	
CV41	13°N	Side of black smoker chimney
374	Biosynthesis	
	13	Amino acid
	355	Nucleotide
	4	Fatty acid
	2	Cofactors/vitamins
52	Metabolism	
	18	Carbohydrate
	1	Phosphorus
	14	Nitrogen **(9 from *nap* operon)**
	14	Respiration **(4 from *cco* operon and 1 from *hyn* operon)**
	3	Sulfur **(2 from *apr* operon)**
	2	Other metabolism
16	Cell function	
	2	Cell division
	5	Cell wall
	3	Membrane transport
	1	Motility
	5	DNA transfer
57	Genetics	
	4	DNA replication and repair
	45	Protein translation and degradation
	8	RNA transcription
844	Other	

pure culture experiments and biofilm communities all tested positive for the presence of RNA bands before and after DNase treatment. A RT-PCR negative

control reaction was performed on each sample to test for carryover DNA. For each biofilm or pure culture extraction, I checked for PCR amplification of the 16S rRNA gene with and without a RT step. All extractions tested negative for carryover DNA before continuing with the functional gene analyses.

The primers developed in this study and used from previous work attempted to include as many organisms as possible while still staying with a degeneracy of 512 variations (3; 29; 56; 149). For some of the genes, there were highly conserved regions between genera and even classes of bacteria. One such example is the molybdenum-binding site in the periplasmic nitrate reductase encoding gene, *napA*. The remaining genes were not as conserved as *napA*, and the alignments used for designing the primers were restricted to *Epsilonproteobacteria*.

All RT-PCR amplicons from pure culture and biofilm community samples were sequenced to verify that the correct transcripts were amplified. The identities of gene transcripts were verified using the deduced amino acid sequences against a protein database (BLASTX). The GenBank sequences from the most closely related isolates to each gene transcript clone were downloaded from the database and used in the phylogenetic analyses. More distant pure culture relatives were also included to create proper out-groups on the trees.

In the analyses of gene transcripts for the libraries constructed with the ATP citrate lyase-encoding gene, *aclA,* and with the adenylylsulfate (APS) reductase-encoding gene, *aprA*, the RFLP analysis was not done and all clones were sequenced. The clones selected for *aclA* had a low percentage of inserts (<20%, Table 8), and the *aprA* library was only meant as a preliminary survey. While analyzing the rest of

the libraries, each clone with a unique RFLP pattern was sequenced and analyzed using BLASTX. Most of the sequences were assembled to the full length of the amplicon. Even those clones with unique RFLP patterns sometimes fell in the same clades within the phylogenetic trees. Rarefaction analysis was performed on the same RFLP fingerprints to determine species richness (Figure 7).

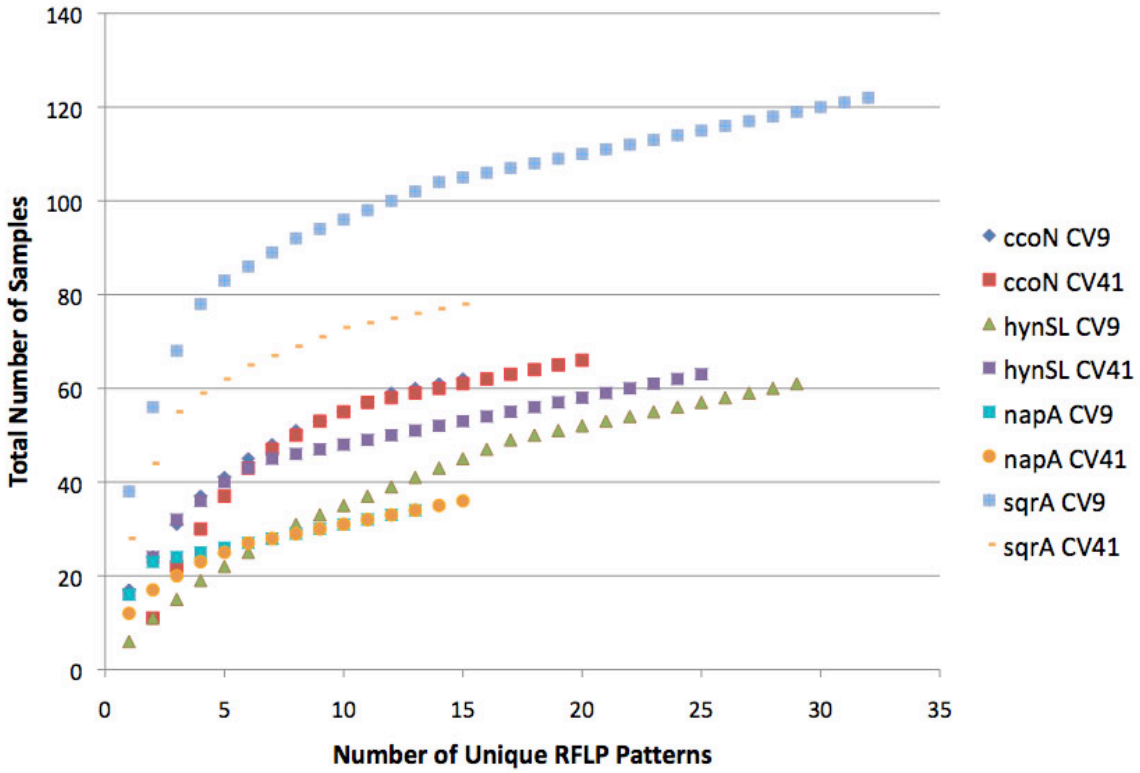

Figure 7: Rarefaction curves for libraries taken from the CV9 and CV41 targeted transcriptome analysis. The total number of samples were added for each unique RFLP pattern found. How close a curve comes to the maximum limit indicates how well the community was sampled.

Phylogenetic analysis of the deduced amino acid sequence form the ATP citrate lyase-encoding gene, *aclA*. The *aclA* insert-containing clones obtained from both the 9°N or 13°N biofilms were sequenced (Table 8). Phylogenetic analysis

Table 8. Number of clone utilized in this study

Sample: gene	#clones picked	#used for further analysis	#unique patterns
CV9: *aclA*	104	16	N/D*
CV41: *aclA*	93	19	N/D*
CV9: *aprA*	15	11	N/D*
CV41: *aprA*	15	11	N/D*
CV9: *ccoN*	72	62	15
CV41: *ccoN*	73	67	20
CV9: *hynSL*	68	61	29
CV41: *hynSL*	68	62	25
CV9: *napA*	40	34	13
CV41: *napA*	40	36	15
CV9: *sqrA*	129	90	32
CV41: *sqrA*	80	74	15
CV9: *soxB*	40	40	1[a]
CV41: *soxB*	40	40	1[a]

*These samples were not subjected to RFLP analysis.
[a]Only one pattern was apparently in the RFLP analysis that returned a 23S rRNA sequence.

of the *aclA* gene transcripts placed the biofilm sequences in five clades. Each of these five clusters was related to a cultured deep-sea vent organism (Figure 8). All the clones retrieved from the CV9 biofilm were closely related to the mesophilic *Epsilonproteobacteria, Sulfurovum* and *Sulfurimonas* (Figure 8). The CV41 biofilm had a predominance of sequences related to two genera (*Nautilia* and *Caminibacter*) of the order *Nautiliales*, which includes only thermophilic *Epsilonproteobacteria* isolated from deep-sea hydrothermal vents. However, two sequences were closely related to the thermophilic *Epsilonproteobacterium Hydrogenimonas thermophila* and three sequences were related to thermophilic members of the *Aquificales*, *Thermovibrio* and *Desulfurobacterium* (Figure 8).

Phylogenetic analysis of the deduced amino acid sequence from the periplasmic nitrate reductase-encoding gene, *napA*. For each biofilm, 40 *napA*

clones were analyzed for the insert of the correct size (Table 8). Thirty-four out of forty *napA* gene transcripts obtained from the CV9 biofilm library and thirty-six out of forty from the CV41 library were used in RFLP analysis. The majority sequences from the CV9 biofilm (n=23) fell into the *Sulfurovum* and *Sulfurimonas* clade. Another vent *Epsilonproteobacteria* genus, *Arcobacter*, formed a clade with ten clones from the CV9 biofilm. One *Epsilonproteobacteria* clone (clone CV9.33) from the CV9 biofilm was not closely related to any cultured strains. The majority of sequences from the CV41 biofilm (n=24) fell into the *Nautilia* and *Caminibacter* clade, although a few clones from this biofilm community was related to the *Sulfurovum*/*Sulfurimonas* group (clones CV41.8, 41.13, 41.14, 41.17 and 41.38). In line with the temperature regime from which the two biofilm communities originated, the clones from the CV9 biofilm were related to mesophilic *Epsilonproteobacteria*, while most of the clones from the CV41 biofilm were related to thermophilic organisms (Figure 10).

Phylogenetic analysis of the deduced amino acid sequence from the cytochrome oxidase-encoding gene, *ccoN*. The thermophilic *C. mediatlanticus* is a strict anaerobe (166) and its genome does not encode for cytochrome oxidase (35). Therefore, only the mesophilic organism, *S. paralvinellae*, was analyzed for *ccoN* expression. The *ccoN* gene was being transcribed in *S. paralvinellae* grown under aerobic conditions ($H_2/S_2O_3^{=}/O_2$). However, a fainter band was also obtained when this organism was grown under anaerobic conditions ($H_2/S^0/NO_3^-$) (Figure 11).

A total of sixty-two out of the seventy-two clones picked contained the *ccoN* insert from the CV9 biofilm library (Table 8). The CV41 biofilm library had sixty-

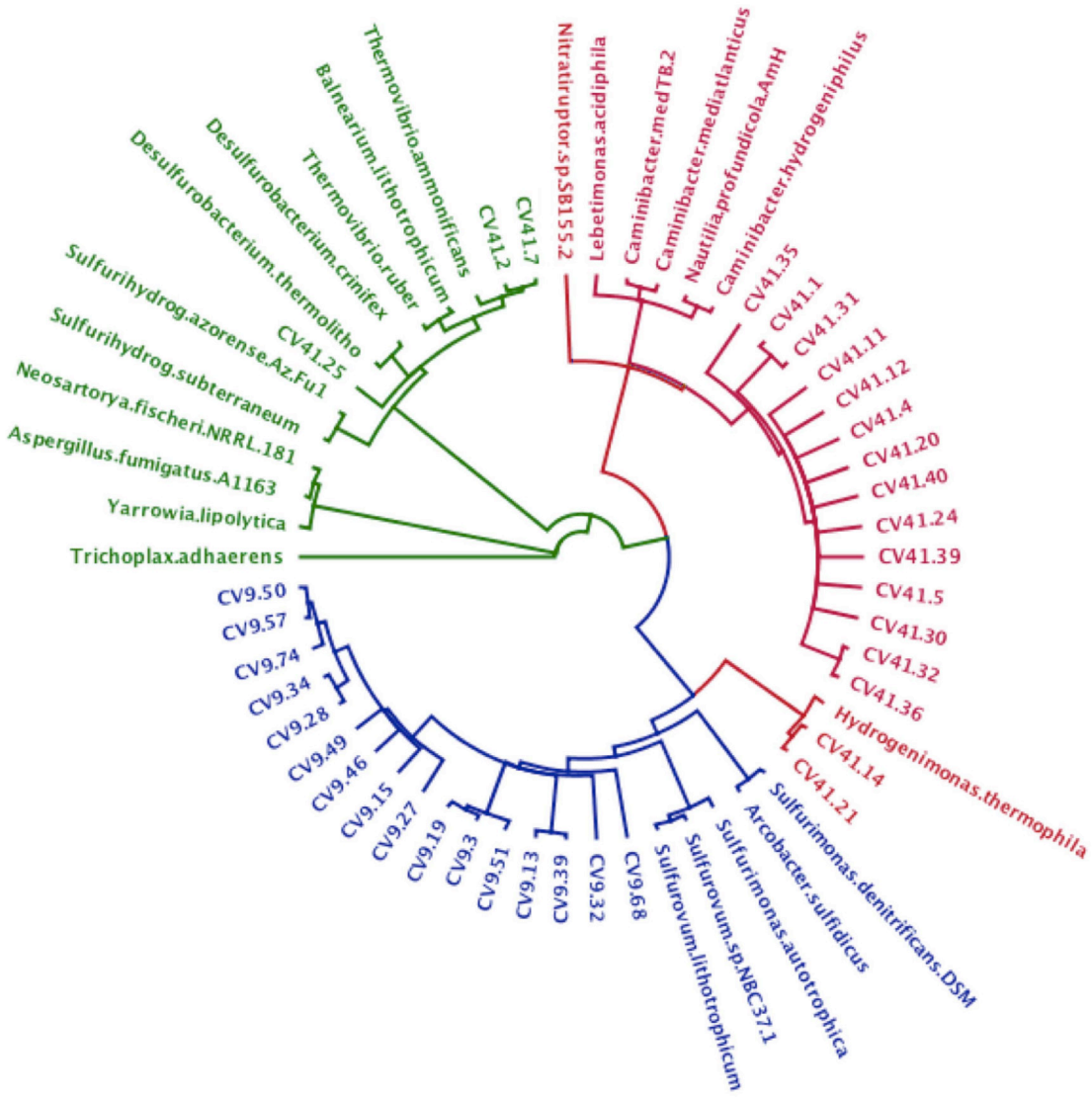

Figure 8: *aclA* phylogenetic distribution. CV9 clones were collected from the diffuse flow vent at EPR 9°N. CV41 clones were collected from the side of a black smoker chimney at EPR 13°N. Red represents thermophilic *Epsilonproteobacteria*. Blue represents mesophilic *Epsilonproteobacteria*. Green represents all non-*Epsilonproteobacteria* samples found, along with sequences from pure culture isolates. The alignment was performed using the observed divergence algorithm.

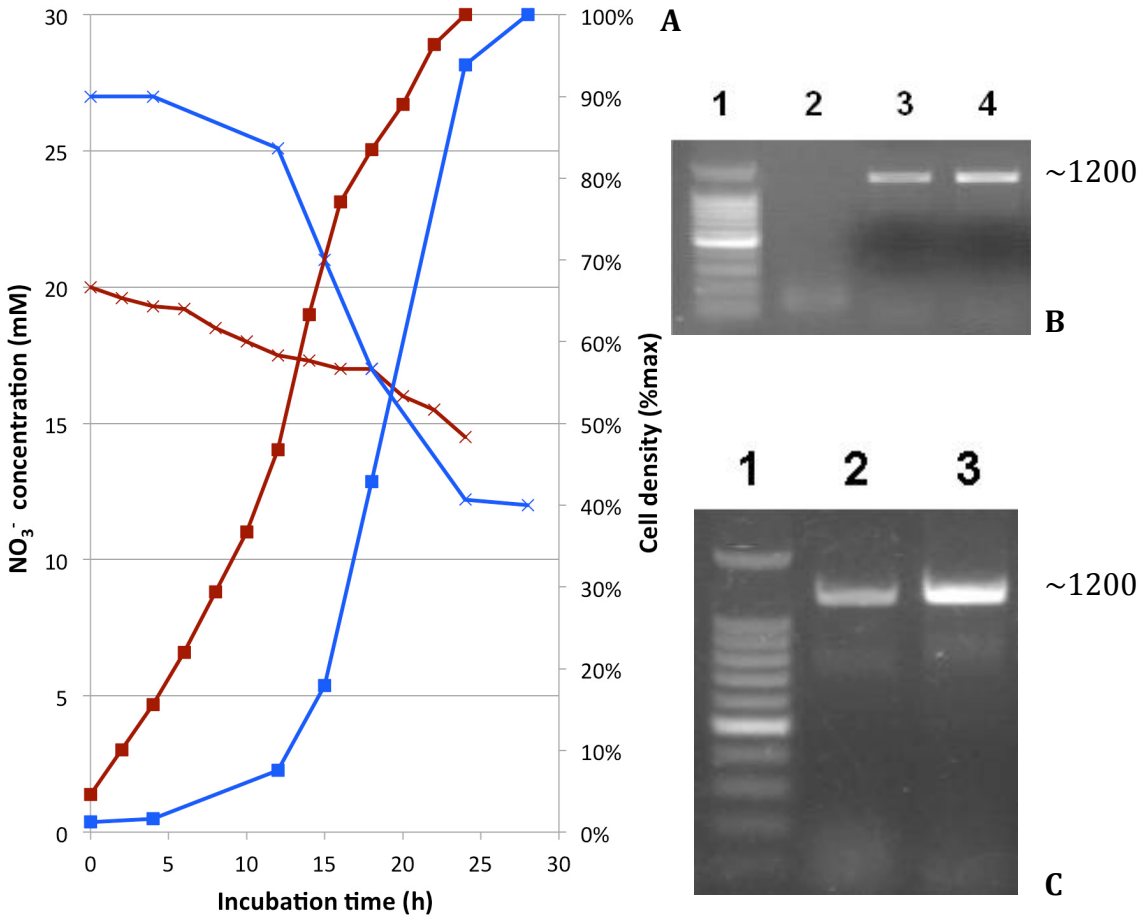

Figure 9. Evidence of nitrate reduction in pure cultures. (a) Growth curves of *S. lithotrophicum* and *C. mediatlanticus* superimposed with the rate of nitrate respiration (60; 166). The squares are the growth curves and the X's are the NO_3^- consumption curves. The blue curves represent data from *S. lithotrophicum* and the red lines represent *C. mediatlanticus*. (b) Detection of *napA* transcripts from *C. mediatlanticus* and *C. profundus* (Voordeckers *et. al.*, in revision). Lane 1 is ladder; lane 2 is the no-RT control for the RNA; lane 3 is the *C. mediatlanticus napA* RT-PCR product; lane 4 is the *C. profundus napA* RT-PCR product. (c) *napA* transcripts detected from mesophilic *Epsilonproteobacteria*. Lane 1 is ladder; lane 2 is the *S. lithotrophicum napA* RT-PCR product; lane 3 is the *S. paralvinellae napA* RT-PCR product.

seven out of seventy-three clones containing an insert of the correct size. Phylogenetic analysis placed most of the *ccoN* gene transcripts from the two biofilm communities in three clusters, each related to mesophilic *Epsilonproteobacteria* of the genera *Sulfurovum*, *Sulfurimonas* and *Arcobacter*, respectively (Figure 12). One clone from the CV41 biofilm (clone CV41.32) was closely related to the *Nitratiruptor* sp. strain SB1552, a thermophilic, facultative microaerobic *Epsilonproteobacterium*. Ten clones from the CV41 biofilm (represented by clones CV41.1, 41.8 and 41.55) were placed within the *Epsilonproteobacteria* but were not related to any known isolate.

Phylogenetic analysis of the deduced amino acid sequence from the sulfide quinone oxidoreductase-encoding gene, *sqrA*. The primer sets for sulfide quinone reductase (*sqrA*) were developed from two sequence alignments. The first alignment included mesophilic bacteria that utilize *sqrA* for oxidation of sulfur. The second set included the thermophilic *Epsilonproteobacteria* that have a *sqrA* gene in their genome annotated as sulfur oxidoreductase. The first primer set, amplified transcripts of the *sqrA* gene from cultures of *S. paralvinellae* utilizing the $S_2O_3^{=}/NO_3^-$ redox couple (with H_2/CO_2 gas in the headspace) and the $S_2O_3^{=}/O_2$ redox couple (with $H_2/CO_2/O_2$ gas in the headspace). Transcripts were not detected in the culture grown with the S^0/NO_3^- redox couple (with H_2/CO_2 gas) (Figure 13a). While using the second set of *sqrA* primers, transcripts were detected in *S. paralvinellae* under the same conditions (Figure 13b). Transcripts were also detected in *C. mediatlanticus* grown with S^0 under H_2/CO_2 gas (Figure 13b).

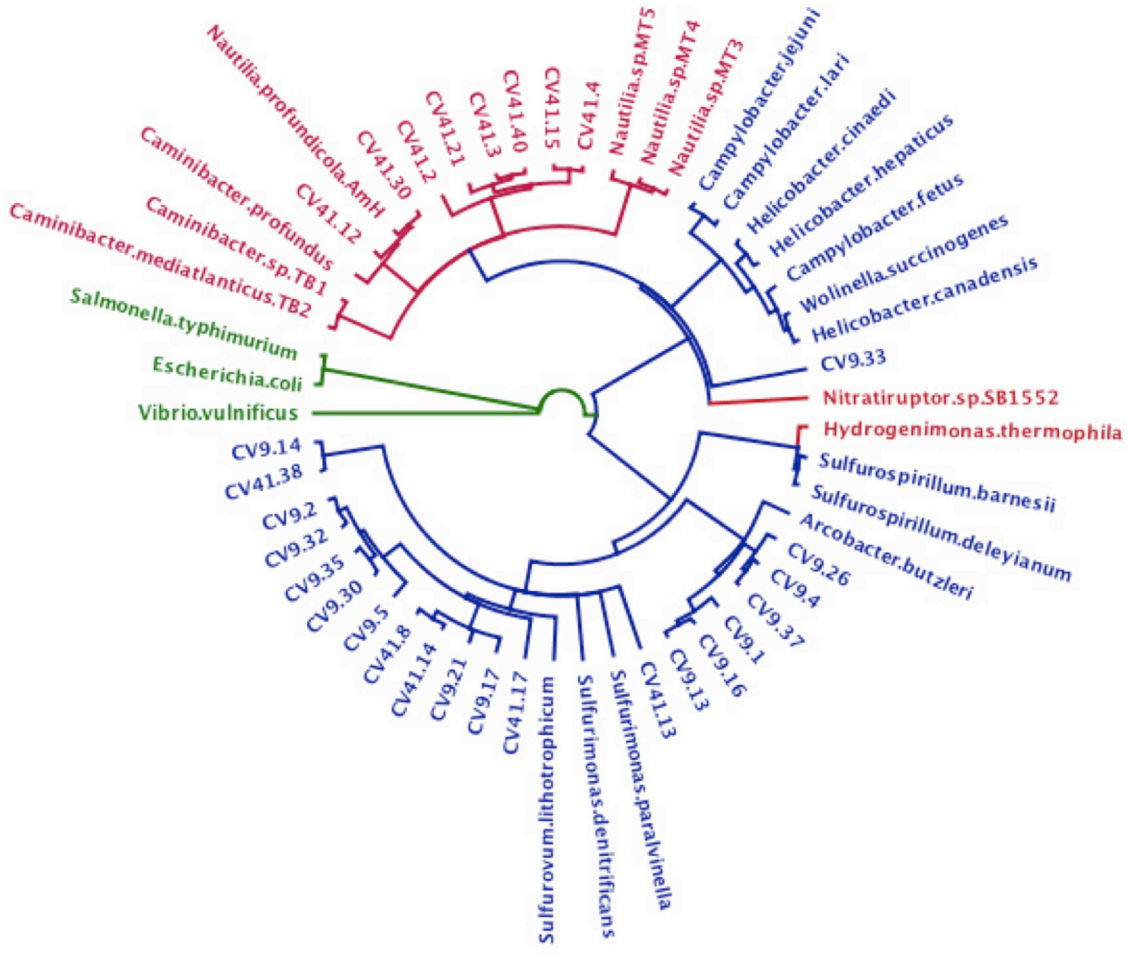

Figure 10: *napA* phylogenetic distribution. CV9 clones were collected from the diffuse flow vent at EPR 9°N. CV41 clones were collected from the side of a black smoker chimney at EPR 13°N. Red represents thermophilic *Epsilonproteobacteria*. Blue represents mesophilic *Epsilonproteobacteria*. Green represents a *Gammaproteobacteria* outgroup. The alignment was performed using the observed divergence algorithm.

Having two sets of primers designed from sequences of mesophilic and thermophilic *Epsilonproteobacteria*, respectively, allowed for a broader recovery of *sqrA* transcripts. The primer set designed on sequences from mesophiles amplified *sqrA* transcripts only from the low temperature biofilm (CV9). However, the primer set designed on sequences from thermophiles amplified *sqrA* transcripts from both

the low and higher temperature biofilms. This is consistent with the detection of both mesophilic and thermophilic *Epsilonproteobacteria* in the higher temperature biofilm, CV41. A total of 90/129 plasmids contained the correct insert size for the CV9 biofilm, while 74/80 inserts of the correct size were detected for the CV41 biofilm (Table 8). Phylogenetic analysis revealed many clades within the mesophilic *Epsilonproteobacteria*. A large portion (n=32 based on RFLP analysis) of the *sqrA* transcripts from the CV41 biofilm was related to the thermophilic, sulfur reducing *Caminibacter mediatlanticus* (Figure 14). Two clones (represented by CV41.7) were related to the green sulfur bacterial genus *Chlorobium*. The remaining *sqrA* sequences, derived for the most part from the low temperature biofilm, CV9, were related to the genera *Sulfurovum*/*Nitratifractor* (n=18 for CV9 and n=10 for CV41 based on RFLP patterns) and *Sulfurimonas* (n=19 for CV9 based on RFLP patterns) clones. All other clones from the CV9 and CV41 biofilms were related to *Epsilonproteobacteria* without clustering tightly to any known cultured isolate (Figure 14). All three libraries – two from the CV9 biofilm (using both primer sets) and one from CV41 (using only the primer set designed using the thermophilic organisms) – were combined in the phylogenetic analysis shown in Figure 14.

Phylogenetic analysis of the deduced amino acid sequence from the hydrogenase-encoding gene, *hynSL*. Sixty-eight *hynSL* clones were picked from each biofilm library (Table 8). Seven of the clones from the CV9 biofilm and 6 from the CV41 biofilm did not contain an insert. The RFLP fingerprints diverse in these two libraries. Phylogenetic analysis showed that, overall, the *hynSL* transcripts were related to mesophilic *Epsilonproteobacteria* of the genus *Sulfurimonas* (all from the

low temperature CV9 biofilm) and to thermophilic *Epsilonproteobacteria* of the order Nautiliales, genera *Caminibacter, Nautilia and Lebetimonas* (All from the higher temperature CV41 biofilm). Furthermore, a number of *hynSL* sequences from the CV9 and CV41 biofilm communities clustered within the sulfate-reducing *Deltaproteobacterium, Desulfotalea psychrophila,* and with a *Deltaproteobacteria*-related clade, respectively (Figure 15).

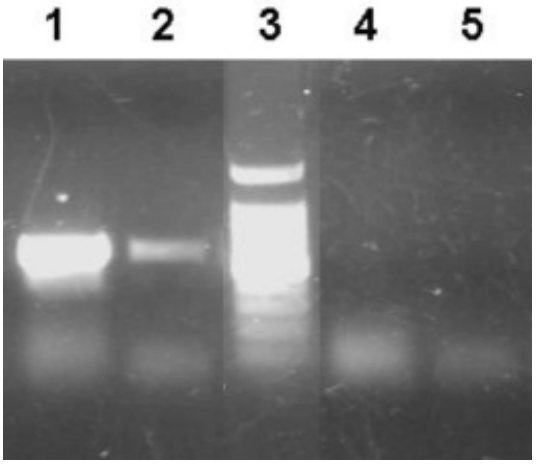

Figure 11. Detection of the gene transcripts for cbb3-type cytochrome oxidase (*ccoN*) in *S. paralvinellae*. Lane 1 is the sample from the $H_2/S_2O_3^{=}/O_2$ *ccoN* RT-PCR product; lane 2 is the sample from the S^0/NO_3^- *ccoN* RT-PCR product; lane 3 is the ladder; lane 4 is the no-RT control from the $H_2/S_2O_3^{=}/O_2$ culture; lane 5 is the no-RT control from the S^0/NO_3^- culture.

Phylogenetic analysis of the deduced amino acid sequence from the adenylylsulfate reductase-encoding gene, *aprA*. I did not carry out a set of experiments to detect the *aprA* transcripts in representative strains of *Epsilonproteobacteria*. However, it is known that *S. lithotrophicum*, *S. paralvinellae* and the *Nautiliales* organism, *L. acidophila*, do not have APS reductase activity (149). Because the APS reductase is not represented in the *Epsilonproteobacteria*, I performed a preliminary survey using *aprA*. For each of the biofilm communities,

eleven out of fifteen plasmids contained the correct size insert for *aprA* (Table 8). Because of the small size of the *aprA* amplicon, I did not carry out the RFLP analysis and all the clones were sequenced. Phylogenetic analysis of the amino acid sequence deduced from the *aprA* transcripts placed the sequences with either various sulfate-reducing *Deltaproteobacteria* or in a clade related to sulfide-oxidizing *Beta*- and *Gammaproteobacteria* of the genera *Thiocapsa*, *Thiobacillus*, *Thiococcus* and symbionts of the marine nematode *Robbea.* No *aprA* transcripts related to *Epsilonproteobacteria* were detected in this analysis (Figure 16).

Discussion

Composition of the active fraction of the vent biofilm communities. *Epsilonproteobacteria* were the dominant active members of the two biofilm communities based on the MEGAN and MG-RAST analytical tools used to assess the diversity of the transcripts recovered from two biofilm communities: the CV9 biofilm, which developed at a temperature range of 10-28 °C and the CV41 biofilm, which developed at a temperature range of 20-50 °C (Table 2, Figure 6 and Table 6). Transcripts related to *Sulfurovum* and *Sulfurimonas* spp. were the most abundant in the low temperature biofilm, CV9, although a number of transcripts related to *Arcobacter* spp. and other members of the *Campylobacterales* were also detected (Figure 6). *Sulfurovum lithotrophicum, Sulfurimonas autotrophica* and *S. paralvinellae* are three mesophilic *Epsilonproteobacteria* isolated from deep-sea hydrothermal vents in the western Pacific Ocean (59; 60; 152). These organisms grow optimally in the 25-30 °C temperature range and couple the oxidation of reduced sulfur species (and hydrogen in the case of *S. paralvinellae*) to the reduction

of oxygen (microaerobically) and/or nitrate. *Arcobacter* spp. are known to produce sulfur filaments in reducing environments (153). The finding of transcripts related to these *Epsilonproteobacteria* in the CV9 biofilm is consistent with the temperature (10-28 °C) and geochemical regimes (sulfide in fluids ~ 100 µM; up to 20% elemental sulfur embedded in the biofilm) of this diffuse flow vent.

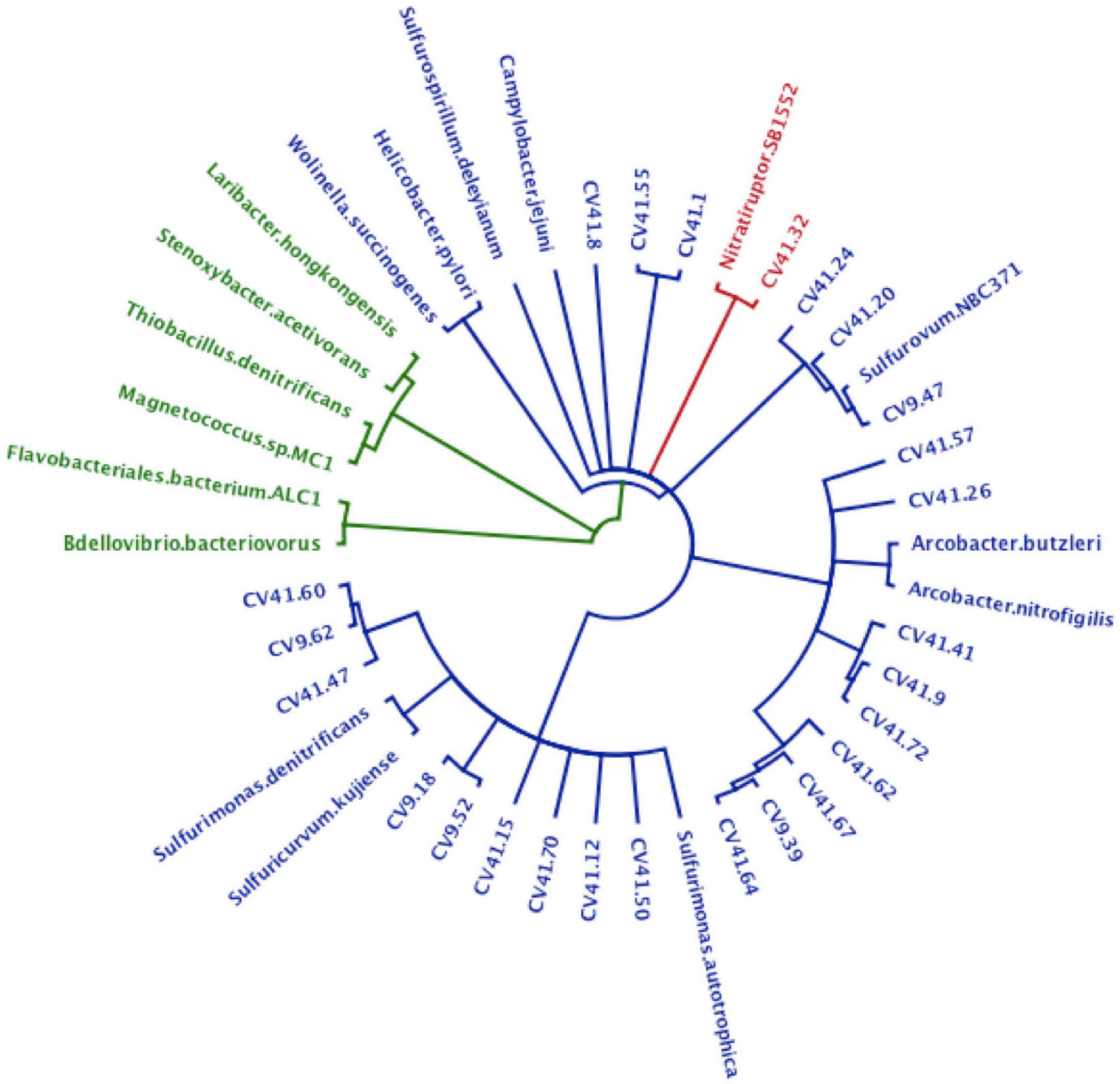

Figure 12: *ccoN* phylogenetic distribution. CV9 clones were collected from the diffuse flow vent at EPR 9°N. CV41 clones were collected from the side of a black smoker chimney at EPR 13°N. Blue represents mesophilic *Epsilonproteobacteria*. Red represents the thermophilic *Epsilonproteobacteria*. Green represents all non-*Epsilonproteobacteria* outgroups formed in the alignment. The alignment was performed using the observed divergence algorithm.

Epsilonproteobacteria also dominated the higher temperature biofilm, CV41. However, most of the transcripts recovered from this community were related to members of the order *Nautiliales*, which includes only thermophilic *Epsilonproteobacteria* isolated from deep-sea hydrothermal vents (100). In particular, most of the transcripts from the CV41 biofilm were related to *Caminibacter* and *Nautilia* spp. These *Epsilonproteobacteria* grow optimally at temperatures between 40-60°C by coupling the oxidation of hydrogen to the reduction of nitrate and/or elemental sulfur. Interestingly, a small fraction of the transcripts from the CV41 biofilm was related to mesophilic *Sulfurovum* and *Sulfurimonas* spp. The presence of active members of both thermophilic and mesophilic *Epsilonproteobacteria* in this biofilm may be explained by the broader temperature range (20-50°C) at which this biofilm developed. It is worth mentioning that transcripts related to the *Thermotogales* and *Aquificales*, two orders that include the most thermophilic *Bacteria* known, were also detected in the CV41 biofilm.

The accuracy of MG-RAST transcript assignment may be skewed towards organisms whose genome sequences are available or towards genes with assigned functions. Given that caveat, the CV41 community is actively expressing the genes encoding for anaerobic respiration (periplasmic nitrate reductase), aerobic and/or microaerobic respiration (cytochrome c oxidase), hydrogen oxidation (NiFe associated hydrogenase) and sulfur oxidation/reduction (adenylylsulfate reductase). Considering that one of the possible biofilm inhabitants, *Caminibacter mediatlanticus* TB-2 is predicted to have 1,826 protein coding genes (35), it is

impressive that 9 out of the 844 contigs created by MG-RAST were for periplasmic nitrate reductase (Table 7). This over-expression of *nap* related genes might indicate that nitrate is the primary electron acceptor used by the biofilm community. However, without knowing the exact rates of mRNA degradation for each gene (24; 125), this is unconfirmed. We did attempt to minimize the mRNA degradation by immediately storing the biofilms in RNAlater upon collection.

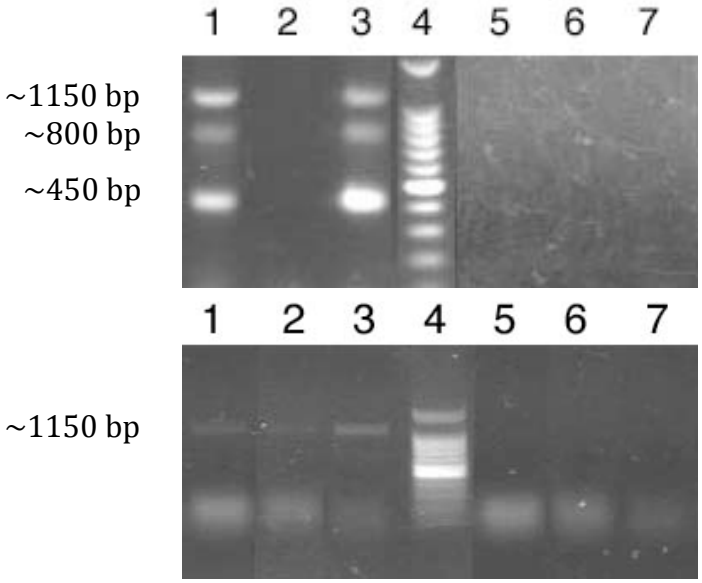

Figure 13. Indication of sulfur metabolism occurring *in vivo*. (top) Transcripts were detected from cultures using the primer sets for sulfide quinone reductase (*sqrA* in mesophiles) from *S. paralvinellae*. Lane 1 is the $H_2/S_2O_3^=/NO_3^-$ *sqrA* RT-PCR product; lane 2 is the S^0/NO_3^- *sqrA* RT-PCR product; lane 3 is the $H_2/S_2O_3^=/O_2$ *sqrA* RT-PCR product; lane 4 is the ladder; lane 5 is the $H_2/S_2O_3^=/NO_3^-$ No-RT control; lane 6 is the S^0/NO_3^- No-RT control; lane 7 is the $H_2/S_2O_3^=/O_2$ No-RT control. The 450 bp and 800 bp bands sequenced to be non-specific 16S rRNA gene products. (bottom) Transcripts were detected from cultures using the primer sets for sulfur oxidoreductase (*sqrA* in thermophiles). Lane 1 is *C. mediatlanticus* H_2/S^0 *sqrA* RT-PCR product; lane 2 is *S. paralvinellae* $H_2/S_2O_3^=/NO_3^-$ *sqrA* RT-PCR product; lane 3 is *S. paralvinellae* $H_2/S_2O_3^=/O_2$ *sqrA* RT-PCR product; lane 4 is the ladder; lane 5 is *C. mediatlanticus* H_2/S^0 No-RT control; lane 6 is *S. paralvinellae* $H_2/S_2O_3^=/NO_3^-$ No-RT control; lane 7 is *S. paralvinellae* $H_2/S_2O_3^=/O_2$ No-RT control.

Detection of transcripts for CO_2 fixation and nitrate reduction. On the basis of the established dominance of *Epsilonproteobacteria* as the active members of the two biofilm communities, I proceeded to identify the gene transcripts known to be involved in autotrophic carbon fixation (rTCA cycle) and energy metabolism in these organisms. Pure culture isolates were chosen as representatives from the major clades of *Epsilonproteobacteria* found in this, as well as previous studies, of deep-sea hydrothermal vents (Figure 6 and (1; 78)). These organisms were also chosen for their abilities to use alternative redox couples for their respiratory metabolism (Figure 2; (139). A thermophilic organism, with growth temperature optimum at 55 ^{o}C, and a mesophilic organism, with growth optimum at 30 ^{o}C, were chosen. The two organisms can fix CO_2, oxidize hydrogen and reduce nitrate (152; 166). They differed in their usage of sulfur species, as the thermophilic *Caminibacter mediatlanticus* reduces oxidized sulfur species (166), and the mesophilic *Sulfurimonas paralvinellae* oxidizes reduced sulfur species (152). *S. paralvinellae* has also been characterized as microaerobic (152). Taking into account the physiology and metabolism of these organisms, and establishing the presence of specific transcripts of interest in these representative isolates, I was able to better interpret the detection of functional gene transcripts in the natural biofilms.

Previous studies done in our laboratory and by others established that vent *Epsilonproteobacteria* and *Aquificales* use the rTCA cycle for autotrophic carbon fixation. The entire cycle was reconstructed in several vent *Epsilonproteobacteria* (14; 35; 111) and *Aquificales* (36). The activity of all the enzymes involved the rTCA cycle, including the ATP citrate lyase, was measured in both vent

Epsilonproteobacteria and *Aquificales* (149; 165) establishing that these organisms encode and express the enzymes for the rTCA cycle during autotrophic growth (Table 1 and Figure 1). Hence, when I detected the transcripts of the ATP citrate lyase-encoding gene, *aclA*, in the vent biofilms, I can reasonably conclude that, at the time of sampling, the biofilm organisms were fixing carbon dioxide via the rTCA cycle.

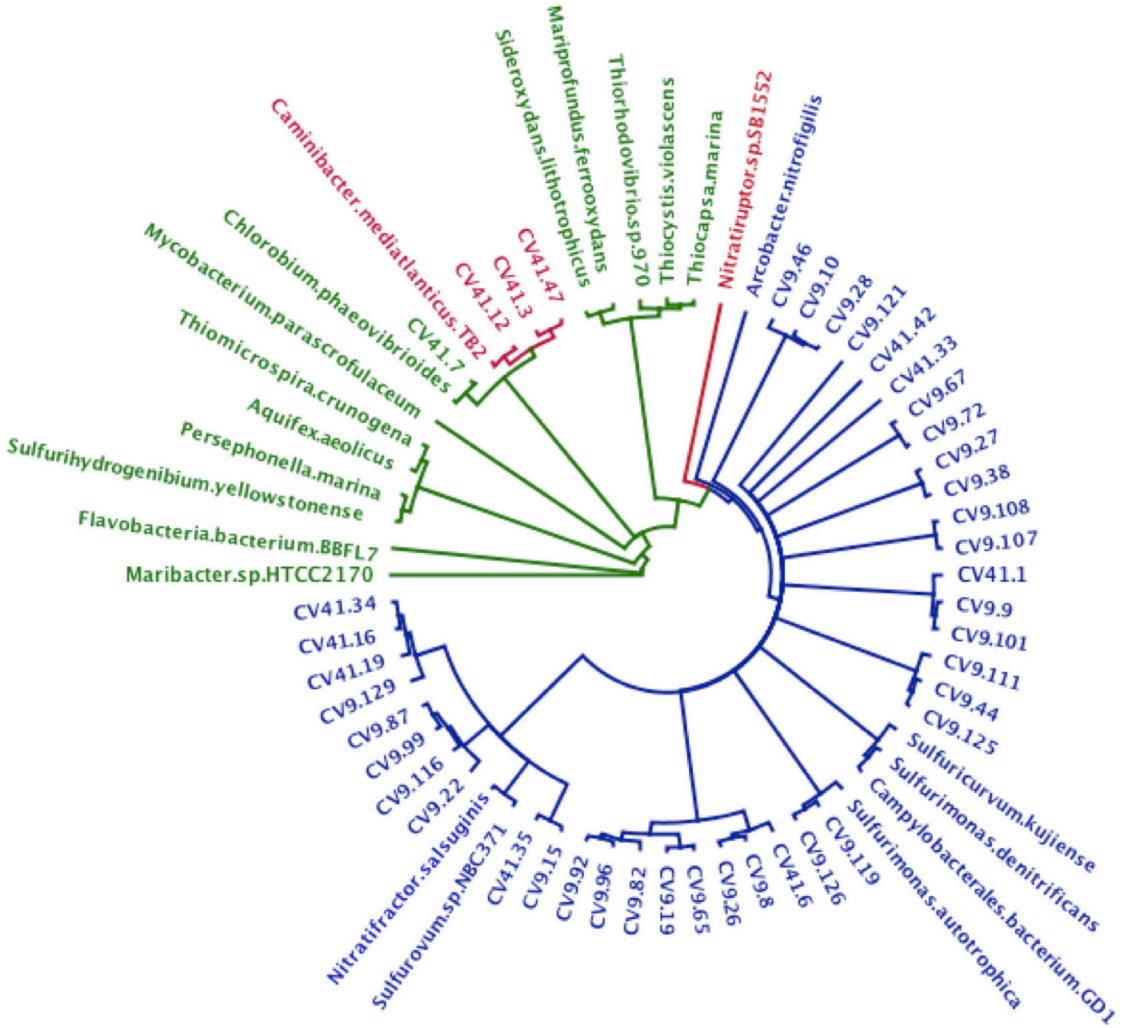

Figure 14: *sqrA* phylogenetic distribution. CV9 clones were collected from the diffuse flow vent at EPR 9°N. CV41 clones were collected from the side of a black smoker chimney at EPR 13°N. Red represents thermophilic *Epsilonproteobacteria*. Blue represents mesophilic *Epsilonproteobacteria*. Green represents all non-*Epsilonproteobacteria* samples found, along with sequences from pure culture isolates. The alignment was performed using the observed divergence algorithm.

Within the *Epsilonproteobacteria*, both *C. mediatlanticus* and *S. lithotrophicum* steadily consume nitrate during growth, indicating that they use it as an electron acceptor (60; 166), Figure 9a). The transcript for the periplasmic nitrate reductase (*napA*) has been detected, in our laboratory, in two different *Caminibacter* species – *C. mediatlanticus* and from the close relative *C. profundus* (Figure 9b). I was also able to detect *napA* transcripts from *S. paralvinellae* grown with nitrate (Figure 9c). Since no other nitrate reductase-encoding gene has been identified in the genomes of vent *Epsilonproteobacteria*, the physiology, expression and genomic data taken together indicate that these bacteria use the periplasmic nitrate reductase when grown under nitrate reducing conditions. Hence, based on the detection of the periplasmic nitrate reductase-encoding gene, *napA*, transcripts in the vent biofilms, one can reasonably conclude that, at the time of sampling, the biofilm organisms were actively respiring nitrate.

In the *aclA* and *napA* phylogenetic trees (Figures 8 and 10), the dominant sequences from the mesophilic biofilm were in the *Sulfurovum* and *Sulfurimonas* clusters. Likewise, the thermophilic biofilm had a dominance of *Caminibacter* and *Nautilia* sequences. These correlated well with the metatranscriptome data, from what we know from the physiology of these organisms, and from the temperature and geochemical regimes of the two vent sites (Figures 8 and 10; (60; 119; 147; 152; 165; 166). In one clade for *napA* transcript phylogeny, both CV9 and CV41 contained *Sulfurovum*/*Sulfurimonas* spp. actively expressing the gene (Figure 10). This again correlated well what we see in the metatranscriptome, as that same clade was the only one with overlapping sequences in both samples (Figure 6). This suggests that,

at vents characterized by fluctuating temperatures, such as the site where the CV41 biofilm developed, both mesophilic and thermophilic *Epsilonproteobacteria* co-exist and are active members of the community.

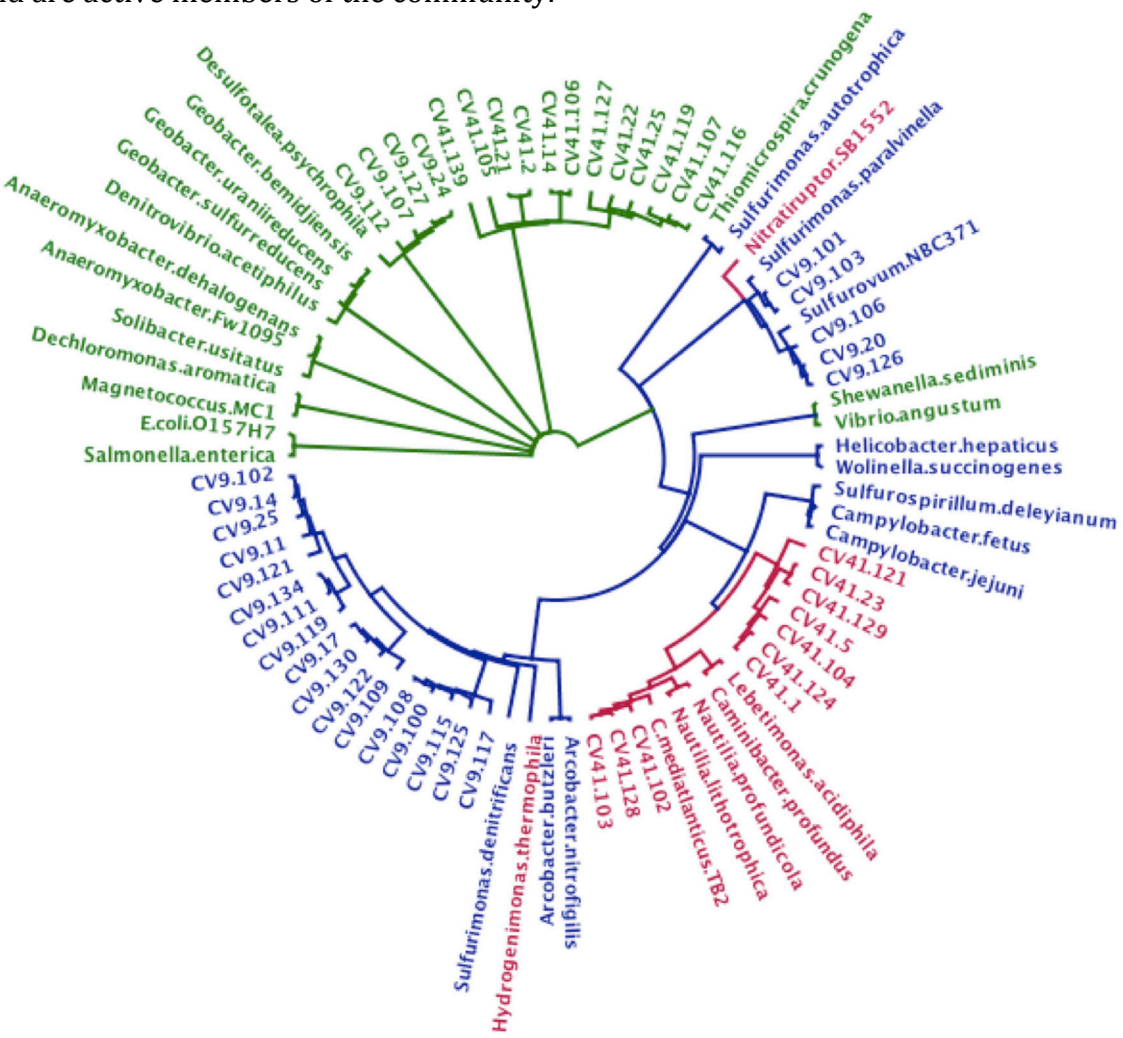

Figure 15: *hynSL* phylogenetic distribution. CV9 clones were collected from the diffuse flow vent at EPR 9°N. CV41 clones were collected from the side of a black smoker chimney at EPR 13°N. Red represents thermophilic *Epsilonproteobacteria*. Blue represents mesophilic *Epsilonproteobacteria*. Green represents all non-*Epsilonproteobacteria* samples found, along with sequences from pure culture isolates. The alignment was performed using the observed divergence algorithm.

Detection of transcripts for microaerobic respiration. The transcript for cbb3-type cytochrome oxidase-encoding gene was detected in cultures of *S. paralvinellae* grown microaerobically, suggesting that this bacterium used the *ccoN*

for microaerobic respiration (Figure 11). However, a fainter band for the *ccoN* transcript was also detected when *S. paralvinellae* was grown with nitrate, rather than oxygen, as the terminal electron acceptor. The *ccoN* gene being constitutively active seems unlikely unless the organisms are constantly subjected to oxidative stress in the environment. A more probable explanation is that residual oxygen was still present in the media. This is possible, as the MJ media used to grow *S. paralvinellae* is not supplemented with a reducing agent or with a redox indicator. Even though the media is boiled and kept under anaerobic conditions, there is no way to be certain whether residual oxygen is present. Because *S. paralvinellae* is microaerobic, it would be expressing its cytochrome oxidase in the presence of trace quantities of oxygen.

Transcripts of the *ccoN* gene were detected in both biofilm communities, and were mostly related to mesophilic *Epsilonproteobacteria* of the genera *Sulfurovum* and *Sulfurimonas* (Figure 12). Since oxygen tends to become more depleted as the temperature of the hydrothermal fluids increases, I was surprised to find several *ccoN* transcripts in the higher temperature biofilm, CV41, biofilm (Figure 12). In the metatranscriptome analysis, only 4/844 contigs in the MG-RAST analysis for the CV41 biofilm were related to the *cco* operon (Table 7). Again, this may be interpreted in the context of the broad temperature variability measured during the development of the CV41 biofilm. Interestingly, one *ccoN* gene transcript detected in the CV41 biofilm was related to the microaerobic, thermophilic *Epsilonproteobacterium, Nitratiruptor* strain SB155-2, again confirming that in this biofilm both mesophilic and thermophilic *Epsilonproteobacteria* coexist and are

active (Figure 12). In this biofilm, microaerobic *Nitratiruptor* spp. appears to share the same temperature niche of thermophilic and anaerobic members of the order *Nautiliales* (e.g., *Caminibacter* and *Nautilia* spp.), without competing for the same terminal electron acceptors.

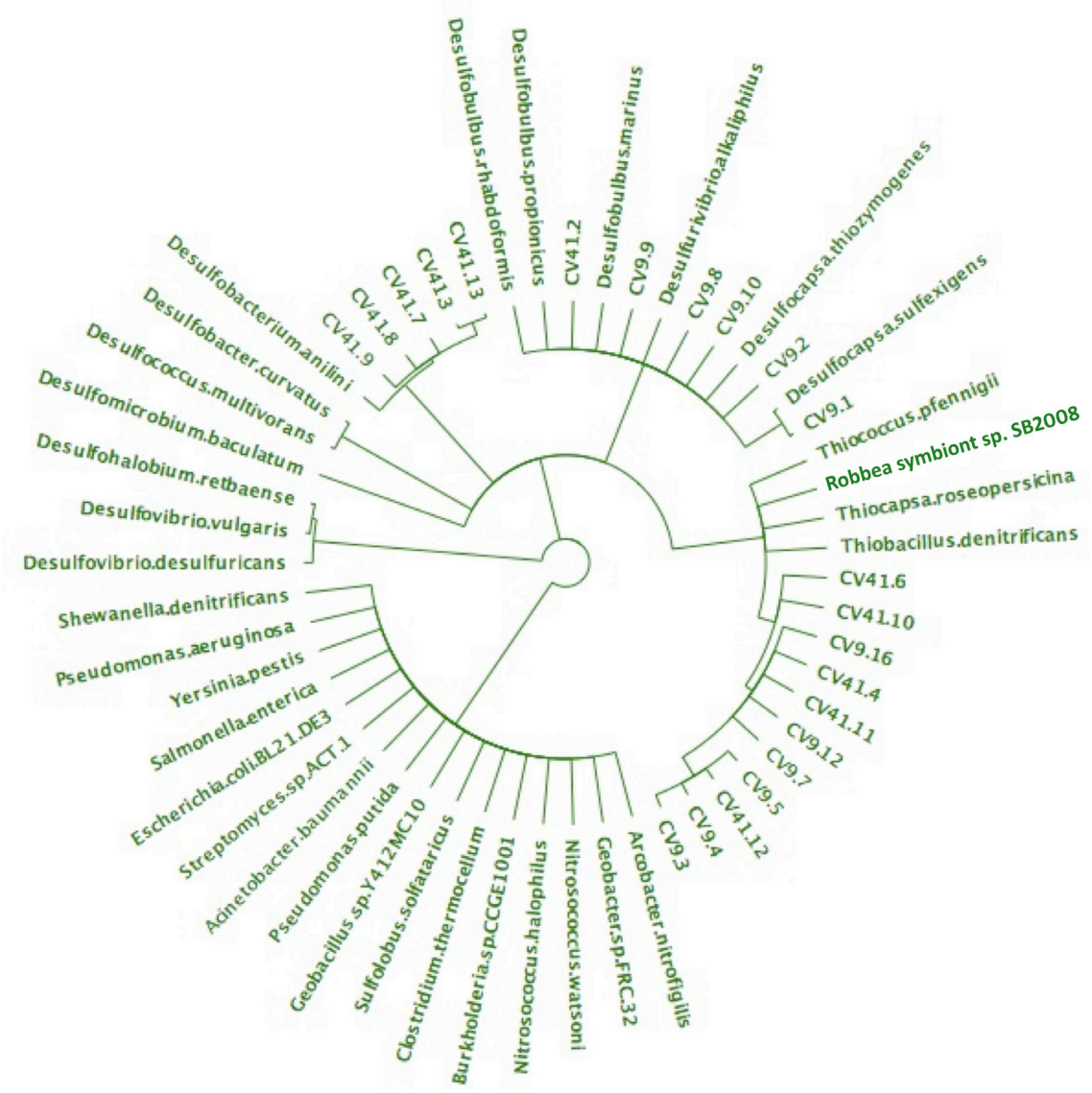

Figure 16: *aprA* phylogenetic distribution. CV9 clones were collected from the diffuse flow vent at EPR 9°N. CV41 clones were collected from the side of a black smoker chimney at EPR 13°N. The top branches contain representatives of the *Deltaproteobacteria*. The branch coming off to the right side contains *Gamma* and *Betaproteobacteria*. The out-group on the bottom contains a mix of *Beta*, *Delta* and *Gammaproteobacteria*. The alignment was performed using the observed divergence algorithm.

Detection of transcripts for sulfur oxidation/reduction. While investigating sulfur oxidation and reduction pathways, the *sqrA* and *aprA* genes worked well for analyzing both sulfur oxidation and sulfur reduction, respectively. The exact mechanism for the *sqrA* reactions are not known, making *in vivo* and *in situ* experiments involving *sqrA* that much more intriguing. Regardless of whether it is a bi-directional enzyme or structurally similar sulfide quinone reductase and sulfur oxidoreductase, the *sqrA* gene is present in both thermophiles and mesophiles (35; 111; 138). *C. mediatlanticus* only expressed *sqrA* in the presence of sulfur as an electron acceptor, and not when nitrate was present (Figure 13b). For *S. paralvinellae*, the *sqrA* transcripts were detected even with hydrogen being present in the headspace (Figure 13a and b). This confirms what has been reported for *S. paralvinellae.* It is described as utilizing hydrogen as a secondary source of electrons when either S^0 or $S_2O_3^=$ are present (152). The absence of transcripts in the $H_2/S^0/NO_3^-$ sample is a little perplexing. One possibility is that because of the extremely inefficient growth in that treatment, *sqrA* transcripts were below the detection limit.

The a*prA* gene was not expressed in pure cultures of *Epsilonproteobacteria*, however it is known to be expressed in the vent *Gammaproteobacterium Thiomicrospira thermophila* (149). The APS reductase is generally reported as a reductase (97), and sulfide quinone reductase is reported to oxidize hydrogen sulfide (42). We entered these experiments expecting them to act as such. The mesophilic biofilm did only had sulfur oxidizers expressing *sqrA* as we had expected (Figure 14). However, in CV41, putative thermophilic sulfur reducers were

expressing *aprA* and co-existed with mesophilic sulfur-oxidizing *Epsilonproteobacteria* (expressing *sqrA*) and *Gamma* and *Betaproteobacteria* (possibly expressing the *aprA* in reverse). The *aprA* expression followed the same pattern of both sulfur oxidizers and reducers co-inhabiting each biofilm (Figure 15). The *Deltaproteobacteria* were most likely expressing *aprA* to reduce APS, while the *Betaproteobacteria* and *Gammaproteobacteria* in the biofilms were probably oxidizing sulfite to APS. The results from both of these functional genes was very exciting as it suggests that these organisms may be interacting by transferring products from their sulfur metabolism across a thermal and redox gradient.

Detection of transcripts for hydrogen oxidation. Based on previous analyses on vent isolates, there are a large number of organisms that can oxidize hydrogen (139; 149). This ability is present more so in the thermophilic organisms than in the mesophilic ones (Table 1; (149)). Previous work from Takai, *et. al.* 2005, described the hydrogen oxidation activity *in vitro* (149). The work included *S. paralvinellae*, *S. lithotrophicum*, and the *Nautiliales* organisms, *L. acidophila*. Both *S. paralvinellae* and *L. acidophila* had the *hyn* genes detected from their genomic DNA and had hydrogen oxidation activity from cell lysates (Table 1). Transcripts for the *hynSL* genes were not detectable in any of the pure culture RNA extractions used in this study. Because of these previous studies, we were expecting to see more diversity of organisms expressing *hynSL* in the higher temperature CV41 biofilm. The phylogenetic analysis of the transcripts shows three major clades of organisms expressing the *hynSL* genes (Figure 16). Furthermore, the rarefaction analysis shows more species richness in the mesophilic environment of CV9 (Figure 7). We

do see the dominant *Epsilonproteobacteria* expressing these genes, as many transcripts fall very close to *Sulfurovum*/*Sulfurimonas* coming from CV9 and *Caminibacter*/*Nautilia* coming from CV41 (Figure 16).

Conclusion. Many of the mesophilic organisms can be found in higher temperature biofilms, however no thermophilic organisms are found in the lower temperatures. These results and results from the clone libraries indicate that the metabolically versatile *Epsilonproteobacteria* make great pioneers in the newly forming biofilms. The *Epsilonproteobacteria* fix CO_2 via the rTCA cycle and express the genes necessary for utilize the redox couples available to them. These results also indicate that the *Epsilonproteobacteria* co-exist with many other active members in the biofilm communities. This is seen more in the higher temperature biofilm as the influx of seawater may create a fluctuating environment. Within their own class, mesophilic, thermophilic, microaerobic and strictly anaerobic *Epsilonproteobacteria* all seem to fill their own niche without competing for electron donors and acceptors. My results also indicate that the *Epsilonproteobacteria* interact with each other and other *Bacteria* by sharing resources and products of their metabolism with the biofilm community..

Chapter 4 – Conclusions

The knowledge gaps with regards to hydrothermal vents are slowly getting smaller (139). The benthic megafauna inhabiting the points of fluid escape were the original identifying factors for these type of ecosystems (77). This was quickly changed after the detection of white particulate spewing from the vents, determined to be chemosynthetic bacteria (62). After an eruption at a hydrothermal vent, the bacteria are the first organisms to recolonize the ecosystem. They do so along chemical gradients where chemical disequilibrium in the form of different redox couples provides them with sufficient energy to fix carbon dioxide. Following colonization by chemosynthetic microorganisms, the tubeworms and other invertebrates repopulate the vent ecosystem. The focus of my work is to understand which central metabolic pathways are expressed by the microorganisms during the colonization of the vent ecosystems.

In this thesis dissertation, my overall hypothesis for this work was that *Epsilonproteobacteria* are particularly fit to be the pioneer colonizers of diffuse flow vents because of their versatile metabolism. I attempted to find the link between pioneering microorganisms and the development of the vent ecosystem. More specifically, I also aimed to identify specific bacterial species involved in early colonization of post eruptive vents and how their metabolic diversity plays a role.

My first hypotheses stated that *the composition of the microbial biofilm communities that colonize the newly formed vents is affected by different temperature and redox regimes, and that specific chemolithoautotrophic bacteria influence the*

presence/absence of specific vent macrofauna. To test this hypothesis, I used DGGE and phylogenetic analysis of 16S rRNA genes to correlate the distribution of microorganisms with macrofaunal and environmental measurements.

The aim of this part of my PhD work, which was done in close collaboration with invertebrate biologists and vent chemists, was to identify, for the first time, correlations between microbial biofilms, fluid temperature and geochemistry and vent invertebrates. The area of diffuse flow (diffuse-flow experiments) contained higher H_2S and lower oxygen concentrations than closely located areas outside of the flow of hydrothermal fluids (no-flow controls). The diffuse-flow samples were also at a higher temperature than the no-flow controls. My results showed that the microbial communities that inhabited the diffuse-flow areas and the no-flow communities were dramatically different. The DGGE analysis alone showed similar banding patterns for diffuse-flow samples and similar, but different, fingerprints for no-flow samples. My 16S rRNA gene phylogenetic libraries confirm that the microbial communities colonizing these two habitats did indeed have different compositions. *Epsilonproteobacteria* dominated the diffuse-flow samples and *Gammaproteobacteria* dominated the no-flow samples. Siboglinid-type tubeworms only colonized biofilms that were diffuse-flow. However, not every diffuse-flow community contained tubeworm colonists. Out of the biofilms tested, the community that was less than 80% *Epsilonproteobacteria* contained one section of the colonization device that did not have any tubeworms. My findings suggest that there is some type of selective pressure dictating siboglinid tubeworm colonization. This may be accomplished via the tubeworms sensing the composition of the biofilm

through cross-kingdom communication, as what has already been described between Eukaryotes and Bacteria before (67). It may also be that tubeworm eggs land randomly in all environments, including the no-flow area, and then succeed or fail to further develop depending on where they end up. One possible explanation of the lack of tubeworms in the no-flow area may be that the biofilms of the no-flow areas were dominated by the filamentous *Gammaproteobactium, Leucothrix mucor,* known for infesting and parasitizing the eggs of higher organisms before they can hatch (65). Another possible explanation is that the low concentration of hydrogen sulfide in the no-flow sites can't support chemosynthetic primary production and the associate vent invertebrates.

My second hypothesis stated that *during the formation of biofilms, vent Epsilonproteobacteria fix carbon dioxide via the reductive tricarboxylic acid (rTCA) cycle and express genes involved in several respiratory pathways in response to different temperature and redox regimes.* To test this hypothesis, I integrated information obtained from experiments on pure cultures of *Epsilonproteobacteria* and from metatranscriptomic studies of the vent biofilms to design experiments for the detection of gene transcripts in chemosynthetic microbial biofilm communities collected from deep-sea hydrothermal vents.

The metatranscriptome samples used were 3 and 7-day old biofilms from the EPR at 13^{o}N and 9^{o}N, respectively. My analysis using MG-RAST and the previous work using MEGAN, taken from the metatranscriptome, only showed a major taxonomic difference at the genus level. All four sample sites and biofilm development times showed a dominance of *Epsilonproteobacteria*. The higher

temperature environment, taken from 13°N, contains transcripts dominated by species from the thermophilic genera *Caminibacter* and *Nautilia*. All three lower temperature environments at 9°N, contain transcripts mostly related to the mesophiles *Sulfurovum* and/or *Sulfurimonas*. This indicates that not only are the *Epsilonproteobacteria* the most abundant group of organisms in the communities, they are also the most active. Again using MG-RAST, I looked at the types of functional genes actively expressed in the biofilms. I found transcripts matching metabolic genes of interest – from the operons for periplasmic nitrate reductase (*nap*), cbb3-type cytochrome oxidase (*cco*), NiFe-type hydrogenase (*hyn*), and adenylylsulfate reductase (*apr*).

We already knew from previous work that the genes required for fixing CO_2 via the reductive tricarboxylic acid cycle (rTCA) are expressed in pure culture *Epsilonproteobacteria* (56; 165). In order to investigate this process *in-situ*, I utilized biofilms collected by the EPR to perform surveys of gene expression. Reverse transcription libraries were created from the RNA extracted from the biofilm communities. To test my hypothesis, I focused on transcripts for *aclA* (encoding for the ATP citrate lyase), as a marker for the rTCA cycle. Because the vent *Epsilonproteobacteria* have been shown to both encode and express the enzymes for rTCA cycle during autotrophic growth (56), the transcripts I detected are a good indication that the organisms in each biofilm were actively fixing CO_2 via the rTCA cycle.

To test my hypothesis that *Epsilonproteobacteria* express several respiratory pathways in response to different temperature and redox regimes, I constructed RT-

PCR clone libraries focusing on genes involved in respiratory metabolism. The genes included in this analysis were *napA* (encoding for a periplasmic nitrate reductase), *ccoN* (encoding for a cbb3-type cytochrome oxidase), *hynSL* (encoding for a NiFe-type hydrogenase), *sqrA* (encoding for sulfide quinone reductase) and *aprA* (encoding for an APS reductase). For the *napA* and *ccoN*, the transcripts were detected *in vivo* from pure culture *Epsilonproteobacteria*. The periplasmic nitrate reductase and a cbb3 cytochrome oxidase are the only known enzymes for vent *Epsilonproteobacteria* to reduce nitrate and oxygen, respectively. Therefore, I can reasonably conclude that the biofilm organisms were actively respiring nitrate and oxygen at the time of sampling. Pure cultures of *Epsilonproteobacteria* have also been shown to oxidize hydrogen (149).My *hynSL* clone libraries revealed that there are many organisms, both from the *Epsilonproteobacteria* class and outside of it, expressing the *hynSL* gene. The results for *sqrA* and *aprA* clone libraries are very exciting as I found both sulfur oxidizers and reducers in the same biofilm community.

Overall, these results show that the metabolically versatile *Epsilonproteobacteria* make great pioneers in the newly forming biofilms. The first indication is that they can dominate diffuse-flow biofilms that are subjected to steep redox gradients. They also have influence on the types of animals that colonize the area. Finally, the *Epsilonproteobacteria* fix CO_2 via the rTCA cycle and express the genes necessary for utilizing several redox couples. My data also indicate that the *Epsilonproteobacteria* co-exist with many other active members in the biofilm communities. This is seen more in the higher temperature biofilm as the influx of

seawater may create a fluctuating environment. Within their own class, mesophilic, thermophilic, microaerobic and strictly anaerobic *Epsilonproteobacteria* all seem to form their own niches without competing for electron donors and acceptors. By working as a community, filling their own niche and sharing resources with other *Bacteria*, the *Epsilonproteobacteria* dominated biofilms would have greater stability when environmental conditions change.

Appendix 1 – Addendum to Chapter 3

Introduction

In addition to studying the sulfide quinone reductase/oxidoreductase (*sqr*) and adenylylsulfate reductase (*apr*) *in situ* expression, we also wanted to include the thiosulfate oxidase (*sox*) and polysulfide reductase (*psr*). This would give us a more complete survey into the sulfur cycle in the hydrothermal vent systems. While *sqr* and *apr* work in both directions for oxidation or reduction (3; 9; 42; 97), the *sox* and *psr* are only known to work in one direction (69; 121).

The thiosulfate oxidase (*sox*) system is a series of reactions that completely oxidize thiosulfate to sulfate and polysulfides (Figure 1) (96). This system is very well studied in vent systems (54; 121). The operon and *sox* system have been identified in *Epsilonproteobacteria* dominated vent biofilms (54). The genes for thiosulfate oxidase have also been indentified in *Epsilonproteobacterial* genomes (19; 140; 171). Although a survey for *soxB* (an essential in the catalytic center; (169)) gene expression has never been performed, the Huber group at Josephine Bay Paul Center is working on a quantitative analysis of *soxB* in biofilm communities in the Juan de Fuca Ridge vent systems (unpublished).

Polysulfide reductase (*psr*) is a periplasmic, membrane-bound, protein that couples quinone oxidation with the reduction of polysulfides (69; 129). The *psr* operon is found in many thermophilic *Bacteria* and *Archaea* the live around hydrothermal vents and hot springs (4; 69). The only studies into *psr* in the *Epsilonproteobacterial* class come from the host-associated genus *Wolinella* (61).

Aside from studying how *psr* expression fits into the sulfur, this operon is of interest to us because polysulfide reduction gets coupled directly to hydrogenase activity (61). Since *psr* is found in vent *Epsilonproteobacteria* genomes (35; 171), our intent is to have the first *psr* phylogenetic analysis and expression survey in the vent system.

The goals of this part of the work included 1) linking *soxB* expression to the previous studies looking pure culture isolates and vent biofilm phylogenetic surveys; 2) surveying the biofilm communities for *psrA* expression after grounding them in pure cultures; 3) relating the gene expression of each, *soxB* and *psrA*, to the other genes expressed in biofilm communities (*aclA*, *napA*, *ccoN*, *sqrA*, *aprA*, *hynSL*); 4) developing a quantitative reverse transcription assay to elucidate the relative usage of substrates in the vent system.

Material and Methods

Biofilm sample collection. Experimental colonizers were deployed and collected from the East Pacific Rise (EPR) during rapid response dives in 2006. The colonizer designated CV9 was deployed on to an active diffuse-flow vent at 9^{o}N. The CV41 colonizer was deployed on the side of a black smoker chimney at a point of diffuse-flow. Upon collection, the meshes were removed from the solid support. Both the top and bottom portions of the colonizers were treated in RNAlater and frozen to preserve the transcripts and biomass.

Pure strains and conditions. The strains used in this study were *Caminibacter mediatlanticus* TB-2 (166) and *Sulfurimonas paralvinellae* (152). *S.*

paralvinellae was grown in MJ-N medium supplemented with KNO_3, NaS_2O_3, NaH_2CO_3 and tungstic acid with H_2/CO_2 gas in the headspace and was grown at 30°C. *C. mediatlanticus* was grown in HB-1 medium pH 5.5 at 55°C under H_2/CO_2. Each organism was grown to exponential phase. Sampling was performed using the standard conditions with alternate electron pairs. *S. paralvinellae* was grown with $S_2O_3^=$, H_2/CO_2 gas and KNO_3, $S_2O_3^=$ and $H_2/CO_2/O_2$, S^0, H_2/CO_2 and KNO_3, or $S_2O_3^=$, N_2/CO_2 and KNO_3. *C. mediatlanticus was* grown with H_2/CO_2 and KNO_3 or H_2/CO_2 and S^0.

RNA extraction. For biofilm community analysis, total RNA was extracted from the stored RNAlater samples. The steel meshes were thawed briefly just to the point where pieces of the biofilm could be sterilely chipped off. The RNA was then extracted using a RNAeasy kit (Qiagen) and the manufacturer's protocol. For pure culture samples, RNA from late exponential phase cultures was extracted by first pelleting the cells and then performing an extraction using the RNAeasy kit (Qiagen). For these samples, the amount of reagents was scaled depending on the size of the pellet. At minimum, twice the amount of lysozyme, RLT and ethanol was used for resuspension and lysis steps. For cultures containing S^0, up to 6 times the amount of lysozyme, RLT and ethanol were utilized, as well as the optional step for removing debris. In each case, the entire lysed sample was loaded on to a single spin column after multiple spins. The rest of the extraction was performed using the manufacturer's protocol. Residual genomic DNA was removed from all samples with a TURBODNAse kit (Ambion). The only modification to the protocol was incubating twice for 30 min at 37°C adding 0.5 ul of DNAse before each incubation. The samples

were further checked for residual DNA contamination by PCR with bacterial universal 16S rRNA gene primers. PCR conditions for 16S rRNA gene amplification reactions were as follow: 35 cycles of denaturation at 94°C for 30 s, annealing at 50°C for 30 s, and extension at 72°C for 30 s with a final extension time of 5 min.

Polymerase chain reaction. Primers for *soxB* were soxB432F (5'-GAYGGNGGNGAYCANTGG-3') and soxB1446R (5'-TTRTCNGCNACRTCYTC-3') (121). The *soxB* reactions used a touchdown of 10 cycles with 53°C annealing temperature, followed by 25 cycles at 47°C (121). The *psrA* primers, PsrA995-Forward (5'-AYACNCCDGARTGGGC-3') and PsrA2703-Reverse (5'-TYACACCYTYCTWAKYKYWAC-3'), were created off of an alignment including all pure culture *Epsilonproteobacteria* containing the gene. The *psrA* reactions were optimized to use 40 cycles with an annealing temperature of 48°C. The RT-PCR reactions were performed utilizing the One-Step Reverse Transcription kit (Invitrogen). The positive control for each gene was either *S. lithotrophicum* or *C. mediatlanticus* genomic. After each sample was mixed, 10 µl was removed and placed in a separate tube to be run without the reverse transcription step (30 min hold at 55°C) as a no-RT control. The reactions were set up according to the manufacturer's protocol with the exception of the primers and annealing temperatures adjusted for each functional gene. PCR reactions for optimizing qPCR primers were optimized using either *S. lithotrophicum* or *C. mediatlanticus* genomic DNA as controls. The primers and PCR conditions for the quantitative analysis are located in Table 1.

Construction of clone libraries. Immediately upon completion of the RT-PCRs on biofilm community samples, the products were sub-cloned into pCR4-TOPO using a TOPO-TA cloning kit (Invitrogen) and the manufacturer's protocol. The ligations were incubated at room temperature before being transformed into One-Shot Top10 *Escherichia coli* cells (Invitrogen). The only modification to the procedure was the use of LB media in place of SOC.

Restriction fragment length polymorphism (RFLP) analysis. Libraries were screened via RFLP to determine the amount of diversity in each sample and to consolidate the number of clones that would need to be sequenced. The isolated clones were first cultured and then subjected PCR using the associated primers and cycle parameters (Table 1). RFLP conditions were as previously reported (80). Reactions were run on 3% Metaphor Agarose (Lonza) gels for 90 min at 75 volts.

Nucleotide Sequence Analysis. Clones from libraries were selected for sequencing based primarily on unique fingerprints in the RFLP analysis. As only one RFLP pattern was present for *soxB* clone libraries, multiple clones were sent for sequencing. The plasmids were extracted from liquid cultures using a Spin Miniprep kit (Qiagen) and the manufacturer's protocol. All of the DNA sequencing was outsourced to GENEWIZ (South Plainfield, NJ). Sequences were assembled with AutoAssembler Program (Applied Biosystems) analyzed using 4Peaks (www.mekentosj.com). The assembled fragments were assessed using the NCBI Basic Local Alignment Search Tool (BLAST).

Results

Analysis of *soxB* transcripts. Previous studies, by Hügler *et. al.*, focused on distribution of *soxB* genes in biofilms located at the Logatchev hydrothermal vent (54). They found that ~75% of the biofilms organisms with *soxB* in their genomes were *Epsilonproteobacteria* (54). From each community, CV9 and CV41, 40 clones were picked after RT-PCR, ligation and transformation into *E. coli* Top10. All 40 clones contained the correct size insert. RFLP analysis resulted in each clone having the same fingerprint. The samples picked for sequencing were determined to be from a 23S rRNA gene.

Analysis of *psrA* transcripts. The *psrA* degenerate primers were optimized using *C. mediatlanticus* genomic DNA. The same conditions did not give consistent results when focusing on mRNA transcripts. Without having a functional procedure for working with *psrA* mRNA, the experiment was not continued into the biofilm community samples.

Quantitative PCR optimization. Primer sets for quantitative analysis were developed based on alignments of pure culture *Epsilonproteobacterial* sequences and environment samples from clone libraries. The degeneracy of each primer was kept below 512 variations. All of the primer sets were optimized to produce one amplicon from pure culture genomic DNA. These amplicons were all sequenced and verified to be from the correct gene and organism. The optimized conditions are listed in Table 1.

Discussion

For both *soxB* and *psrA* reactions, it was clear that the primers would need adjustments before being used on mRNA transcripts. In the case of *soxB*, the reactions produced an amplicon related to 23S rRNA. Most rRNA removal kits are focused on 16S rRNA removal. We will either have to find a kit optimized for 23S rRNA removal or redesign the primers to make them more specific to *Epsilonproteobacteria*. The *psrA* primer set most likely created an amplicon that was too large for the reverse transcriptase to completely reverse transcribe before falling off. Our future experiments involving *psrA* will focus on amplifying fragments <1200 basepairs, as that size seems to work well with our current methods.

All of the other *Epsilonproteobacterial* genes used in our metabolic surveys, *aclA*, *napA*, *ccoN*, *sqrA*, and *hynSL*, now have quantitative primers developed for future experiments. These will be used to test relative expression levels in *Epsilonproteobacterial*-dominated biofilms. As the primers were created using just *Epsilonproteobacterial* sequences, any community analyses will take into account that in some cases (e.g. *hynSL* and *sqrA*), the biofilm communities have a significant portion of the total expression occurring from non-*Epsilonproteobacteria*. *Epsilonproteobacteria* were the primary organisms expressing *aclA, napA,* and especially *ccoN* from the *in situ* biofilm communities. These primers would also be useful for pure culture experiments involving alternate redox couples. We plan to investigate metabolic gene regulation in time course growth experiments.

Table 5. Primers used in this study

Primer name	Primer Sequence	Expected length	Annealing Temp	Reference
16S361F*	TCC TAC GGG AGG CAG C	155	47 ^{o}Cx40	This study
16S515R*	GCA CGG AGT TAG CCG G			
AclA409F	TGT ACD ATY TCY GAY GAY MGR GG	190	49 ^{o}Cx10; 47 ^{o}Cx40	This study
AclA598R	SHC CRT GGT CKG CDA CWG			
CcoN180F	CCV TCH TGG GGW WSW GC	184	50 ^{o}Cx10; 48 ^{o}Cx40	This study
CcoN363R	SRA TCC ART CNG TRA AGT GWG C			
Hyn1641F	MRT CWC KWG GGT CHC KYC C	141	49 ^{o}Cx10; 47 ^{o}Cx40	This study
Hyn1781R	ACC CNR TWA CMA GRA THG ARG G			
NapA341F	AAY GCH MGW CAC TGT ATG GC	134	49 ^{o}Cx10; 47 ^{o}Cx40	This study
NapA474R	YTC HGC CAT RTT NGM WCC CC			
SqrA546F	YAC HTG YCA RGG DGC NGC	132	49 ^{o}Cx10; 47 ^{o}Cx40	This study
SqrA677R	CCR SCS ATD CCD AAR TCD C			
SqrA682F	GGH GAY TTH GGW ATS GSH GG	215	49 ^{o}Cx10; 47 ^{o}Cx40	This study
SqrA896R	GGH GGD ATD RRC ATW GCA AAR TC			

*16S rRNA gene primers were constructed using an alignment of pure culture *Epsilonproteobacterial* sequence from genbank.

± All other primers were created from alignments using clones from phylogenetic trees from Chapter 4 along with both *Sulfurovum* NBC37-1 and *Caminibacter mediatlanticus* TB-2 sequences taken from their respectively genomes. The primers for *ccoN* did not include *Caminibacter mediatlanticus* in the alignment.

Appendix 2: Closest relatives for clone libraries obtained in Chapter 3

gene	CV	Clone #	#same RFLP patterns	Closest relative	%identity	Accession#
aclA	9	3	1	Sulfurimonas autotrophica DSM 16294	83%	YP_003892636.1
aclA	9	13	1	Sulfurimonas autotrophica DSM 16294	86%	YP_003892636.1
aclA	9	15	1	Sulfurimonas autotrophica DSM 16294	65%	YP_003892636.1
aclA	9	19	1	Hydrogenimonas thermophila	70%	ABV48825.1
aclA	9	27	1	Sulfurimonas autotrophica DSM 16294	50%	YP_003892636.1
aclA	9	28	1	Sulfurimonas autotrophica DSM 16294	69%	YP_003892636.1
aclA	9	32	1	Sulfurimonas autotrophica DSM 16294	84%	YP_003892636.1
aclA	9	34	1	Sulfurimonas autotrophica DSM 16294	85%	YP_003892636.1
aclA	9	39	1	Sulfurimonas autotrophica DSM 16294	85%	YP_003892636.1
aclA	9	46	1	Sulfurimonas autotrophica DSM 16294	76%	YP_003892636.1
aclA	9	49	1	Sulfurimonas autotrophica DSM 16294	75%	YP_003892636.1
aclA	9	50	1	Sulfurimonas autotrophica DSM 16294	86%	YP_003892636.1
aclA	9	51	1	Sulfurimonas autotrophica DSM 16294	82%	YP_003892636.1
aclA	9	57	1	Sulfurimonas autotrophica DSM 16294	70%	YP_003892636.1
aclA	9	68	1	Sulfurovum lithotrophicum	90%	ABV48828.1
aclA	9	74	1	Sulfurimonas autotrophica DSM 16294	72%	YP_003892636.1
aclA	41	1	1	Caminibacter mediatlanticus TB-2	88%	ZP_01872360.1
aclA	41	2	1	Thermovibrio ammonificans	98%	ABI50081.1
aclA	41	4	1	Caminibacter mediatlanticus TB-2	88%	ZP_01872360.1
aclA	41	5	1	Caminibacter mediatlanticus TB-2	87%	ZP_01872360.1
aclA	41	7	1	Thermovibrio ammonificans	98%	ABI50081.1
aclA	41	11	1	Caminibacter mediatlanticus TB-2	88%	ZP_01872360.1
aclA	41	12	1	Caminibacter mediatlanticus TB-2	88%	ZP_01872360.1
aclA	41	14	1	Nitratifractor salsuginis DSM 16511	89%	YP_004167594.1
aclA	41	20	1	Caminibacter mediatlanticus TB-2	87%	ZP_01872360.1
aclA	41	21	1	Nitratifractor salsuginis DSM 16511	89%	YP_004167594.1
aclA	41	24	1	Caminibacter mediatlanticus TB-2	87%	ZP_01872360.1
aclA	41	25	1	Thermovibrio ammonificans	87%	ABI50081.1
aclA	41	30	1	Caminibacter mediatlanticus TB-2	88%	ZP_01872360.1
aclA	41	31	1	Caminibacter mediatlanticus TB-2	87%	ZP_01872360.1
aclA	41	32	1	Caminibacter mediatlanticus TB-2	88%	ZP_01872360.1
aclA	41	35	1	Caminibacter mediatlanticus TB-2	91%	ZP_01872360.1
aclA	41	36	1	Caminibacter mediatlanticus TB-2	87%	ZP_01872360.1
aclA	41	39	1	Caminibacter mediatlanticus TB-2	87%	ZP_01872360.1

aclA	41	40	1	Caminibacter mediatlanticus TB-2	86%	ZP_01872360.1
aprA	9	1	1	Desulfocapsa sulfexigens	95%	AAL57398.1
aprA	9	2	1	Desulfocapsa thiozymogenes DSM 7269	90%	ABR92531.1
aprA	9	3	1	Thermochromatium tepidum	93%	ABV80058.1
aprA	9	4	1	Thermochromatium tepidum	93%	ABV80058.1
aprA	9	5	1	Thermochromatium tepidum	94%	ABV80058.1
aprA	9	7	1	Thermochromatium tepidum	91%	ABV80058.1
aprA	9	8	1	Desulfocapsa sulfexigens	94%	AAL57398.1
aprA	9	9	1	Desulfobulbus marinus	96%	ABR92523.1
aprA	9	10	1	Desulfocapsa thiozymogenes DSM 7269	96%	ABR92531.1
aprA	9	12	1	Allochromatium warmingii	92%	ABV80048.1
aprA	9	16	1	Allochromatium warmingii	93%	ABV80048.1
aprA	41	2	1	Desulfobulbus sp. DSM 2033	98%	ABR92527.1
aprA	41	3	1	Archaeoglobus profundus DSM 5631	96%	AAL57401.1
aprA	41	4	1	Allochromatium warmingii	93%	ABV80048.1
aprA	41	6	1	Thermochromatium tepidum	93%	ABV80058.1
aprA	41	7	1	Archaeoglobus profundus DSM 5631	95%	AAL57401.1
aprA	41	8	1	Archaeoglobus profundus DSM 5631	95%	AAL57401.1
aprA	41	9	1	Archaeoglobus profundus DSM 5631	95%	AAL57401.1
aprA	41	10	1	Thermochromatium tepidum	93%	ABV80058.1
aprA	41	11	1	AprA [Thiococcus pfennigii]	91%	ABV80070.1
aprA	41	12	1	Thermochromatium tepidum	94%	ABV80058.1
aprA	41	13	1	Archaeoglobus profundus DSM 5631	96%	AAL57401.1
ccoN	9	1	7	Sulfurovum sp. NBC37-1	94%	YP_001357495.1
ccoN	9	8	3	Arcobacter sp. L	87%	YP_005554769.1
ccoN	9	64	2	Sulfurimonas autotrophica DSM 16294	93%	YP_003893020.1
ccoN	9	38	1	Sulfurimonas autotrophica DSM 16294	94%	YP_003893020.1
ccoN	9	24	1	Nitratifractor salsuginis DSM 16511	94%	YP_004168931.1
ccoN	9	2	17	Arcobacter sp. L	88%	YP_005554769.1
ccoN	9	5	2	Arcobacter sp. L	91%	YP_005554769.1
ccoN	9	20	6	Sulfurimonas gotlandica GD1	92%	ZP_05070516.1
ccoN	9	6	7	Arcobacter sp. L	91%	YP_005554769.1
ccoN	9	26	1	Arcobacter butzleri RM4018	87%	YP_001490968.1
ccoN	9	18	2	Sulfurimonas autotrophica DSM 16294	89%	YP_003893020.1
ccoN	9	39	4	Arcobacter sp. L	91%	YP_005554769.1
ccoN	9	47	2	Sulfurovum sp. NBC37-1	95%	YP_001357495.1
ccoN	9	52	3	Sulfurimonas autotrophica DSM 16294	89%	YP_003893020.1
ccoN	9	62	3	Sulfurimonas autotrophica DSM 16294	88%	YP_003893020.1
ccoN	41	1	1	Thiovulum sp. ES	87%	ZP_10404729.1

ccoN	41	8	2	Sulfurimonas autotrophica DSM 16294	88%	YP_003893020.1
ccoN	41	9	1	Arcobacter butzleri RM4018	87%	YP_001490968.1
ccoN	41	12	11	Sulfurimonas autotrophica DSM 16294	94%	YP_003893020.1
ccoN	41	15	3	Sulfurimonas autotrophica DSM 16294	93%	YP_003893020.1
ccoN	41	20	11	Sulfurovum sp. NBC37-1	94%	YP_001357495.1
ccoN	41	24	8	Nitratifractor salsuginis DSM 16511	94%	YP_004168931.1
ccoN	41	26	2	Arcobacter sp. L	88%	YP_005554769.1
ccoN	41	32	1	Nitratiruptor sp. SB155-2	93%	YP_001357081.1
ccoN	41	41	4	Arcobacter sp. L	87%	YP_005554769.1
ccoN	41	47	1	Sulfurimonas autotrophica DSM 16294	93%	YP_003893020.1
ccoN	41	50	1	Sulfurimonas autotrophica DSM 16294	95%	YP_003893020.1
ccoN	41	55	7	Sulfurospirillum barnesii SES-3	88%	YP_006404887.1
ccoN	41	57	1	Arcobacter sp. L	86%	YP_005554769.1
ccoN	41	60	1	Sulfurimonas autotrophica DSM 16294	87%	YP_003893020.1
ccoN	41	62	1	Arcobacter sp. L	89%	YP_005554769.1
ccoN	41	64	6	Arcobacter sp. L	91%	YP_005554769.1
ccoN	41	67	1	Arcobacter sp. L	91%	YP_005554769.1
ccoN	41	70	3	Sulfurimonas gotlandica GD1	92%	ZP_05070516.1
ccoN	41	72	1	Arcobacter butzleri RM4018	87%	YP_001490968.1
hynSL	9	11	2	Sulfurimonas denitrificans DSM 1251	83%	YP_393947.1
hynSL	9	14	4	Sulfurimonas denitrificans DSM 1251	84%	YP_393947.1
hynSL	9	17	3	Sulfurimonas denitrificans DSM 1251	82%	YP_393947.1
hynSL	9	24	2	Desulfocapsa sulfexigens DSM 10523	97%	YP_007467378.1
hynSL	9	25	4	Sulfurimonas denitrificans DSM 1251	83%	YP_393947.1
hynSL	9	100	1	Sulfurimonas denitrificans DSM 1251	79%	YP_393947.1
hynSL	9	101	3	Sulfurimonas paralvinella	86%	BAE44407.1
hynSL	9	102	3	Sulfurimonas denitrificans DSM 1251	82%	YP_393947.1
hynSL	9	103	1	Sulfurovum sp. NBC37-1	85%	YP_001358969.1
hynSL	9	106	5	Sulfurovum sp. NBC37-1	84%	YP_001358969.1
hynSL	9	107	2	Desulfocapsa sulfexigens DSM 10523	94%	YP_007467378.1
hynSL	9	108	3	Sulfurimonas denitrificans DSM 1251	79%	YP_393947.1
hynSL	9	109	2	Sulfurimonas denitrificans DSM 1251	81%	YP_393947.1
hynSL	9	111	1	Sulfurimonas denitrificans DSM 1251	82%	YP_393947.1
hynSL	9	112	2	Desulfocapsa sulfexigens DSM 10523	82%	YP_007467378.1
hynSL	9	115	1	Sulfurimonas denitrificans DSM 1251	82%	YP_393947.1
hynSL	9	117	1	Sulfurimonas denitrificans DSM 1251	84%	YP_393947.1
hynSL	9	119	1	Sulfurimonas denitrificans DSM 1251	82%	YP_393947.1
hynSL	9	121	2	Sulfurimonas denitrificans DSM 1251	83%	YP_393947.1
hynSL	9	122	1	Sulfurimonas denitrificans DSM 1251	79%	YP_393947.1

hynSL	9	125	2	Sulfurimonas denitrificans DSM 1251	81%	YP_393947.1
hynSL	9	126	6	Sulfurovum sp. NBC37-1	85%	YP_001358969.1
hynSL	9	127	2	Desulfocapsa sulfexigens DSM 10523	93%	YP_007467378.1
hynSL	9	130	2	Sulfurimonas denitrificans DSM 1251	82%	YP_393947.1
hynSL	9	134	1	Sulfurimonas denitrificans DSM 1251	82%	YP_393947.1
hynSL	41	1	1	Nautilia profundicola AmH]	76%	YP_002606991.1
hynSL	41	2	3	Thermovibrio ammonificans HB-1	93%	YP_004151729.1
hynSL	41	5	16	Nautilia profundicola AmH]	81%	YP_002606991.1
hynSL	41	14	1	Thermovibrio ammonificans HB-1	93%	YP_004151729.1
hynSL	41	21	1	Thermovibrio ammonificans HB-1	93%	YP_004151729.1
hynSL	41	22	1	Thermovibrio ammonificans HB-1	90%	YP_004151729.1
hynSL	41	23	1	Caminibacter mediatlanticus TB-2	68%	ZP_01871474.1
hynSL	41	25	1	Thermovibrio ammonificans HB-1	91%	YP_004151729.1
hynSL	41	102	1	Nautilia profundicola AmH]	83%	YP_002606991.1
hynSL	41	103	1	Caminibacter mediatlanticus TB-2	83%	ZP_01871474.1
hynSL	41	104	4	Nautilia profundicola AmH]	80%	YP_002606991.1
hynSL	41	105	4	Thermovibrio ammonificans HB-1	94%	YP_004151729.1
hynSL	41	106	8	Thermovibrio ammonificans HB-1	93%	YP_004151729.1
hynSL	41	107	8	Thermovibrio ammonificans HB-1	90%	YP_004151729.1
hynSL	41	116	1	Thermovibrio ammonificans HB-1	89%	YP_004151729.1
hynSL	41	119	1	Thermovibrio ammonificans HB-1	90%	YP_004151729.1
hynSL	41	121	1	Nautilia profundicola AmH]	81%	YP_002606991.1
hynSL	41	134	1	Nautilia profundicola AmH]	81%	YP_002606991.1
hynSL	41	127	1	Thermovibrio ammonificans HB-1	94%	YP_004151729.1
hynSL	41	128	1	Caminibacter mediatlanticus TB-2	83%	ZP_01871474.1
hynSL	41	129	1	Caminibacter mediatlanticus TB-2	81%	ZP_01871474.1
hynSL	41	139	1	Thermovibrio ammonificans HB-1	91%	YP_004151729.1
napA	9	1	1	Sulfurimonas paralvinellae	80%	ABV30920.1
napA	9	2	1	Sulfurovum sp. NBC37-1	88%	YP_001357616.1
napA	9	4	7	Arcobacter sp. L	81%	YP_005552684.1
napA	9	5	16	Sulfurovum sp. NBC37-1	91%	YP_001357616.1
napA	9	13	1	Arcobacter sp. L	83%	YP_005552684.1
napA	9	14	1	Arcobacter sp. L	80%	YP_005552684.1
napA	41	16	1	Arcobacter sp. L	82%	YP_005552684.1
napA	9	17	1	Sulfurovum sp. NBC37-1	83%	YP_001357616.1
napA	9	21	1	Sulfurovum sp. NBC37-1	84%	YP_001357616.1
napA	9	26	1	Arcobacter sp. L	82%	YP_005552684.1
napA	9	30	1	Sulfurovum sp. NBC37-1	83%	YP_001357616.1
napA	9	32	1	Sulfurovum sp. NBC37-1	89%	YP_001357616.1

napA	41	33	1	Helicobacter bizzozeronii CCUG 35545	74%	ZP_16313031.1
napA	9	35	1	Sulfurovum sp. NBC37-1	82%	YP_001357616.1
napA	9	37	1	Arcobacter sp. L	82%	YP_005552684.1
napA	41	2	5	Caminibacter mediatlanticus TB-2	90%	ZP_01871445.1
napA	41	3	12	Caminibacter hydrogeniphilus	84%	ABV48844.1
napA	41	4	1	Caminibacter hydrogeniphilus	84%	ABV48844.1
napA	41	8	3	Sulfurovum sp. NBC37-1	82%	YP_001357616.1
napA	41	12	1	Caminibacter hydrogeniphilus	94%	ABV48844.1
napA	41	13	3	Nitratifractor salsuginis DSM 16511	85%	YP_004168605.1
napA	41	14	1	Sulfurovum sp. NBC37-1	81%	YP_001357616.1
napA	41	15	1	Caminibacter hydrogeniphilus	89%	ABV48844.1
napA	41	17	1	Sulfurovum sp. NBC37-1	88%	YP_001357616.1
napA	41	21	1	Caminibacter hydrogeniphilus	82%	ABV48844.1
napA	41	30	1	Nautilia profundicola AmH	93%	YP_002606972.1
napA	41	38	1	Sulfurimonas denitrificans DSM 1251	80%	YP_394026.1
napA	41	40	1	Caminibacter hydrogeniphilus	83%	ABV48844.1
sqrA	9	8	1	Sulfurimonas autotrophica DSM 16294	84%	YP_003892602.1
sqrA	9	9	2	Sulfurimonas autotrophica DSM 16294	83%	YP_003892602.1
sqrA	9	10	1	Sulfurimonas autotrophica DSM 16294	75%	YP_003892602.1
sqrA	9	15	4	Sulfurovum sp. NBC37-1	74%	YP_001357509.1
sqrA	9	19	2	Sulfurimonas autotrophica DSM 16294	84%	YP_003892602.1
sqrA	9	22	10	Sulfurovum sp. NBC37-1	83%	YP_001357509.1
sqrA	9	26	2	Sulfurimonas autotrophica DSM 16294	84%	YP_003892602.1
sqrA	9	27	2	Sulfurimonas autotrophica DSM 16294	83%	YP_003892602.1
sqrA	9	28	1	Sulfurimonas autotrophica DSM 16294	73%	YP_003892602.1
sqrA	9	38	28	Sulfurimonas autotrophica DSM 16294	80%	YP_003892602.1
sqrA	9	44	5	Sulfurimonas autotrophica DSM 16294	81%	YP_003892602.1
sqrA	9	46	3	Sulfurimonas autotrophica DSM 16294	75%	YP_003892602.1
sqrA	9	65	3	Sulfurimonas autotrophica DSM 16294	83%	YP_003892602.1
sqrA	9	67	1	Sulfurimonas autotrophica DSM 16294	80%	YP_003892602.1
sqrA	9	72	2	Sulfurimonas autotrophica DSM 16294	82%	YP_003892602.1
sqrA	9	82	2	Sulfurimonas autotrophica DSM 16294	85%	YP_003892602.1
sqrA	9	87	1	Sulfurovum sp. NBC37-1	83%	YP_001357509.1
sqrA	9	92	1	Sulfurimonas autotrophica DSM 16294	83%	YP_003892602.1
sqrA	9	96	1	Sulfurimonas autotrophica DSM 16294	84%	YP_003892602.1
sqrA	9	99	2	Sulfurovum sp. NBC37-1	84%	YP_001357509.1
sqrA	9	101	1	Sulfurimonas autotrophica DSM 16294	84%	YP_003892602.1
sqrA	9	107	1	Sulfurovum sp. NBC37-1	81%	YP_001357509.1
sqrA	9	108	1	Sulfurimonas autotrophica DSM 16294	82%	YP_003892602.1

sqrA	9	111	1	Sulfurimonas autotrophica DSM 16294	85%	YP_003892602.1
sqrA	9	116	1	Sulfurovum sp. NBC37-1	83%	YP_001357509.1
sqrA	9	119	2	Sulfurimonas autotrophica DSM 16294	87%	YP_003892602.1
sqrA	9	121	1	Sulfurovum sp. NBC37-1	80%	YP_001357509.1
sqrA	9	125	1	Sulfurimonas autotrophica DSM 16294	84%	YP_003892602.1
sqrA	9	126	18	Sulfurimonas autotrophica DSM 16294	87%	YP_003892602.1
sqrA	9	129	1	Sulfurovum sp. NBC37-1	81%	YP_001357509.1
sqrA	41	1	11	Sulfurimonas autotrophica DSM 16294	84%	YP_003892602.1
sqrA	41	3	28	Caminibacter mediatlanticus TB-2	78%	ZP_01871251.1
sqrA	41	6	1	Sulfurimonas autotrophica DSM 16294	84%	YP_003892602.1
sqrA	41	7	2	Chlorobium chlorochromatii CaD3	67%	YP_379190.1
sqrA	41	12	1	Caminibacter mediatlanticus TB-2	91%	ZP_01871251.1
sqrA	41	16	3	Sulfurovum sp. NBC37-1	85%	YP_001357509.1
sqrA	41	19	2	Sulfurovum sp. NBC37-1	86%	YP_001357509.1
sqrA	41	33	2	Sulfurimonas autotrophica DSM 16294	79%	YP_003892602.1
sqrA	41	34	2	Sulfurovum sp. NBC37-1	85%	YP_001357509.1
sqrA	41	35	3	Sulfurovum sp. NBC37-1	80%	YP_001357509.1
sqrA	41	42	1	Sulfurimonas autotrophica DSM 16294	88%	YP_003892602.1
sqrA	41	47	1	Caminibacter mediatlanticus TB-2	83%	ZP_01871251.1

References

1. Alain, K., M. Zbinden, N. Le Bris, F. Lesongeur, J. Querellou, F. Gaill and M. A. Cambon-Bonavita (2004). Early steps in microbial colonization processes at deep-sea hydrothermal vents. Environmental Microbiology **6**(3): 227-241.

2. Bach, W. and G. L. Frueh-Green (2010). Alteration of the Oceanic Lithosphere and Implications for Seafloor Processes. Elements **6**(3): 173-178.

3. Blazejak, A., C. Erseus, R. Amann and N. Dubilier (2005). Coexistence of bacterial sulfide oxidizers, sulfate reducers, and spirochetes in a gutless worm (Oligochaeta) from the Peru margin. Applied and Environmental Microbiology **71**(3): 1553-1561.

4. Blochl, E., R. Rachel, S. Burggraf, D. Hafenbradl, H. W. Jannasch and K. O. Stetter (1997). Pyrolobus fumarii, gen. and sp. nov., represents a novel group of archaea, extending the upper temperature limit for life to 113 degrees C. Extremophiles **1**(1): 14-21.

5. Bonatti, E., Guerstein-Honnorez, B.-M., Honnorez, J. (1976). Copper-iron sulfide mineralizations from the equatorial Mid-Atlantic Ridge. Economic Geology **71**: 1515-1525.

6. Bond, A. M., Jones, R.D. (1980). The analytical performance of direct current, normal pulse and differential polarography with static mercury drop electrodes. Analytica Chimica Acta **121**: 1-11.

7. Brendel, P. J. and G. W. Luther (1995). Development of a Gold Amalgam Voltammetric Microelectrode for the Determination of Dissolved Fe, Mn, O-2, and S(-Ii) in Porewaters of Marine and Fresh-Water Sediments. Environmental Science & Technology **29**(3): 751-761.

8. Bright, M. and S. Bulgheresi (2010). A complex journey: transmission of microbial symbionts. Nature Reviews Microbiology **8**(3): 218-230.

9. Brito, J. A., F. L. Sousa, M. Stelter, T. M. Bandeiras, C. Vonrhein, M. Teixeira, M. M. Pereira and M. Archer (2009). Structural and Functional Insights into Sulfide:Quinone Oxidoreductase. Biochemistry **48**(24): 5613-5622.

10. Brock, T. D. (1966). The Habitat of Leucothrix Mucor, a Widespread Marine Microorganism. Limnology and Oceanography **11**(2): 303-307.

11. Campbell, B. J. and S. C. Cary (2004). Abundance of reverse tricarboxylic acid cycle genes in free-living microorganisms at deep-sea hydrothermal vents. Applied and Environmental Microbiology **70**(10): 6282-6289.

12. Campbell, B. J., A. S. Engel, M. L. Porter and K. Takai (2006). The versatile epsilon-proteobacteria: key players in sulphidic habitats. Nature Reviews Microbiology **4**(6): 458-468.

13. Campbell, B. J., C. Jeanthon, J. E. Kostka, G. W. Luther and S. C. Cary (2001). Growth and phylogenetic properties of novel bacteria belonging to the epsilon subdivision of the Proteobacteria enriched from Alvinella pompejana and deep-sea hydrothermal vents. Applied and Environmental Microbiology **67**(10): 4566-4572.

14. Campbell, B. J., J. L. Smith, T. E. Hanson, M. G. Klotz, L. Y. Stein, C. K. Lee, D. Y. Wu, J. M. Robinson, H. M. Khouri, J. A. Eisen and S. C. Cary (2009). Adaptations to Submarine Hydrothermal Environments Exemplified by the Genome of Nautilia profundicola. Plos Genetics **5**(2).

15. Campbell, B. J., J. L. Stein and S. C. Cary (2003). Evidence of chemolithoautotrophy in the bacterial community associated with Alvinella pompejana, a hydrothermal vent polychaete. Applied and Environmental Microbiology **69**(9): 5070-5078.

16. Carbotte, S. and K. C. Macdonald (1994). Comparison of seafloor tectonic fabric at intermediate, fast, and super fast spreading ridges: Influence of spreading rate, plate motions, and ridge segmentation on fault patterns. Journal of Geophysical Research **99**(B7): 13609-13631.

17. Chor, B., M. D. Hendy and S. Snir (2006). Maximum likelihood Jukes-Cantor triplets: Analytic solutions. Molecular Biology and Evolution **23**(3): 626-632.

18. Clarke, K. R. and R. M. Warwick (2001). A further biodiversity index applicable to species lists: variation in taxonomic distinctness. Marine Ecology-Progress Series **216**: 265-278.

19. Class, U. G., S. M. Sievert, K. M. Scott, M. G. Klotz, P. S. G. Chain, L. J. Hauser, J. Hemp, M. Hugler, M. Land, A. Lapidus, F. W. Larimer, S. Lucas, S. A. Malfatti, F. Meyer, I. T. Paulsen, Q. Ren and J. Simon (2007). The Genome of the Epsilonproteobacterial Chemolithoautotroph Sulfurimonas dentrificans. Journal Name: Applied and Environmental Microbiology; Journal Volume: 74; Journal Issue: 4; Related Information: Journal Publication Date: February 2008: Medium: ED; Size: 61.

20. Cline, J. D. (1969). Spectrophotometric determination of hydrogen sulfide in natural waters. Limnology and Oceanography **14**(3): 454-458.

21. Comtet, T., D. Jollivet, A. Khripounoff, M. Segonzac and D. R. Dixon (2000). Molecular and morphological identification of settlement-stage vent mussel larvae, Bathymodiolus azoricus (Bivalvia : Mytilidae), preserved in situ at active vent fields on the Mid-Atlantic Ridge. Limnology and Oceanography **45**(7): 1655-1661.

22. Corre, E., A. L. Reysenbach and D. Prieur (2001). epsilon-Proteobacterial diversity from a deep-sea hydrothermal vent on the Mid-Atlantic Ridge. Fems Microbiology Letters **205**(2): 329-335.

23. Cowen, J. P., Glazer, B., Fornari, D.J., Shank, T.M., Soule, S.A., Love, B., Treusch, A., Pomrainig, K.R., Holmes, R.C., Tolstoy, M., Baker, E.T. (2007). Volcanic eruptions at East Pacific Rise near 9°50′N. Eos Trans. AGU **88**(7).

24. Deutscher, M. P. (2006). Degradation of RNA in bacteria: comparison of mRNA and stable RNA. Nucleic Acids Research **34**(2): 659-666.

25. Edwards, K. J., W. Bach and T. M. McCollom (2005). Geomicrobiology in oceanography: microbe-mineral interactions at and below the seafloor. Trends in Microbiology **13**(9): 449-456.

26. Ferrini, V. L., D. J. Fornari, T. M. Shank, J. C. Kinsey, M. A. Tivey, S. A. Soule, S. M. Carbotte, L. L. Whitcomb, D. R. Yoerger and J. Howland (2007). Submeter bathymetric mapping of volcanic and hydrothermal features on the East Pacific Rise crest at 9-degrees 50'N. Geochemistry Geophysics Geosystems **8**(1): 1-33.

27. Fisher, A. T. and K. Becker (2000). Channelized fluid flow in oceanic crust reconciles heat-flow and permeability data. Nature **403**(6765): 71-74.

28. Fisher, C. R., K. Takai and N. Le Bris (2007). Hydrothermal Vent Ecosystems. Oceanography **20**(1): 14-23.

29. Flanagan, D. A., L. G. Gregory, J. P. Carter, A. Karakas-Sen, D. J. Richardson and S. Spiro (1999). Detection of genes for periplasmic nitrate reductase in nitrate respiring bacteria and in community DNA. Fems Microbiology Letters **177**(2): 263-270.

30. France, S. C. and T. D. Kocher (1996). DNA sequencing of formalin-fixed crustaceans from archival research collections. Molecular Marine Biology and Biotechnology **5**(4): 304-313.

31. Friedrich, C. G., F. Bardischewsky, D. Rother, A. Quentmeier and J. Fischer (2005). Prokaryotic sulfur oxidation. Current Opinion in Microbiology **8**(3): 253-259.

32. Friedrich, C. G., D. Rother, F. Bardischewsky, A. Quentmeier and J. Fischer (2001). Oxidation of reduced inorganic sulfur compounds by bacteria: Emergence of a common mechanism? Applied and Environmental Microbiology **67**(7): 2873-2882.

33. Galtier, N., Gouy, M., Gaultier, C. (1996). Seaview and Phylo_Win: two graphic tools for sequence alignment and molecular phylogeny. Computer Applications In The Biosciences **12**: 543-548.

34. Gillan, D. C. and N. Dubilier (2004). Novel epibiotic Thiothrix bacterium on a marine amphipod. Applied and Environmental Microbiology **70**(6): 3772-3775.

35. Giovannelli, D., S. Ferriera, J. Johnson, S. Kravitz, I. Perez-Rodriguez, J. Ricci, C. O'Brien, J. W. Voordeckers, E. Bini and C. Vetriani (2011). Draft genome sequence of Caminibacter mediatlanticus strain TB-2(T), an epsilonproteobacterium isolated from a deep-sea hydrothermal vent. Standards in Genomic Sciences **5**(1): 135-143.

36. Giovannelli, D., J. Ricci, I. Perez-Rodriguez, M. Hugler, C. O'Brien, R. Keddis, A. Grosche, L. Goodwin, D. Bruce, K. W. Davenport, C. Detter, J. Han, S. S. Han, N. Ivanova, M. L. Land, N. Mikhailova, M. Nolan, S. Pitluck, R. Tapia, T. Woyke and C. Vetriani (2012). Complete genome sequence of Thermovibrio ammonificans HB-1(T), a thermophilic, chemolithoautotrophic bacterium isolated from a deep-sea hydrothermal vent. Standards in Genomic Sciences **7**(1): 82-90.

37. Glud, R. N., S. Rysgaard, T. Fenchel and P. H. Nielsen (2004). A conspicuous H2S-oxidizing microbial mat from a high-latitude Arctic fjord (Young Sound, NE Greenland). Marine Biology **145**(1): 51-60.

38. Gorley, C. a. (2001). "PRIMER v5, Primer-E." from http://www.primer-e.com.

39. Govenar, B. and C. R. Fisher (2007). Experimental evidence of habitat provision by aggregations of Riftia pachyptila at hydrothermal vents on the East Pacific Rise. Marine Ecology-an Evolutionary Perspective **28**(1): 3-14.

40. Govenar, B., M. Freeman, D. C. Bergquist, G. A. Johnson and C. R. Fisher (2004). Composition of a one-year-old Riftia pachyptila community following a clearance experiment: Insight to succession patterns at deep-sea hydrothermal vents. Biological Bulletin **207**(3): 177-182.

41. Gregersen, L. H., D. A. Bryant and N.-U. Frigaard Mechanisms and evolution of oxidative sulfur metabolism in green sulfur bacteria. Frontiers in Microbiology **2**.

42. Griesbeck, C., M. Schutz, T. Schodl, S. Bathe, L. Nausch, N. Mederer, M. Vielreicher and G. Hauska (2002). Mechanism of sulfide-quinone reductase investigated using site-directed mutagenesis and sulfur analysis. Biochemistry **41**(39): 11552-11565.

43. Gundersen, J. K., Jorgensen, B.B., Larsen, E., and Jannasch, H.W. (1992). Mats of giant sulphur bacteria on deep-sea sediments due to fluctuating hydrothermal flow. Nature **360**: 454-456.

44. Harmer, T. L., R. D. Rotjan, A. D. Nussbaumer, M. Bright, A. W. Ng, E. G. DeChaine and C. M. Cavanaugh (2008). Free-living tube worm endosymbionts found at deep-sea vents. Applied and Environmental Microbiology **74**(12): 3895-3898.

45. Harold, R. and R. Y. Stanier (1955). The genera Leucothrix and Thiothrix. Bacteriology Reviews **19**(2): 49-64.

46. Haymon, R. M., D. J. Fornari, M. H. Edwards, S. Carbotte, D. Wright and K. C. Macdonald (1991). Hydrothermal Vent Distribution Along the East Pacific Rise Crest (9-Degrees-09'-54'n) and Its Relationship to Magmatic and Tectonic Processes on Fast-Spreading Midocean Ridges. Earth and Planetary Science Letters **104**(2-4): 513-534.

47. Haymon, R. M., D. J. Fornari, K. L. Vondamm, M. D. Lilley, M. R. Perfit, J. M. Edmond, W. C. Shanks, R. A. Lutz, J. M. Grebmeier, S. Carbotte, D. Wright, E. Mclaughlin, M. Smith, N. Beedle and E. Olson (1993). Volcanic-Eruption of the Midocean Ridge Along the East Pacific Rise Crest at 9-Degrees-45-52'n - Direct Submersible Observations of Sea-Floor Phenomena Associated with an Eruption Event in April, 1991. Earth and Planetary Science Letters **119**(1-2): 85-101.

48. He, P. Q., Y. Liu, W. J. Yue and X. H. Huang (2013). Key genes expression of reductive tricarboxylic acid cycle from deep-sea hydrothermal chemolithoautotrophic Caminibacter profundus in response to salinity, pH and O-2. Acta Oceanologica Sinica **32**(2): 35-41.

49. Hessler, R. R. (1985). Citation Classic - Faunal Diversity in the Deep-Sea. Current Contents/Agriculture Biology & Environmental Sciences(11): 18-18.

50. Hoffman, P. S. and T. G. Goodman (1982). Repiratory physiology and energy conservation efficiency of Campylobacter jejuni. Journal of Bacteriology **150**(1): 319-326.

51. Holden, J. F., M. Summit and J. A. Baross (1998). Thermophilic and hyperthermophilic microorganisms in 3-30 degrees C hydrothermal fluids following a deep-sea volcanic eruption. Fems Microbiology Ecology **25**(1): 33-41.

52. Honjo, S. and S. J. Manganini (1993). Annual Biogenic Particle Fluxes to the Interior of the North-Atlantic Ocean - Studied at 34-Degrees-N 21-Degrees-W and 48-Degrees-N 21-Degrees-W. Deep-Sea Research Part Ii-Topical Studies in Oceanography **40**(1-2): 587-607.

53. Huber, J. A., D. A. Butterfield and J. A. Baross (2003). Bacterial diversity in a subseafloor habitat following a deep-sea volcanic eruption. Fems Microbiology Ecology **43**(3): 393-409.

54. Hugler, M., A. Gartner and J. F. Imhoff (2010). Functional genes as markers for sulfur cycling and CO2 fixation in microbial communities of hydrothermal vents of the Logatchev field. Fems Microbiology Ecology **73**(3): 526-537.

55. Hugler, M., J. M. Petersen, N. Dubilier, J. F. Imhoff and S. M. Sievert (2011). Pathways of Carbon and Energy Metabolism of the Epibiotic Community Associated with the Deep-Sea Hydrothermal Vent Shrimp Rimicaris exoculata. Plos One **6**(1).

56. Hugler, M., C. O. Wirsen, G. Fuchs, C. D. Taylor and S. M. Sievert (2005). Evidence for autotrophic CO2 fixation via the reductive tricarboxylic acid cycle by members of the epsilon subdivision of proteobacteria. Journal of Bacteriology **187**(9): 3020-3027.

57. Hung, O. S., O. O. Lee, V. Thiyagarajan, H. P. He, Y. Xu, H. C. Chung, J. W. Qiu and P. Y. Qian (2009). Characterization of cues from natural multi-species biofilms that induce larval attachment of the polychaete Hydroides elegans. Aquatic Biology **4**(3): 253-262.

58. Huson, D. H., A. F. Auch, J. Qi and S. C. Schuster (2007). MEGAN analysis of metagenomic data. Genome Research **17**(3): 377-386.

59. Inagaki, F., K. Takai, K. I. Hideki, K. H. Nealson and K. Horikishi (2003). Sulfurimonas autotrophica gen. nov., sp nov., a novel sulfur-oxidizing epsilon-proteobacterium isolated from hydrothermal sediments in the Mid-Okinawa Trough. International Journal of Systematic and Evolutionary Microbiology **53**: 1801-1805.

60. Inagaki, F., K. Takai, K. H. Nealson and K. Horikoshi (2004). Sulfurovum lithotrophicum gen. nov., sp nov., a novel sulfur-oxidizing chemolithoautotroph within the epsilon-Proteobacteria isolated from Okinawa Trough hydrothermal sediments. International Journal of Systematic and Evolutionary Microbiology **54**: 1477-1482.

61. Jankielewicz, A., O. Klimmek and A. Kroger (1995). The Electron-Transfer from Hydrogenase and Formate Dehydrogenase to Polysulfide Reductase in the Membrane of Wolinella-Succinogenes. Biochimica Et Biophysica Acta-Bioenergetics **1231**(2): 157-162.

62. Jannasch, H. W. (1985). The Chemosynthetic Support of Life and the Microbial Diversity at Deep-Sea Hydrothermal Vents. Proceedings of the Royal Society B-Biological Sciences **225**(1240): 277-297.

63. Jannasch, H. W. (1995). Microbial Ecology - Life at the Sea-Floor. Nature **374**(6524): 676-677.

64. Johnson, K. S., C. L. Beehler, C. M. Sakamotoarnold and J. J. Childress (1986). Insitu Measurements of Chemical-Distributions in a Deep-Sea Hydrothermal Vent Field. Science **231**(4742): 1139-1141.

65. Johnson, P., Sieburth, JM., Sastry, A., Arnold, CR., Doty, M. (1971). Leucothrix Mucor Infestation of Benthis Crustacea, Fish Eggs, and Tropical Algae. Limnology and Oceanography **16**(6): 962-969.

66. Johnson, P. W., J. M. Sieburth, A. Sastry, C. R. Arnold and M. S. Doty (1971). Leucothrix mucor infestation of benthic crustacea, fish eggs, and tropical algae. Limnology and Oceanography **16**(6): 962-969.

67. Joint, I., K. Tait and G. Wheeler (2007). Cross-kingdom signalling: exploitation of bacterial quorum sensing molecules by the green seaweed Ulva. Philosophical Transactions of the Royal Society B-Biological Sciences **362**(1483): 1223-1233.

68. Jones, C. M., B. Stres, M. Rosenquist and S. Hallin (2008). Phylogenetic analysis of nitrite, nitric oxide, and nitrous oxide respiratory enzymes reveal a complex evolutionary history for denitrification. Molecular Biology and Evolution **25**(9): 1955-1966.

69. Jormakka, M., K. Yokoyama, T. Yano, M. Tamakoshi, S. Akimoto, T. Shimamura, P. Curmi and S. Iwata (2008). Molecular mechanism of energy conservation in polysulfide respiration. Nature Structural & Molecular Biology **15**(7): 730-737.

70. Karl, D. M. (1995). Ecology of free-living, hydrothermal vent microbial communities. The microbiology of deep-sea hydrothermal vents. D. M. Karl. Boca Raton, CRC press**:** 35-124.

71. Kelly, D. P., J. K. Shergill, W. P. Lu and A. P. Wood (1997). Oxidative metabolism of inorganic sulfur compounds by bacteria. Antonie Van Leeuwenhoek International Journal of General and Molecular Microbiology **71**(1-2): 95-107.

72. Kelly, N., A. Metaxas and D. Butterfield (2007). Spatial and temporal patterns of colonization by deep-sea hydrothermal vent invertebrates on the Juan de Fuca Ridge, NE Pacific. Aquatic Biology **1**(1): 1-16.

73. Kern, M. and J. Simon (2009). Electron transport chains and bioenergetics of respiratory nitrogen metabolism in Wolinella succinogenes and other Epsilonproteobacteria. Biochimica Et Biophysica Acta-Bioenergetics **1787**(6): 646-656.

74. Kulajta, C., J. O. Thumfart, S. Haid, F. Daldal and H. G. Koch (2006). Multi-step assembly pathway of the cbb(3)-type cytochrome c oxidase complex. Journal of Molecular Biology **355**(5): 989-1004.

75. Lilley, M. D., D. A. Butterfield, J. E. Lupton and E. J. Olson (2003). Magmatic events can produce rapid changes in hydrothermal vent chemistry. Nature **422**(6934): 878-881.

76. Longnecker, K. and A. L. Reysenbach (2001). Expansion of the geographic distribution of a novel lineage of epsilon-Proteobacteria to a hydrothermal vent site on the Southern East Pacific Rise. Fems Microbiology Ecology **35**(3): 287-293.

77. Lonsdale, P. (1977). Clustering of suspension-feeding macrobenthos near abyssal hydrothermal vents at oceanic spreading centers. Deep Sea Research **24**(9): 857-858.

78. Lopez-Garcia, P., S. Duperron, P. Philippot, J. Foriel, J. Susini and D. Moreira (2003). Bacterial diversity in hydrothermal sediment and epsilon proteobacterial dominance in experimental microcolonizers at the Mid-Atlantic Ridge. Environmental Microbiology **5**(10): 961-976.

79. Lopez-Garcia, P., H. Philippe, F. Gail and D. Moreira (2003). Autochthonous eukaryotic diversity in hydrothermal sediment and experimental microcolonizers at the Mid-Atlantic Ridge. Proceedings of the National Academy of Sciences of the United States of America **100**(2): 697-702.

80. Luo, J. F., W. T. Lin and Y. Guo (2011). Functional genes based analysis of sulfur-oxidizing bacteria community in sulfide removing bioreactor. Applied Microbiology and Biotechnology **90**(2): 769-778.

81. Luther, G. W., A. Gartman, M. Yucel, A. S. Madison, T. S. Moore, H. A. Nees, D. B. Nuzzio, A. Sen, R. A. Lutz, T. M. Shank and C. R. Fisher (2012). Chemistry, Temperature, and Faunal Distributions at Diffuse-Flow Hydrothermal Vents Comparison of Two Geologically Distinct Ridge Systems. Oceanography **25**(1): 234-245.

82. Luther, G. W., B. T. Glazer, S. F. Ma, R. E. Trouwborst, T. S. Moore, E. Metzger, C. Kraiya, T. J. Waite, G. Druschel, B. Sundby, M. Taillefert, D. B. Nuzzio, T. M. Shank, B. L. Lewis and P. J. Brendel (2008). Use of voltammetric solid-state (micro)electrodes for studying biogeochemical processes: Laboratory measurements to real time measurements with an in situ electrochemical analyzer (ISEA). Marine Chemistry **108**(3-4): 221-235.

83. Luther, G. W., T. F. Rozan, M. Taillefert, D. B. Nuzzio, C. Di Meo, T. M. Shank, R. A. Lutz and S. C. Cary (2001). Chemical speciation drives hydrothermal vent ecology. Nature **410**(6830): 813-816.

84. Luther, G. W., M. Taillefert, D. B. Nuzzio, S. C. Cary and T. F. Rozan (2000). In situ voltammetry at hydrothermal vents. Abstracts of Papers of the American Chemical Society **219**: U701-U701.

85. Lutz, R. A., D. Desbruyeres, T. M. Shank and R. C. Vrijenhoek (1998). A deep-sea hydrothermal vent community dominated by Stauromedusae. Deep-Sea Research Part Ii-Topical Studies in Oceanography **45**(1-3): 329-334.

86. Lutz, R. A., T. M. Shank and R. Evans (2001). Life after death in the deep sea. American Scientist **89**(5): 422-431.

87. Lutz, R. A., T. M. Shank, G. W. Luther, C. Vetriani, M. Tolstoy, D. B. Nuzzio, T. S. Moore, F. Waldhauser, M. Crespo-Medina, A. D. Chatziefthimiou, E. R. Annis and A. J. Reed (2008). Interrelationships between vent fluid chemistry, temperature, seismic activity, and biological community structure at a mussel-dominated, deep-sea hydrothermal vent along the East Pacific Rise. Journal of Shellfish Research **27**(1): 177-190.

88. M. Tolstoy, J. P. C., E. T. Baker, D. J. Fornari, K. H. Rubin, T. M. Shank, F. Waldhauser, D. R. Bohnenstiehl, D. W. Forsyth, R. C. Holmes, B. Love, M. R. Perfit, R. T. Weekly, S. A. Soule, B. Glazer (2006). A Sea-Floor Spreading Event Captured by Seismometers. Science **314**: 1920-1922.

89. Maidak, B. L., J. R. Cole, C. T. Parker, G. M. Garrity, N. Larsen, B. Li, T. G. Lilburn, M. J. McCaughey, G. J. Olsen, R. Overbeek, S. Pramanik, T. M. Schmidt, J. M. Tiedje and C. R. Woese (1999). A new version of the RDP (Ribosomal Database Project). Nucleic Acids Research **27**(1): 171-173.

90. Maier, R. J., C. Fu, J. Gilbert, F. Moshiri, J. Olson and A. G. Plaut (1996). Hydrogen uptake hydrogenase in Helicobacter pylori. Fems Microbiology Letters **141**(1): 71-76.

91. McCollom, T. M. (2000). Experimental investigation of abiotic synthesis of organic compounds under hydrothermal conditions. Abstracts of Papers of the American Chemical Society **219**: U692-U692.

92. McCollom, T. M. (2000). Geochemical constraints on primary productivity in submarine hydrothermal vent plumes. Deep-Sea Research Part I-Oceanographic Research Papers **47**(1): 85-101.

93. McCollom, T. M. and E. L. Shock (1997). Geochemical constraints on chemolithoautotrophic metabolism by microorganisms in seafloor hydrothermal systems. Geochimica Et Cosmochimica Acta **61**(20): 4375-4391.

94. McMullin, E. R., S. Hourdez, S. W. Schaeffer and C. R. Fisher (2003). Phylogeny and biogeography of deep sea vestimentiferan tubeworms and their bacterial symbionts. Symbiosis **34**(1): 1-41.

95. Meinersmann, R. J., C. M. Patton, G. M. Evins, I. K. Wachsmuth and P. I. Fields (2002). Genetic diversity and relationships of Campylobacter species and subspecies. International Journal of Systematic and Evolutionary Microbiology **52**: 1789-1797.

96. Meyer, B., J. F. Imhoff and J. Kuever (2007). Molecular analysis of the distribution and phylogeny of the soxB gene among sulfur-oxidizing bacteria - evolution of the Sox sulfur oxidation enzyme system. Environmental Microbiology **9**(12): 2957-2977.

97. Meyer, B. and J. Kuever (2007). Phylogeny of the alpha and beta subunits of the dissimilatory adenosine-5'-phosphosulfate (APS) reductase from sulfate-reducing prokaryotes - origin and evolution of the dissimilatory sulfate-reduction pathway. Microbiology-Sgm **153**: 2026-2044.

98. Meyer, F., D. Paarmann, M. D'Souza, R. Olson, E. M. Glass, M. Kubal, T. Paczian, A. Rodriguez, R. Stevens, A. Wilke, J. Wilkening and R. A. Edwards (2008). The metagenomics RAST server - a public resource for the automatic phylogenetic and functional analysis of metagenomes. Bmc Bioinformatics **9**: -.

99. Micheli, F., C. H. Peterson, L. S. Mullineaux, C. R. Fisher, S. W. Mills, G. Sancho, G. A. Johnson and H. S. Lenihan (2002). Predation structures communities at deep-sea hydrothermal vents. Ecological Monographs **72**(3): 365-382.

100. Miroshnichenko, M. L. (2004). Thermophilic microbial communities of deep-sea hydrothermal vents. Microbiology **73**(1): 1-13.

101. Miroshnichenko, M. L., S. L'Haridon, P. Schumann, S. Spring, E. A. Bonch-Osmolovskaya, C. Jeanthon and E. Stackebrandt (2004). Caminibacter profundus sp nov., a novel thermophile of Nautiliales ord. nov within the class 'Epsilonproteobacteria', isolated from a deep-sea hydrothermal vent. International Journal of Systematic and Evolutionary Microbiology **54**: 41-45.

102. Moore, T. S., K. M. Mullaugh, R. R. Holyoke, A. S. Madison, M. Yucel and G. W. Luther (2009). Marine Chemical Technology and Sensors for Marine Waters: Potentials and Limits. Annual Review of Marine Science **1**: 91-115.

103. Moussard, H., E. Corre, M. A. Cambon-Bonavita, Y. Fouquet and C. Jeanthon (2006). Novel uncultured Epsilonproteobacteria dominate a filamentous sulphur mat from the 13 degrees N hydrothermal vent field, East Pacific Rise. Fems Microbiology Ecology **58**(3): 449-463.

104. Moyer, C. L., F. C. Dobbs and D. M. Karl (1995). Phylogenetic Diversity of the Bacterial Community from a Microbial Mat at an Active, Hydrothermal Vent System, Loihi Seamount, Hawaii. Applied and Environmental Microbiology **61**(4): 1555-1562.

105. Mullineaux, L. S., C. R. Fisher, C. H. Peterson and S. W. Schaeffer (2000). Tubeworm succession at hydrothermal vents: use of biogenic cues to reduce habitat selection error? Oecologia **123**(2): 275-284.

106. Mullineaux, L. S., S. W. Mills and E. Goldman (1998). Recruitment variation during a pilot colonization study of hydrothermal vents (9 degrees 50 ' N, East Pacific Rise). Deep-Sea Research Part Ii-Topical Studies in Oceanography **45**(1-3): 441-464.

107. Mullineaux, L. S., C. H. Peterson, F. Micheli and S. W. Mills (2003). Successional mechanism varies along a gradient in hydrothermal fluid flux at deep-sea vents. Ecological Monographs **73**(4): 523-542.

108. Nakagawa, S. and K. Takai (2008). Deep-sea vent chemoautotrophs: diversity, biochemistry and ecological significance. FEMS Microbiol Ecol **65**(1): 1-14.

109. Nakagawa, S., K. Takai, F. Inagaki, H. Hirayama, T. Nunoura, K. Horikoshi and Y. Sako (2005). Distribution, phylogenetic diversity and physiological characteristics of epsilon-Proteobacteria in a deep-sea hydrothermal field. Environmental Microbiology **7**(10): 1619-1632.

110. Nakagawa, S., K. Takai, F. Inagaki, K. Horikoshi and Y. Sako (2005). Nitratiruptor tergarcus gen. nov., sp. nov. and Nitratifractor salsuginis gen. nov., sp. nov., nitrate-reducing chemolithoautotrophs of the epsilon-Proteobacteria isolated from a deep-sea hydrothermal system in the Mid-Okinawa Trough (vol 55, pg 925, 2005). International Journal of Systematic and Evolutionary Microbiology **55**: 2233-2233.

111. Nakagawa, S., Y. Takaki, S. Shimamura, A. L. Reysenbach, K. Takai and K. Horikoshi (2007). Deep-sea vent epsilon-proteobacterial genomes provide insights into emergence of pathogens. Proc Natl Acad Sci U S A **104**(29): 12146-50.

112. Nakagawa, S., Y. Takaki, S. Shimamura, A. L. Reysenbach, K. Takai and K. Horikoshi (2007). Deep-sea vent epsilon-proteobacterial genomes provide insights into emergence of pathogens. Proceedings of the National Academy of Sciences of the United States of America **104**(29): 12146-12150.

113. Nees, H. A., T. S. Moore, K. M. Mullaugh, R. R. Holyoke, C. P. Janzen, S. Ma, E. Metzger, T. J. Waite, M. Yucel, R. A. Lutz, T. M. Shank, C. Vetriani, D. B. Nuzzio and G. W. Luther (2008). Hydrothermal vent mussel habitat chemistry, pre- and post-eruption at 9 degrees 50 ' North on the East Pacific Rise. Journal of Shellfish Research **27**(1): 169-175.

114. Nees, H. L., RA | Shank, TM | Luther, GW (2009). Pre- and post-eruption diffuse flow variability among tubeworm habitats at 9 super(o)50' north on the East Pacific Rise. Deep Sea Research **56**(19-20): 1607-1615.

115. Nelson, D. C., B. B. Jorgensen and N. P. Revsbech (1986). Growth-Pattern and Yield of a Chemoautotrophic Beggiatoa Sp in Oxygen-Sulfide Microgradients. Applied and Environmental Microbiology **52**(2): 225-233.

116. Nishimura, H., Y. Kitano, T. Inoue, K. Nomura and Y. Sako (2010). Purification and Characterization of Membrane-Associated Hydrogenase from the Deep-Sea Epsilonproteobacterium Hydrogenimonas thermophila. Bioscience Biotechnology and Biochemistry **74**(8): 1624-1630.

117. Nussbaumer, A. D., C. R. Fisher and M. Bright (2006). Horizontal endosymbiont transmission in hydrothermal vent tubeworms. Nature **441**(7091): 345-348.

118. Parkhill, J., B. W. Wren, K. Mungall, J. M. Ketley, C. Churcher, D. Basham, T. Chillingworth, R. M. Davies, T. Feltwell, S. Holroyd, K. Jagels, A. V. Karlyshev, S. Moule, M. J. Pallen, C. W. Penn, M. A. Quail, M. A. Rajandream, K. M. Rutherford, A. H. M. van Vliet, S. Whitehead and B. G. Barrell (2000). The genome sequence of the food-borne pathogen Campylobacter jejuni reveals hypervariable sequences. Nature **403**(6770): 665-668.

119. Perez-Rodriguez, I., J. Ricci, J. W. Voordeckers, V. Starovoytov and C. Vetriani (2010). Nautilia nitratireducens sp nov., a thermophilic, anaerobic, chemosynthetic, nitrate-ammonifying bacterium isolated from a deep-sea hydrothermal vent. International Journal of Systematic and Evolutionary Microbiology **60**: 1182-1186.

120. Petersen, J. M., A. Ramette, C. Lott, M. A. Cambon-Bonavita, M. Zbinden and N. Dubilier (2010). Dual symbiosis of the vent shrimp Rimicaris exoculata with filamentous gamma- and epsilonproteobacteria at four Mid-Atlantic Ridge hydrothermal vent fields. Environmental Microbiology **12**(8): 2204-2218.

121. Petri, R., L. Podgorsek and J. F. Imhoff (2001). Phylogeny and distribution of the soxB gene among thiosulfate-oxidizing bacteria. Fems Microbiology Letters **197**(2): 171-178.

122. Pitcher, R. S. and N. J. Watmough (2004). The bacterial cytochrome cbb(3) oxidases. Biochimica Et Biophysica Acta-Bioenergetics **1655**(1-3): 388-399.

123. Preuss, A., R. Schauder, G. Fuchs and W. Stichler (1989). Carbon Isotope Fractionation by Autotrophic Bacteria with 3 Different Co2 Fixation Pathways. Zeitschrift Fur Naturforschung C-a Journal of Biosciences **44**(5-6): 397-402.

124. R. Hekinian, J. F., V. Renard, R. D. Ballard, P. Choukroune, J. L. Cheminee, F. Albarede, J. F. Minster, J. L. Charlou, J. C. Marty and J. Boulegue (1983). Intense hydrothermal activity at the axis of the east pacific rise near 13°N: Sumbersible witnesses the growth of sulfide chimney. Marine Geophysical Researches **6**(1): 1-14.

125. Rauhut, R. and G. Klug (1999). mRNA degradation in bacteria. Fems Microbiology Reviews **23**(3): 353-370.

126. Rawlings, D. E. (2005). Characteristics and adaptability of iron- and sulfur-oxidizing microorganisms used for the recovery of metals from minerals and their concentrates. Microbial Cell Factories **4**.

127. Rohlf, F. J. (1998). NTSYS-PC numerical taxonomy and multivariate analysis system. Setauket, N.Y., Exeter Publications.

128. Rosenberg, N. D., F. J. Spera and R. M. Haymon (1993). The Relationship between Flow and Permeability Field in Sea-Floor Hydrothermal Systems. Earth and Planetary Science Letters **116**(1-4): 135-153.

129. Rothery, R. A., N. Kalra, R. J. Turner and J. H. Weiner (2002). Sequence similarity as a predictor of the transmembrane topology of membrane-intrinsic subunits of bacterial respiratory chain enzymes. Journal of Molecular Microbiology and Biotechnology **4**(2): 133-150.

130. Rothschild, L. (2002). Life at the limits: Organisms in extreme environments. Nature **417**(6889): 593-593.

131. Rothschild, L. J. (2008). The evolution of photosynthesis ... again? Philosophical Transactions of the Royal Society B-Biological Sciences **363**(1504): 2787-2801.

132. Saitou, N. and M. NEI (1986). The Neighbor-Joining Method - a New Method for Reconstructing Phylogenetic Trees. Japanese Journal of Genetics **61**(6): 611-611.

133. Scheirer, D. S., T. M. Shank and D. J. Fornari (2006). Temperature variations at diffuse and focused flow hydrothermal vent sites along the northern East Pacific Rise. Geochemistry Geophysics Geosystems **7**.

134. Schrenk, M. O., J. A. Huber and K. J. Edwards (2010). Microbial Provinces in the Subseafloor. Annual Review of Marine Science **2**: 279-304.

135. Seyfried, W. E. and D. R. Janecky (1985). Heavy-Metal and Sulfur Transport during Subcritical and Supercritical Hydrothermal Alteration of Basalt - Influence of Fluid Pressure and Basalt Composition and Crystallinity. Geochimica Et Cosmochimica Acta **49**(12): 2545-2560.

136. Shank, T. M., D. J. Fornari, K. L. Von Damm, M. D. Lilley, R. M. Haymon and R. A. Lutz (1998). Temporal and spatial patterns of biological community development at nascent deep-sea hydrothermal vents (9 degrees 50 ' N, East Pacific Rise). Deep-Sea Research Part Ii-Topical Studies in Oceanography **45**(1-3): 465-+.

137. Shiozawa, D. K., J. Kudo, R. P. Evans, S. R. Woodward and R. N. Williams (1992). DNA Extraction from Preserved Trout Tissues. Great Basin Naturalist **52**(1): 29-34.

138. Sievert, S. M., K. A. Scott, M. G. Klotz, P. S. G. Chain, L. J. Hauser, J. Hemp, M. Hugler, M. Land, A. Lapidus, F. W. Larimer, S. Lucas, S. A. Malfatti, F. Meyer, I. T. Paulsen, Q. Ren, J. Simon and U. G. Class (2008). Genome of the epsilonproteobacterial chemolithoautotroph Sulfurimonas denitrificans. Applied and Environmental Microbiology **74**(4): 1145-1156.

139. Sievert, S. M. and C. Vetriani (2012). Chemoautotrophy at Deep-Sea Vents Past, Present, and Future. Oceanography **25**(1): 218-233.

140. Sikorski, J., C. Munk, A. Lapidus, O. D. N. Djao, S. Lucas, T. G. Del Rio, M. Nolan, H. Tice, C. Han, J. F. Cheng, R. Tapia, L. Goodwin, S. Pitluck, K. Liolios, N. Ivanova, K. Mavromatis, N. Mikhailova, A. Pati, D. Sims, L. Meincke, T. Brettin, J. C. Detter, A. Chen, K. Palaniappan, M. Land, L. Hauser, Y. J. Chang, C. D. Jeffries, M. Rohde, E. Lang, S. Spring, M. Goker, T. Woyke, J. Bristow, J. A. Eisen, V. Markowitz, P. Hugenholtz, N. C. Kyrpides and H. P. Klenk (2010). Complete genome sequence of Sulfurimonas autotrophica type strain (OK10(T)). Standards in Genomic Sciences **3**(2): 194-202.

141. Sneath, P. H. A. and R. R. Sokal (1973). Numerical taxonomy; the principles and practice of numerical classification. San Francisco,, W. H. Freeman.

142. Soule, S. A., J. Escartin and D. J. Fornari (2009). A record of eruption and intrusion at a fast spreading ridge axis: Axial summit trough of the East Pacific Rise at 9-10 degrees N. Geochemistry Geophysics Geosystems **10**: -.

143. Sparks, R. S., H. E. Huppert, T. Koyaguchi and M. A. Hallworth (1993). Origin of Modal and Rhythmic Igneous Layering by Sedimentation in a Convecting Magma Chamber. Nature **361**(6409): 246-249.

144. Stein, J. L., S. C. Cary, R. R. Hessler, S. Ohta, R. D. Vetter, J. J. Childress and H. Felbeck (1988). Chemoautotrophic Symbiosis in a Hydrothermal Vent Gastropod. Biological Bulletin **174**(3): 373-378.

145. Stephenson, M. and L. H. Stickland (1931). Hydrogenase: a bacterial enzyme activating molecular hydrogen. Biochemical Journal **25**(1): 205-214.

146. Stetter, K. O. (1999). Extremophiles and their adaptation to hot environments. Febs Letters **452**(1-2): 22-25.

147. Suzuki, Y., T. Sasaki, M. Suzuki, Y. Nogi, T. Miwa, K. Takai, K. H. Nealson and K. Horikoshi (2005). Novel chemoautotrophic endosymbiosis between a member of the Epsilonproteobacteria and the hydrothermal-vent gastropod Alviniconcha aff. hessleri (Gastropoda : Provannidae) from the Indian Ocean. Applied and Environmental Microbiology **71**(9): 5440-5450.

148. Sylvan, J. B., B. M. Toner and K. J. Edwards (2012). Life and Death of Deep-Sea Vents: Bacterial Diversity and Ecosystem Succession on Inactive Hydrothermal Sulfides. Mbio **3**(1).

149. Takai, K., B. J. Campbell, S. C. Cary, M. Suzuki, H. Oida, T. Nunoura, H. Hirayama, S. Nakagawa, Y. Suzuki, F. Inagaki and K. Horikoshi (2005). Enzymatic and genetic characterization of carbon and energy metabolisms by deep-sea hydrothermal chemolithoautotrophic isolates of Epsilonproteobacteria. Applied and Environmental Microbiology **71**(11): 7310-7320.

150. Takai, K., T. Gamo, U. Tsunogai, N. Nakayama, H. Hirayama, K. H. Nealson and K. Horikoshi (2004). Geochemical and microbiological evidence for a hydrogen-based, hyperthermophilic subsurface lithoautotrophic microbial ecosystem (HyperSLiME) beneath an active deep-sea hydrothermal field. Extremophiles **8**(4): 269-282.

151. Takai, K., K. H. Nealson and K. Horikoshi (2004). Hydrogenimonas thermophila gen. nov., sp nov., a novel thermophilic, hydrogen-oxidizing chemolithoautotroph within the epsilon-Proteobacteria, isolated from a black smoker in a Central Indian Ridge hydrothermal field. International Journal of Systematic and Evolutionary Microbiology **54**: 25-32.

152. Takai, K., M. Suzuki, S. Nakagawa, M. Miyazaki, Y. Suzuki, F. Inagaki and K. Horikoshi (2006). Sulfurimonas paralvinellae sp nov., a novel mesophilic, hydrogen- and sulfur-oxidizing chemolithoautotroph within the Epsilonproteo-bacteria isolated from a deep-sea hydrothermal vent polychaete nest, reclassification of Thiomicrospira denitrificans as Sulfurimonas denitrificans comb. nov and emended description of the genus Sulfurimonas. International Journal of Systematic and Evolutionary Microbiology **56**: 1725-1733.

153. Taylor, C. D. and C. O. Wirsen (1997). Microbiology and ecology of filamentous sulfur formation. Science **277**(5331): 1483-1485.

154. Taylor, C. D., C. O. Wirsen and F. Gaill (1999). Rapid microbial production of filamentous sulfur mats at hydrothermal vents. Applied and Environmental Microbiology **65**(5): 2253-2255.

155. Thompson, J. D., Gibson, T.J., Plewniak, F., Jeanmougin, F., Higgins, D.G. (1997). The ClustalX window interface: flexible strategies for multiple sequence alignment aided by quality analysis tools. Nucleic Acids Research **25**: 4876-4882.

156. Thompson, J. D., D. G. Higgins and T. J. Gibson (1994). Clustal-W - Improving the Sensitivity of Progressive Multiple Sequence Alignment through Sequence Weighting, Position-Specific Gap Penalties and Weight Matrix Choice. Nucleic Acids Research **22**(22): 4673-4680.

157. Tolstoy, M., J. P. Cowen, E. T. Baker, D. J. Fornari, K. H. Rubin, T. M. Shank, F. Waldhauser, D. R. Bohnenstiehl, D. W. Forsyth, R. C. Holmes, B. Love, M. R. Perfit, R. T. Weekly, S. A. Soule and B. Glazer (2006). A sea-floor spreading event captured by seismometers. Science **314**(5807): 1920-1922.

158. Tomb, J. F., O. White, A. R. Kerlavage, R. A. Clayton, G. G. Sutton, R. D. Fleischmann, K. A. Ketchum, H. P. Klenk, S. Gill, B. A. Dougherty, K. Nelson, J. Quackenbush, L. X. Zhou, E. F. Kirkness, S. Peterson, B. Loftus, D. Richardson, R. Dodson, H. G. Khalak, A. Glodek, K. McKenney, L. M. Fitzegerald, N. Lee, M. D. Adams, E. K. Hickey, D. E. Berg, J. D. Gocayne, T. R. Utterback, J. D. Peterson, J. M. Kelley, M. D. Cotton, J. M. Weldman, C. Fujii, C. Bowman, L. Watthey, E. Wallin, W. S. Hayes, J. M. Weidman, C. Fujii, M. Borodovsky, P. D. Karp, H. O. Smith, C. M. Fraser and J. C. Venter (1997). The complete genome sequence of the gastric pathogen Helicobacter pylori. Nature **388**(6642): 539-547.

159. Vetriani, C., H. W. Jannasch, B. J. MacGregor, D. A. Stahl and A. L. Reysenbach (1999). Population structure and phylogenetic characterization of marine benthic archaea in deep-sea sediments. Applied and Environmental Microbiology **65**(10): 4375-4384.

160. Vignais, P. M., B. Billoud and J. Meyer (2001). Classification and phylogeny of hydrogenases. Fems Microbiology Reviews **25**(4): 455-501.

161. Von Damm, K. L. and M. D. Lilley (2004). Diffuse flow hydrothermal fluids from 9-degrees-50'N East Pacific Rise: origin, evolution and biogeochemical controls. Geophysical Monograph Series **144**: 245-268.

162. Von Damm, K. L., Lilley, M.D. (2004). Diffuse flow hydrothermal fluids from 9° 50′ N East Pacific Rise: Origin, evolution and biogeochemical controls. GEOPHYSICAL MONOGRAPH SERIES **144**: 245-268.

163. Vondamm, K. L. (1990). Seafloor Hydrothermal Activity - Black Smoker Chemistry and Chimneys. Annual Review of Earth and Planetary Sciences **18**: 173-204.

164. Voordeckers, J. W., Crespo-Medina, M., Lutz, R.A. and Vetriani, C. Detection and phylogenetic analysis of the periplasmic nitrate reductase (NapA) in chemolithoautotrophic Epsilonproteobacteria and microbial communities from deep-sea hydrothermal vents. submitted to Appl. Environ. Microbiol.

165. Voordeckers, J. W., M. H. Do, M. Hugler, V. Ko, S. M. Sievert and C. Vetriani (2008). Culture dependent and independent analyses of 16S rRNA and ATP citrate lyase genes: a comparison of microbial communities from different black smoker chimneys on the Mid-Atlantic Ridge. Extremophiles **12**(5): 627-640.

166. Voordeckers, J. W., V. Starovoytov and C. Vetriani (2005). Caminibacter mediatlanticus sp nov., a thermophilic, chemolithoautotrophic, nitrate-ammonifying bacterium isolated from a deep-sea hydrothermal vent on the Mid-Atlantic Ridge. International Journal of Systematic and Evolutionary Microbiology **55**: 773-779.

167. Ward, B. B. (1996). Nitrification and denitrification: Probing the nitrogen cycle in aquatic environments. Microbial Ecology **32**(3): 247-261.

168. Williams, T. M. and R. F. UNZ (1989). The Nutrition of Thiothrix, Type-021n, Beggiatoa and Leucothrix Strains. Water Research **23**(1): 15-22.

169. Wodara, C., S. Kostka, M. Egert, D. P. Kelly and C. G. Friedrich (1994). Identification and Sequence-Analysis of the Soxb Gene Essential for Sulfur Oxidation of Paracoccus-Denitrificans Gb17. Journal of Bacteriology **176**(20): 6188-6191.

170. Xiaotong, P. and Z. Huaiyang (2005). Growth history of hydrothermal chimneys at EPR 9-10-degrees N: A structural and mineralogical study. Science in China Series D: Earth Sciences **48**(11): 1891-1899.

171. Yamamoto, M., S. Nakagawa, S. Shimamura, K. Takai and K. Horikoshi (2010). Molecular characterization of inorganic sulfur-compound metabolism in the deep-sea epsilonproteobacterium Sulfurovum sp NBC37-1. Environmental Microbiology **12**(5): 1144-1152.

172. Zumft, W. G. (1997). Cell biology and molecular basis of denitrification. Microbiology and Molecular Biology Reviews **61**(4): 533-+.